6-2018

Myosin Assembly into Elongating Thick Filaments is Dependent on the Function of Conserved APMK-Related Kinase UNC-82 in C. Elegans

NaTasha R. Schiller
Western Michigan University, natasha.r.schiller@gmail.com

MYOSIN ASSEMBLY INTO ELONGATING THICK FILAMENTS IS DEPENDENT ON THE FUNCTION OF CONSERVED APMK-RELATED KINASE UNC-82 IN C. ELEGANS

by

NaTasha R. Schiller

A dissertation submitted to the Graduate College
in partial fulfillment of the requirements
for the degree of Doctor of Philosophy
Biological Sciences
Western Michigan University
June 2018

Doctoral Committee:

Pamela Hoppe, Ph.D., Chair
Wendy Beane, Ph.D.
Donald Kane, Ph.D.
Blair Szymczyna, Ph.D.

MYOSIN ASSEMBLY INTO ELONGATING THICK FILAMENTS IS DEPENDENT ON THE FUNCTION OF CONSERVED APMK-RELATED KINASE UNC-82 IN C. ELEGANS

NaTasha R. Schiller, Ph.D.

Western Michigan University, 2018

The mechanism of assembly of sarcomeric myosins into elongating thick filaments is not well understood. The results of this study suggest a novel mechanistic model in which the AMPK-related kinase UNC-82, which is orthologous to mammalian ARK5/NUAK1 and SNARK/NUAK2, acts as an assemblase on sarcomeric myosin molecules, mediating their addition into the elongating thick filaments of *C. elegans* body-wall muscle. The classical genetic crosses performed in this study produced over 53 different worm strains that contain thick-filament-affecting mutations and/or transgenes in single-, double- or triple-mutant combinations. The phenotypes of these strain were documented and analyzed using viability assays, brood analysis, thrashing assays, immunocytochemistry and polarized light microscopy. This in-depth analysis revealed a vital stoichiometric relationship of UNC-82 kinase with the three homologous myosin-related proteins that are the major structural components of the thick filament: myosin A, the minor filament-initiating myosin; myosin B, the major myosin required for locomotion in adult worms; and paramyosin, the headless myosin that forms the core of the long thick filament structure. The importance of UNC-82 protein dosage in proper filament formation suggests a structural role for UNC-82, which is consistent with the large number of amino acids (more

than 1200) that lie outside the kinase catalytic domain. Experiments with a mutation that impairs only the catalytic activity of the kinase domain suggest that UNC-82 enzymatic activity is specifically required for addition of paramyosin and myosin A, but not myosin B, to elongating filaments. Using chimeric myosin transgenes that are combinations of sequences from both myosin A and myosin B, we have mapped the myosin-A-specific requirement for UNC-82 to a 531-amino-acid region of the coiled-coil rod. The results of this study expand the understanding of the mechanism of thick filament elongation whereby UNC-82 acts to modulate the interactions between myosins A and B with paramyosin in elongating thick filaments. This new knowledge provides important evidence to support further investigation of the UNC-82/NUAK/ARK5/SNARK protein kinase as a potential drug target in managing cardiac and skeletal related myopathies.

TABLE OF CONTENTS

Table of contents—continued

CHAPTER

Table of contents—continued

CHAPTER

Table of contents—continued

LIST OF TABLES

LIST OF FIGURES

List of figures—continued

CHAPTER 1

INTRODUCTION

Myosin Assembly into Elongating Thick Filaments is Dependent on the Function of Conserved Apmk-Related Kinase UNC-82 in *C. elegans*

Human congenital myopathies occur as a result of underlying defects in a complex array of proteins related to neuromuscular function. The variety of the genetic defects can range from impairment in calcium cycling, cellular vesicle trafficking and myosin thick filament assembly and function alterations. These protein impairments can lead to distinct histopathological features with early onset of skeletal and cardiac muscle impairments which often present as muscle weakness or cardiorespiratory insufficiency and, in the case of some cardiomyopathies, sudden cardiac arrest. While there has been an increase in identification of mutant genes correlated with congenital myopathies, the treatment options for individuals with these diseases is more supportive care rather than a cure. As a result of the complexity of molecular interactions required for proper muscle maintenance and contraction of muscle, patient care is limited. Compounding this problem is the lack of clarity in the mechanism for muscle cell organization at the sarcomere level (reviewed in Jungbluth *et al.,* 2017).

Mammalian Sarcomere Organization and Mechanism of Contraction

The contractile units of mammalian muscle cells are composed short sarcomeres of highly organized class II myosin thick filaments, anchored to M-lines, and interdigitated between actin-containing thin filaments which are anchored at the Z-disks. The Z-disks of these short sarcomeres are sites where actin filaments of one sarcomere cross-link with the

actin filaments in an adjacent sarcomere in reversed polarity. These links form the "small-square lattice" sarcomere boundaries that keep the sarcomeres in register and prevent disassociation of muscle when contraction occurs (Goldstein *et al.,* 1990; Luther *et al.*, 2002, Clark *et al.,* 2002; Squire *et al.,* 2005). A network of proteins including Obsl1, myomesin, titin, obscurin interact to compose the M-line (Fukuzawa *et al.,* 2008; Gautel, 2011; Kontrogianni-Konstantopoulos *et al.,* 2009). Anchored to the M-line are thick filaments of class II myosin molecules.

The basic mechanism of sarcomere contraction involves the myosin motor domain interacting cyclically in a cross-bridge with actin, requiring the repeated hydrolysis of ATP, which is bound to myosin, to produce a power stroke. This mechanism requires a careful balance between ATP consumption and production for the continuation of contraction. AMPK is a highly conserved sensor of intracellular adenosine nucleotide levels and promotes the metabolic generation of additional ATP when levels are low (Kahn *et al.*, 2005; Xiao *et al.*, 2011).

Class II Myosins

The Individual subunit of class II myosins are hexameric molecules composed of two motor-containing coiled-coil heavy chains, and four light chains, two essential hinge stabilizing light chains (ELC), and two motor regulating light chains (RLC) (Sellers, 2002). The molecular structure of single myosin molecule includes ~800 amino acids in the motor domain, which contains both ATP and actin binding sites, ~50 amino acids in the neck domain where ELC and RLC bind, a coiled-coil rod domain of varied lengths upwards to ~1100 amino acids, and a nonhelical tailpiece which contains three S_S_A phosphorylation

site motifs. Inter molecular interactions between the coiled-coil rod domain and the nonhelical tailpiece are crucial for formation of the hexamer and its incorporation into thick filament structures (Niederman and Pollard, 1975; Lu and Wong, 1985; Schriefer and Waterston, 1989; Verkhovsky *et al.,* 1995; Hoppe and Waterston, 1996).

Caenorhabditis elegans as a Model Organism

The sarcomeric molecular machinery of the body-wall muscle cells, and associating attachment structures, in the free living microscopic nematode, *Caenorhabditis elegans* (*C. elegans)* and have striking similarities to human striated cell structures. This coupled with the ease of genetic manipulation, and rapid life cycle make *C. elegans* a great tool for investigating sarcomere organization (Benian and Epstein, 2011).

The 95 spindle-shaped body-wall muscle cells of *C. elegans* appear as staggered pairs that run the length of the four longitudinal quadrants of the worm. The long sarcomeres of the muscles cells are organized in oblique striations with the filaments longitudinally parallels to the cell axis (Waterston, 1988). The contractile activity of *C. elegans* body-wall muscle sarcomeres is required for embryonic viability and adult locomotion. The body-wall muscles are attached to the cuticular exoskeleton of the worm through the epidermis via Z-disk-like structures called dense bodies. The dense bodies contribute to the oblique organization of the sarcomeres and serve as the site for actin filament anchoring.

Thick filament proteins of *C. elegans* body wall muscle, are attached to a M-line structure similar to the M-line of mammals and contain two isoforms of a class II myosin: myosin A (encoded by the *myo-3* gene), required for filament initiation, and myosin B (encoded by the *unc-54* gene), required for movement in adults. Divergent from vertebrates,

is the stabilizing inner core of the long thick filament structures which is comprised of hydrophobic "headless myosin" molecule, paramyosin. Thought to have been lost in vertebrates with the evolution of short thick filaments. Paramyosin is homologous to the filament forming light meromyoisn domain of the coiled-coil myosins A and B (Lowey *et al.,* 1969; Waterston, 1980; Cohen *et al.,* 1987; Kagawa *et al.,* 1989; Waterston, 1989).

C. elegans is an ideal candidate for studying the role of the conserved UNC-82 kinase in striated muscle due to the larger size of the sarcomeres, the simplicity of the body plan, and the viability of genetic mutants. The availability of many muscle-affecting mutant strains and the advances in molecular biology techniques for modifying the genome has opened new avenues for testing protein function in vivo.

Conserved AMPK-Related Kinase, UNC-82

Electron and polarized light microscopy revealed spatial arrangement abnormalities of thick filament with aberrant aggregates of paramyosin in worms with mutations in the unc-82 gene which codes for the AMPK-related kinase, UNC-82 (Waterston *et al.,* 1980; Hoppe *et al.,* 2010a). The kinase activity of the conserved AMPK related kinase UNC-82, orthologous to ARK5/NUAK1 and SNARK/NUAK2, which is highly expressed in mammalian striated muscle, is required for proper sarcomere organization in *C. elegans* body-wall muscle (Waterston, 1980; Lefebvre and Rosen, 2005; Hoppe *et al.,* 2010a). Analysis of phosphorylation levels of protein components of the actin-myosin cytoskeleton in a muscle-specific knockout of mammalian NUAK1 revealed changes in phosphorylation levels of myosin whereas an investigation examining the reduction of NUAK2 resulted in an age-dependent loss of muscle mass (Inazuka, 2012). These observations suggest potential

conserved roles for NUAK kinase in the contractile apparatus of mammalian striated muscle. In mouse, early embryonic lethality occurs when either single gene is knocked out requiring tissue specific targeting of these proteins for in vivo analysis. The role of these proteins in muscle structure has likely been over looked in muscle-specific targeting assays due to expression of the paralog protein, which may act redundantly to organize thick filaments. Redundant function of NUAK1 and NUAK2 has been demonstrated for the non-muscle myosin II- dependent cell shape changes that drive folding of embryonic epithelial sheets during morphogenesis. A few studies suggest there may be conserved elements in the roles of UNC-82/NUAK kinases in regulation of myosin II activity in muscle and non-muscle cells (Vallenius *et al.*, 2011; Zogorska *et al.*, 2012). The results of the studies within this document have culminated in the identification of a role for the conserved AMPK-related kinase UNC-82/ARK5/SNARK, in organizing the complex molecular machine of muscle sarcomeres through modulating myosin-myosin interactions within the thick filaments.

CHAPTER 2

THE ROLE OF THE UNC-82 PROTEIN KINASE IN ORGANIZING MYOSIN FILAMENTS IN STRIATED MUSCLE OF *C. ELEGANS*

This chapter has been published in GENETICS (March 1, 2017 vol. 205 no. 3 1195-1213; https://doi.org/10.1534/genetics.116.193029) (see Appendix)

We study the mechanisms that guide the formation and maintenance of the highly-ordered actin-myosin cytoskeleton in striated muscle. The UNC-82 kinase of *Caenorhabditis elegans* is orthologous to mammalian kinases ARK5/NUAK1 and SNARK/NUAK2. UNC-82 localizes to the M-line and is required for proper organization of thick filaments, but its substrate and mechanism of action are unknown. Antibody staining of three mutants with missense mutations in the UNC-82 catalytic domain revealed muscle structure that is less disorganized than in the null *unc-82(0)*, but which contained distinctive ectopic accumulations not found in *unc-82(0)*. These accumulations contain paramyosin and myosin B, but lack myosin A and myosin A-associated proteins as well as proteins of the integrin-associated complex. Fluorescently tagged missense mutant protein UNC-82 E424K localized normally in wild type; however, in *unc-82(0)* the tagged protein was found in the ectopic accumulations, which we also show label with recently synthesized paramyosin. Recruitment of wild-type UNC-82::GFP to aggregates of differing protein composition in five muscle-affecting mutants revealed that colocalization of UNC-82 and paramyosin does not require UNC-96, UNC-98/ZnF, UNC-89/obscurin, CSN-5, myosin A or myosin B individually. Dosage effects in paramyosin mutants suggest that UNC-82 acts as part of a complex in which its stoichiometric relationship with paramyosin is critical. UNC-82 dosage affects muscle organization in the absence of paramyosin, perhaps through myosin B. We present evidence that the interaction of UNC-98/ZnF with myosin A is independent

of UNC-82, and that UNC-82 acts upstream of UNC-98/ZnF in a pathway that organizes paramyosin during thick filament assembly.

The nematode *C. elegans* has been an excellent system for discovery and study of proteins important for proper muscle cell structure and function (reviewed in Waterston, 1988; Moerman and Fire, 1997; Moerman and Williams, 2006; Gieseler *et al.,* 2016). The contractile apparatus of striated muscle is a highly-ordered array of interdigitated actin thin filaments and myosin thick filaments. The myosin filaments in *C. elegans* contain myosin A, myosin B, paramyosin, and the filagenins. The nematode thick filament has been modeled to consist of a series of concentric layers, with an outer layer containing myosins A and B, an intermediate layer of paramyosin, and an inner layer or core of paramyosin and the filagenins (Epstein *et al.,* 1985; Deitiker and Epstein, 1993; Liu *et al.,* 1998). Paramyosin is a "headless myosin" which is homologous to the C-terminal three-fourths of the myosin coiled-coil rod (Kagawa *et al.,* 1989). These three coiled-coil proteins segregate to three distinct compartments within the thick filament. Paramyosin, which has a more hydrophobic surface (Cohen *et al.,* 1987), forms a core that runs the length of the filament. Paramyosin supports formation of the long thick filaments found in invertebrate muscle. The motor protein myosin assembles upon the surface of this paramyosin core, where its motor domain can interact with actin filaments to slide the two filament systems past each other and accomplish contraction of the muscle cell. Myosin A is found in the central region of the thick filament, which is also the site where the thick filament attaches to the M-line. Myosin B, the major myosin isoform, is found in the filament arms that extend on either side of the M-line (Miller *et al.,* 1983).

Contraction of the body-wall muscles, which are attached to the cuticular exoskeleton of the worm through the epidermis, causes the body bends that drive locomotion. In addition, contraction of the body-wall muscle is required for body elongation during embryogenesis. Embryonic body elongation is accomplished through constriction of circumferential actin filaments in the epidermis (Priess and Hirsh, 1986), yet in the absence of muscle contraction, body elongation arrests and worms die as deformed L1 larvae with the Pat phenotype (paralyzed, arrested elongation at the two-fold stage) (Waterston, 1989; Williams and Waterston, 1994). Muscle and epidermal cells in *C. elegans* assemble and organize their cytoskeletons in response to contact with each other through integrin-mediated signaling at focal adhesion-like structures, which are present at the base of M-lines and dense bodies, the sites of thick filament and thin filament attachment, respectively (reviewed in Moerman and Williams, 2006). Identification of many genes/proteins required in muscle occurred through forward genetics screens for Unc (uncoordinated) mutants, which have reduced muscle function and exhibit slow movement as adult worms, or the more severe Pat phenotype.

Mutations that eliminate myosin B, the major myosin (encoded by the gene *unc-54*), or paramyosin (encoded by the gene *unc-15*), cause disorganization of the contractile apparatus, resulting in an Unc phenotype (Epstein *et al*. 1974; Waterston *et al.*, 1977). In contrast, mutations that eliminate the minor isoform myosin A (encoded by the *myo-3* gene) result in the Pat phenotype, an observation that revealed an essential role for myosin A in thick filament initiation (Waterston, 1989). The region of myosin A necessary for the essential myosin A-specific function was mapped using chimeric myosins to two regions of

the coiled-coil rod, consistent with a function in assembly of the thick filament (Hoppe and Waterston, 1996).

The precise placement and structural regularity of thick filaments depend upon the action of many muscle proteins. The M-line, the site of thick filament attachment, comprises many structural and probable signaling proteins (reviewed in Qadota and Benian 2010, Gieseler *et al.* 2016). UNC-89/obscurin is a very large protein with many functional domains that is found at the M-line. TEM analysis revealed that *unc-89*/obscurin mutants lack M-lines, and have disorganized thick filaments (Waterston *et al.* 1980). The mutant alleles that lack the UNC-89/obscurin isoforms that contain the SH3 domain, which is proposed to link thick filaments to the M-line through an interaction with paramyosin, have distinctive paramyosin accumulations at the ends of muscle cells (Qadota *et al.,* 2016). Mutations affecting the M-line-specific proteins UNC-98 and UNC-96 also cause moderate thick filament disorganization coupled with distinctive paramyosin accumulations (Zengel and Epstein, 1980). UNC-98 is a 310 amino acid protein that contains four C2H2 zinc fingers ("UNC-98/ZnF"). UNC-96 is a novel protein (Mercer *et al.,* 2006).

The body-wall muscle of *unc-82* mutant worms, which move more slowly than wild type in adulthood, exhibits abnormalities in myosin thick filament morphology and distribution when examined by polarized-light and electron microscopy (Waterston *et al.* 1980). Antibody staining of the putative null mutant *unc-82(e1323)* revealed that the thick filament components myosin A and paramyosin and the M-line protein UNC-89/obscurin were severely affected and that these defects arose during body elongation of the embryo. A rescuing UNC-82::GFP fusion protein is detected at the M-line in body-wall muscle (Hoppe *et al.,* 2010a). The protein product of *unc-82* is an AMPK-related kinase orthologous

to human ARK5/NUAK1 and SNARK/NUAK2 (Hoppe *et al*., 2010a). Both orthologs are expressed in mammalian striated muscle (Lefebvre and Rosen, 2005). Studies have implicated each of these genes individually in function of the contractile apparatus in mouse muscle. Muscle-specific knock down of ARK5/NUAK1 causes altered phosphorylation of contractile apparatus proteins whereas disruption of SNARK/NUAK2 causes an age dependent reduction in muscle mass (Inazuka *et al.,* 2012; Lessard *et al*., 2016). Double knockouts of these orthologs have not been studied in mammalian muscle; these mutants arrest with defects in embryonic morphogenesis (Ohmura *et al.,* 2012). Interestingly, in human kidney cells, ARK5 has been shown to regulate non-muscle myosin light chain phosphorylation (Zagorska *et al.,* 2010). We propose that the UNC-82 kinase associates stoichiometrically, directly or indirectly, with recently synthesized paramyosin to promote proper assembly of paramyosin into the thick filament. Our results also indicate that UNC-82 affects one or more proteins of the contractile apparatus other than paramyosin, and suggest that one such protein is myosin B.

Materials and Methods

GFP and RFP Fusion Constructs

A previously isolated extrachromosomal array expressing wild-type UNC-82::GFP (*phEx22,* Hoppe *et al.* 2010a) was used in this study. The transgene was generated by recombination in vivo between two overlapping linear DNAs, a 17-kb genomic PCR fragment and a linearized plasmid encoding the C-terminus of UNC-82 fused to GFP, following the method of Yuan *et al.* (2000). The PCR fragment, amplified from cosmid B0496, begins within intron 5, 2.6 kb upstream of exon 6 (which contains the initiator methionine used in the majority of *unc-82* transcripts, unpublished data), and ends within intron 32. The plasmid contains genomic DNA spanning exons 29 – 35, with GFP inserted prior to the stop codon in exon 35. The numbering of the exons within the *unc-82* gene has changed from that in the original publication of this construct (Hoppe *et al.,* 2010a) due to the discovery of minor transcripts that contain five additional 5' exons that were not included in the previously published gene structure.

In this study, full-length UNC-82 E424K::GFP and UNC-82 E424K::RFP fusion constructs were generated by the same method as described above for the wild-type GFP fusion with the exception that genomic DNA from the *unc-82(e1220)* mutant was used as template to make the 17 kb PCR fragment using oligonucleotides GTCTCTGCTAAACAGCAATCG and GTTTGTGTACTTGTTGTGTGTG and LongAmp *Taq* DNA Polymerase (New England Biolabs). The GFP sequences in the plasmid encoding exons 29-35 (Hoppe *et al.,* 2010a) were removed by digestion with *Age*I and *Bsm*I, and replaced with a similarly digested 1240 base-pair fragment containing RFP,

amplified from pKFMbRFP using Platinum Pfx DNA Polymerase (Invitrogen) and oligonucleotides ATTTTCAGGGCAGGG and GTTAGTAGAACTCAG. Prior to injection, plasmids were linearized with *Hin*dIII, extracted with phenol/chloroform, and ethanol precipitated.

Generation of Transgenic Lines

Transgenes expressing UNC-82 fused to GFP or RFP were obtained by injecting a DNA cocktail containing 50 ng of PCR product, 125 ng of linearized plasmid, and 2 µg of pRF4 plasmid containing the *rol-6* coinjection marker (Mello *et al*. 1991), brought up to 10 µL with TE. Transgenic lines expressing *hsp*::UNC-15::GFP were obtained by injecting a 200 ng/µL DNA cocktail containing a 1:100 ratio of the plasmid containing full-length UNC-15::GFP under the control of a heat-shock promoter (described in Miller *et al*. 2008) to pRF4.

Genetic Crosses

Anaesthetizing hermaphrodites for crosses with rolling males: Transgenes in this study were followed in genetic crosses by the dominant rolling (Rol) phenotype conferred by the coinjection marker plasmid pRF4 *rol-6(su1006)* (Mello *et al*., 1991). It is advantageous to pass the transgene from the male because rolling cross progeny are easily distinguished from the hermaphrodites' self progeny. Because Rol males mate poorly, hermaphrodites were temporarily immobilized by treatment with TT: M9 with 0.1% tricaine and 0.01% tetramisole (Sigma Inc.) (McCarter *et al*., 1999). Adult rolling males were picked to the bacterial lawn of a seeded plate. Adult hermaphrodites, about four per Rol male, were

treated for 15 – 30 min. in 0.1 mL TT in a sterile well of a three-well glass slide, and then picked to the unseeded area of the plate to allow the TT to seep into the agar. The hermaphrodites were then moved into the lawn, where they were straightened and placed close to each other, either in rows or in clusters; males were then placed directly on top of a hermaphrodite. The following day, males were removed and hermaphrodites transferred to fresh plates.

Crossing transgenes marked with rol-6 into mutant backgrounds: To introduce a transgene into a single mutant background, rolling transgenic males were crossed to anaesthetized homozygous mutant hermaphrodites (see above), and the rolling F1 heterozygous hermaphrodite progeny picked singly and allowed to self. The rolling F2 progeny were picked singly, and mutant homozygotes identified by movement and polarized light phenotypes of the F2 hermaphrodite and its F3 progeny. Double mutant worm strains were generated in the lab through similar crossing and classical genetic phenotype screening. All viable double mutant strains were verified by outcross to N2 and reisolation of each single mutant. Due to synthetic lethal interaction between *unc-15* alleles and the UNC-82::GFP transgene *phEx22*, a chromosome containing the homozygous sterile mutation *gld-1(q485),* which is closely-linked to *unc-15*, was used to create balanced heterozygous *unc-15/gld-1(q485)* strains carrying the transgene *phEx22*.

Brood Analysis

The lethality of the transgenic array expressing UNC-82::GFP in animals homozygous for an *unc-15* mutation was tested by examination of all progeny in two one-day egg collections from a single balanced heterozygous hermaphrodite [*unc-15* +/+ *gld-*

1(q485) I; *phEx22*]. One day after removal of the parent hermaphrodite, unhatched eggs were moved to a small area of the plate and monitored for an additional two days. Similarly, Unc progeny were grouped and monitored for progress to adulthood. All dead/arrested or Unc animals were mounted on slides to score for the presence of the UNC-82::GFP transgene using fluorescence microscopy. All moving transgenic progeny, identified by the *rol-6* marker, were picked singly for genotyping: animals homozygous wild type at the *unc-15* locus [+ *gld-1(q485)/* + *gld-1(q485)* I; *phEx22*] are sterile with a tumorous germ line; *unc-15* heterozygotes [*unc-15* +/+ *gld-1(q485)* I; *phEx22*] segregate wild-type, Unc and tumorous germ line offspring.

Temperature Enhanced Phenotype Assay

The following strains were used to screen for temperature sensitive phenotypes by polarized light, anti-myosin A and anti-paramyosin: N2, CB1220 *unc-82(e1220)* IV, PZ218 and PZ219 *unc-82(gk205468)* IV and PZ220 and PZ221 *unc-82(gk718459gk718460)* IV. Eggs were harvested from gravid adults grown at both 15° (5 days) and 25° (2 days) via bleaching methods described by Stiernagle (2006). Eggs were placed on unseeded plates at the appropriate temperature to hatch overnight. Hatched animals were washed off the plates with M9, placed on large seeded plates, and incubated at either 15° or 25°. When cultures reached the young adult stage, animals were collected and fixed using the Nonet fixation method (Nonet *et al.*, 1993).

Microscopy

All worms were fixed using the Nonet method (Nonet *et al.*, 1993) and incubated in primary antibodies overnight at room temperature. Mouse monoclonal antibodies 5-6 (1:500 dilution), 5-8 (1:500 dilution), 5-23 (1:200 dilution), and rabbit polyclonal antibody EU131 (1:200) were used for immunofluorescence localization of myosin A, myosin B, paramyosin, and UNC-98 respectively (Miller *et al.,* 1983; Mercer *et al.*, 2003). Rabbit and mouse anti-GFP antibodies from Jackson ImmunoResearch Laboratories (West Grove, PA) were used at 1:250 dilution. Alexa Fluor 488- and 594-conjugated secondary antibodies from Jackson ImmunoResearch Laboratories were used at 1:400 dilutions. Worms were incubated in secondary antibodies for two hours. For staining of UNC-89 the mouse monoclonal MH42(1:200) and rabbit polyclonal EU30(1:200) were used (Benian *et al.* 1996). For staining of UNC-95, UNC-97, CPNA-1, PAT-6, UNC-112, and CSN-5 the following antibodies were used: Benian-13 (1:100), Benian-16 (1:100), anti-CPNA (1:100), anti-PAT-6 (1:100), anti-UNC-112 (1:100), anti-CSN-5 (1:100) (Benian *et al*. 1996; Hitika *et al*. 2005; Miller *et al.* 2006; Qadota *et al*. 2007; Warner *et al*. 2013; Miller *et al.* 2009). The polarized light microscopy procedures of Mackenzie *et al*. (1978) were followed. All images were acquired in ImagePro 6.0 (Rockville, MD) using a Retiga Exi Fast cooling mono12-bit Qimaging camera mounted to a Leica DM5500 microscope equipped with a polarizing lens. All images were processed using Adobe Photoshop CS6 software (San Jose, CA).

Nematode Strains

Unless otherwise noted, worm strains were maintained at 20° on nematode growth medium (NGM) plates seeded with the uracil mutant OP50 strain of *Escherichia coli* (Brenner, 1974).

Strains obtained from Guy Benian or the CGC: Bristol N2 [wild type]; CB1220 [*unc-82(e1220)* IV]; CB1323 [*unc-82(e1323)* IV]; CB73[*unc-15(e73)* I]; GB246 [*unc-98(sf19)* X]; HE75 [*unc-89(su75)* I]; CB1214 [*unc-15(e1214)* I]

Transgenic strains carrying fluorescently tagged wild-type UNC-82: PZ278 [*+; phEx22* (UNC-82::GFP)]; PZ238 [*unc-82(e1323); phEx22*]; PZ236 [*unc-98(sf19)* X*; phEx22*]; PZ237 [*unc-89(su75)* I*; phEx22*]; PZ240 [*unc-82(e1323*) IV; *unc-98(sf19)* X; *phEx22*]; PZ249 [*unc-89(su75)* I*; unc-82(e1323)* IV; *phEx22*]; PZ259 [*unc-15(e1214) +/+ gld-1(q485)* I; *phEx22*]; PZ279 [*unc-96(sf18)* X*; phEx22*]; PZ290 [*unc-15(e73) +/+ gld-1(q485)* I; *phEx22*]; PZ289 [*unc-15(su228) +/+ gld-1(q485)* I; *phEx22*].

Transgenic strains carrying fluorescently tagged E424K UNC-82: PZ169 [*+; phEx67* (E424K UNC-82::GFP)]; PZ171 [*unc-82(e1323)* IV*; phEx67*]; PZ176 [*unc-82(e1323)* IV*; phEx68* (E424K UNC-82::RFP)]

Transgenic strains carrying heat-shock-inducible paramyosin::GFP: PZ182 [*+; phEx70* (UNC-15::GFP)]; PZ187 [*unc-82(e1323)* IV*; phEx70*]; PZ190 [*unc-82(e1220)* IV*; phEx70*].

Missense *unc-82* mutations from the Million Mutation Project (MMP): The MMP created 2000 mutagenized *C. elegans* strains, each of which carries many unique mutations, and determined the genomic DNA sequence of these strains (Thompson *et al.,* 2013). From this collection, 22 lines carrying a missense mutation in *unc-82* were examined in Donald

Moerman's laboratory using polarized light microscopy, with the help of Teresa Rogalski. Two of these strains, VC40608 [*unc-82(gk718459 gk718460)*] and VC40253 [*unc-82(gk537592)*], have abnormal muscle structure, and both have a missense mutation within the UNC-82 kinase domain; VC40608 contains a second *unc-82* missense mutation outside the kinase domain. The strains VC40041 [*unc-82(gk205469)*] and VC40253 [*unc-82(gk537592)*] have a missense mutation in the kinase domain but have normal muscle structure. The remaining eighteen strains examined, which carry *unc-82* missense mutations outside the kinase domain, have normal muscle structure: VC20602 [*unc-82(gk350480)*], VC20766 [*unc-82(gk396209)*], VC40085 [*unc-82(gk455403)*], VC20628 [*unc-82(gk361893)*], VC30173 [*unc-82(gk430314)*], VC20724 [*unc-82(gk384013)*], VC30166 [*unc-82(gk428568)*], VC20233 [*unc-82(gk205474)*], VC40473 [*unc-82(gk654885)*], VC20013 [*unc-82(gk205476)*], VC40884 [*unc-82(gk864500)*], VC20779 [*unc-82(gk400373)*], VC20418 [*unc-82(gk205477)*], VC20013 [*unc-82(gk205482)*], VC20720 [*unc-82(gk382630)*], VC40847 [*unc-82(gk844906)*], VC20144 [*unc-82(gk205484)*], VC30024 [*unc-82(gk405473)*].

Outcrossing of MMP lines: To remove many background mutations and to randomize the background of remaining mutations, wild-type males were mated to each MMP line, and the resulting F1 males crossed again to wild-type hermaphrodites. Single F2 hermaphrodites from this cross were picked, and the F3 progeny examined by polarized light microscopy to identify wells segregating the *unc-82* mutation. Individual Unc animals were picked to establish 2X outcrossed lines. The process was repeated, and two independent 4X outcrossed lines isolated for each MMP allele: PZ218 and PZ219 [*unc-82(gk205468)* IV], and PZ220 and PZ221 [*unc-82(gk718459gk718460)* IV]. The mutational

changes reported for these MMP alleles were confirmed in the outcrossed lines by DNA sequencing.

All strains and reagents generated in this study are available upon request.

Results

Myosin and Paramyosin Distribution in *unc-82* Mutants

Adults homozygous for either of the *unc-82* mutant alleles *e1323* or *e1220* exhibit defects in thick filament and M-line organization when examined using polarized light and electron microscopy. In both mutants, TEM revealed abnormal, large-diameter filaments which, based on analysis of double mutants of *unc-82* with myosin B and paramyosin null mutations, were likely composed of paramyosin (Waterston *et al.,* 1980). Subsequent molecular analyses found that *e1323* is a presumptive null allele [*unc-82(0)*] containing a premature stop codon (Q403stop) within the kinase domain; in Q403stop homozygotes localization of myosin A, paramyosin and the large M-line protein UNC-89/obscurin in adult muscle was severely disrupted, with defects appearing during body elongation stages of embryogenesis (Hoppe *et al.,* 2010a). In contrast, the *e1220* allele was identified as a missense mutation E424K [*unc-82* E424K] that affects a highly conserved residue in the kinase catalytic domain, and therefore likely produces a full-length but catalytically-impaired protein product. The predicted UNC-82 protein contains over one thousand amino acids that are C-terminal to the kinase domain, but these sequences are poorly conserved among species, have no recognizable conserved domain, and their importance to UNC-82 function is not known (Hoppe *et al.,* 2010a). It was therefore of interest to examine the cellular phenotype of the E424K missense mutant and compare it to that of the null mutant.

In wild type, paramyosin and myosins A and B appear in stripes that are localized within the birefringent A bands, which mark the position of the myosin-containing thick filaments in striated body-wall muscle cells (Figure 2.1 A-F). Myosin A is restricted to the

center of the thick filament, and therefore myosin A stain appears in thin stripes that coincide with the position of the M-line, whereas myosin B appears more broadly in the A-band (see Introduction, compare Figure 1 C and E). In the presumptive *unc-82* null Q403stop mutant the staining for paramyosin, myosin A or myosin B coincides with amorphous birefringent patches that are distributed throughout the muscle cell (Figure 1 G-L), suggesting that these patches are disorganized thick filament accumulations that contain all three proteins. In *unc-82* E424K mutants, the overall disruption of muscle cell structure appears less severe than in the null (Figure 1 M-R; Waterston *et al.*, 1980). The polarized light phenotype of *unc-82* E424K shows more uniformly distributed birefringence throughout the body of the cell, and includes more areas that contain discernible striations than found in Q403stop animals. However, most E424K cells also contain small brightly birefringent accumulations at the ends of the spindle-shaped cells; these stain brightly for paramyosin (Figure 1 M-N). Paramyosin is weakly detected elsewhere in the body of these muscle cells. In contrast, myosins A and B are strongly detected throughout the disorganized contractile apparatus. The birefringent accumulations at the ends of muscle cells coincide with a portion of the myosin B stain in the cell. However, the accumulations at the ends of the muscle cell do not stain positive for myosin A. These results suggest that the presence of a full-length, catalytically-impaired UNC-82 protein leads to formation of distinctive abnormal structures at the ends of muscle cells. The birefringence of the structures indicates that they contain organized molecular assemblages. The intensity of the

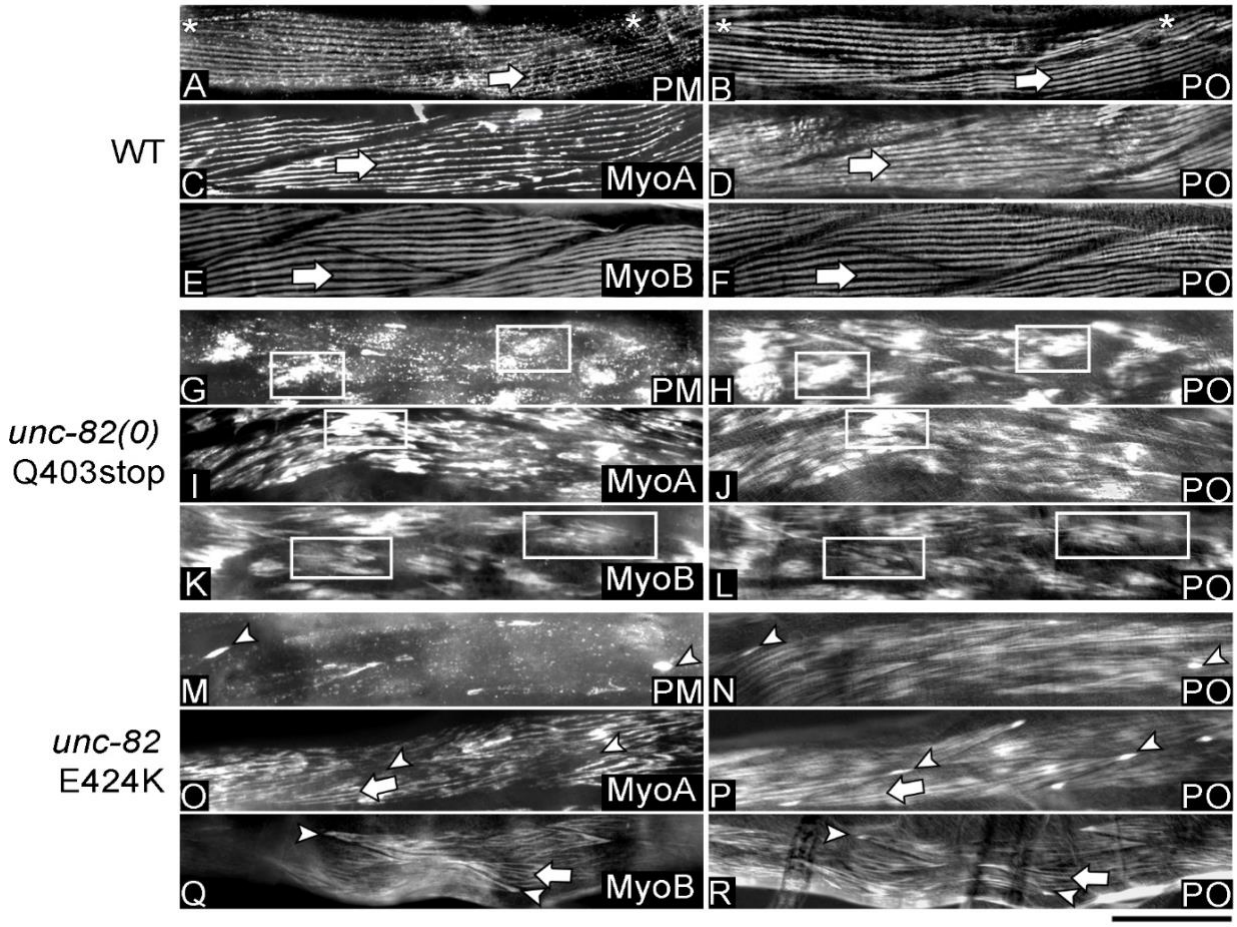

Figure 2.1: Thick filament components paramyosin, myosin A and myosin B have distinct subcellular distribution patterns in the *unc-82* null compared to the E424K missense mutant. **A-F.** In wild type, antibody staining of thick filament components appears in organized lines of signal. Paramyosin (PM) antibody stain (arrow in A) coincides with the birefringent A-bands visible by polarized light (PO) microscopy (arrow in B). Asterisks (A-B) mark the ends of a single spindle-shaped muscle cell. Myosin A (MyoA) staining (arrow in C) is found at the center of the A band (arrow in D). Myosin B (MyoB) staining (arrow in E) is localized more broadly in the A-band (arrow in F). **G-L**. Antibody stains in *unc-82(0)* [PZ96 *unc-82(e1323)*] mutants reveal amorphous patches of paramyosin (rectangles in G), myosin A (rectangle in I), and myosin B (rectangles in K) that coincide with the birefringent amorphous patches present in the polarized light micrographs (rectangles in H, J and L). **M-R**. Antibody staining of paramyosin in *unc-82* E424K [CB1220 *unc-82(e1220)*] worms shows that paramyosin accumulates at the ends of muscle cells in distinctive compact aggregates (arrowheads in M), which are also birefringent (arrowheads in N). Myosin A staining in E424K worms is localized to the disorganized A-bands (broad arrow in O and P) and is not detected in the distinctive birefringent accumulations at the ends of muscle cells (arrowheads in O and P). Myosin B stain in E424K is localized to the disorganized A-bands (broad arrow in Q and R) and the distinctive birefringent accumulations (arrow heads in Q and R). Scale bar is 20 microns

antibody stain suggests that a major component of the assemblages is paramyosin, with some myosin B also present.

The *unc-82(e1220)* E424K substitution introduces a charge change (negative to positive) in a highly conserved residue of the catalytic loop (Figure 2.2 A-B). An alanine substitution at this position in a yeast kinase reduced catalytic activity to 1.7% of wild type (Gibbs and Zoller, 1991). In structural studies of a transition state mimic, the homologous negatively-charged glutamic acid residue E170 of cAMP-dependent kinase (protein kinase A, PKA) forms a salt bridge with a positively-charged arginine in the peptide substrate (Madhusudan *et al.*, 2002). The lysine substitution in UNC-82 E424K changes this to an unfavorable interaction between two positive charges, which likely adversely affects binding of the catalytic loop with the substrate, delaying or preventing transfer of the phosphate group. The distinctive accumulations in this mutant might therefore be the result of disruption of this specific step in catalysis.

To determine whether other alterations in the UNC-82 kinase domain would result in similar distinctive paramyosin-containing accumulations, we used GExplore (Hutter *et al.,* 2009) to identify strains generated by the Million Mutation Project (MMP) (Thompson *et al.,* 2013) that contained novel *unc-82* mutations. Two of the four MMP strains that contained missense mutations within the kinase domain (VC20479, G456R; VC40608, S442P S969F) (see Materials and Methods) had a defective polarized light muscle phenotype. Both alleles are recessive and failed to complement *unc-82(0)*, confirming that the novel *unc-82* mutations in the MMP strains were responsible for the observed muscle defects. Both strains contain a substitution within the activation segment (Figure 2.2 A-B), a region that regulates substrate access to the catalytic cleft in a phosphorylation-dependent

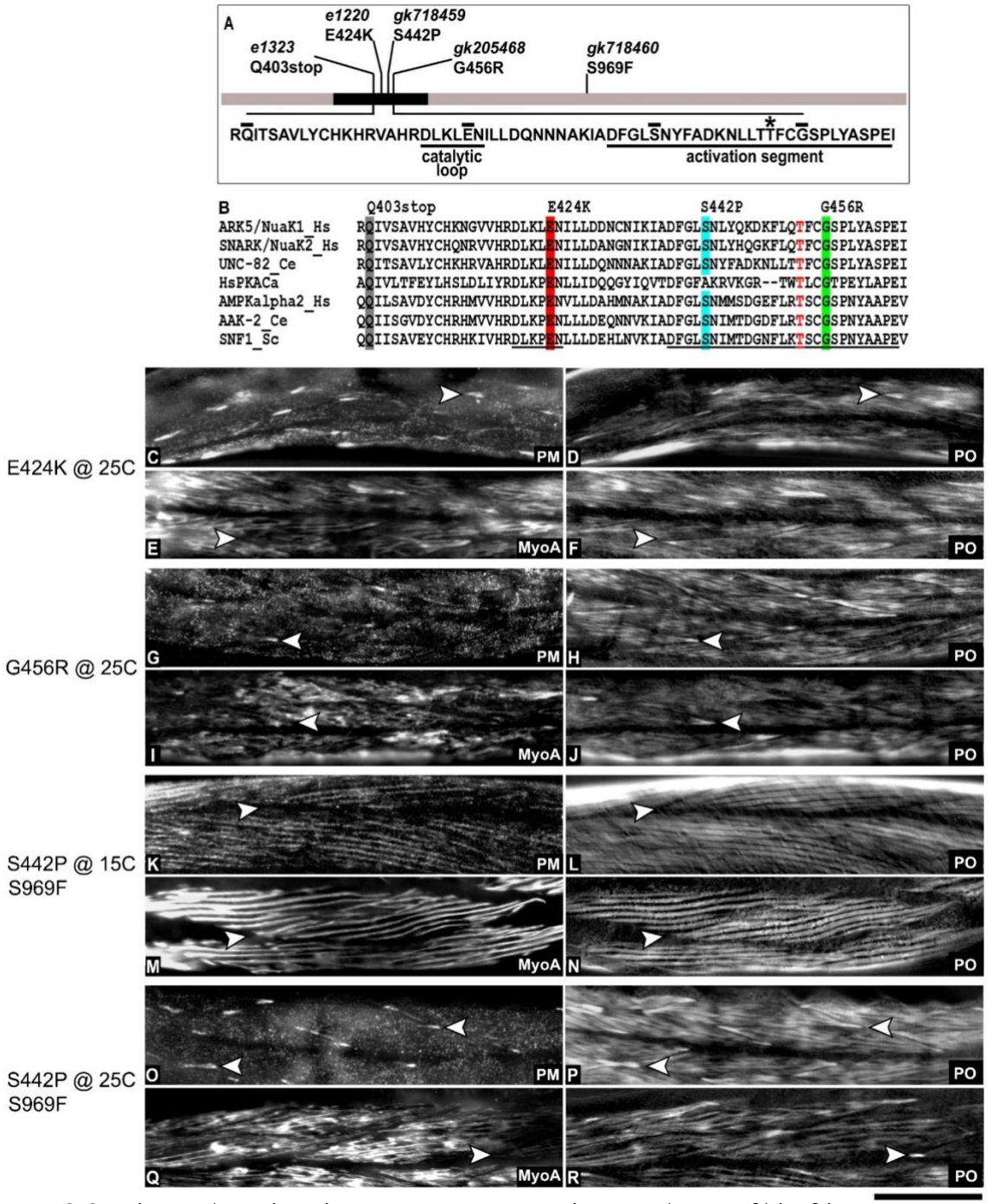

Figure 2.2: Kinase domain missense mutants vary in prevalence of birefringent paramyosin-containing accumulations at ends of muscle cells. **A.** The long rectangle represents the predicted 1817-amino-acid UNC-82 protein made from a hypothetical transcript that contains all 35 exons. The dark shading indicates the kinase domain. The positions of the nonsense and missense mutations used in this study are shown, giving the allele number and the resulting alteration in the protein sequence. The text below the rectangle shows the amino acid sequence of the portion of the kinase domain that contains four of the mutations; affected residues are marked with a bar above the letter.

The residues comprising the catalytic loop and activation segment (underlined), as well as the threonine in the activation segment that is phosphorylated in the active form of the enzyme (asterisk) were assigned by homology. **B.** A Clustal X alignment of protein kinase sequences in the portion of the catalytic domain that is affected in *unc-82* mutants shows the high conservation of affected residues (highlighted positions) in the catalytic loop and activation segment (underlined as in A), and the position of the threonine residue (red T) that is phosphorylated in the activated kinase. ARK5/NUAK1 and SNARK/NUAK2 are the human (Hs) orthologs of UNC-82. Homology to the human cAMP-dependent protein kinase (HsPKACa) sequence was used to define the residues within the catalytic loop and activations segment. The last three sequences are human, worm (Ce) and yeast (Sc) representatives from the closely related AMPK family . Paramyosin and myosin A staining in E424K (C-F) and G456R [PZ219 *unc-82(gk205468)*] worms (G-J) grown at 25° reveals distinctive birefringent accumulations that contain paramyosin but not myosin A at the ends of muscle cells (arrowheads) in both strains, but there are present in fewer cells in G456R. **K-N.** Paramyosin and myosin A staining of the temperature-sensitive mutant S442P S969F [PZ221 *unc-82(gk718456 gk718460)*] grown at 15° shows a near wild-type phenotype (K-N) while most cells in animals grown at 25°exhibit distinctive birefringent accumulations of paramyosin that do not stain for myosin A at the ends of muscle cells (arrowheads in O-R). Scale bar is 20 microns.

manner (reviewed in Johnson *et al.*, 2001; Huse and Kuriyan, 2002). The strain VC40608 contains a second missense mutation in the *unc-82* gene that is located outside the kinase domain (S969F, Figure 2.2 A) Because the residues outside the UNC-82 kinase domain are poorly conserved (Hoppe *et al.*, 2010a) it is unlikely that the second missense mutation is responsible for the observed muscle phenotype. Consistent with this proposal, examination of 18 other MMP strains that contain an *unc-82* missense mutation outside the kinase domain (see Materials and Methods) found that all have a normal polarized light muscle phenotype.

The two MMP strains that have abnormal muscle and a mutation in the activation segment were outcrossed four times to wild type (see Materials and Methods), and the

reported mutational changes in *unc-82* confirmed by DNA sequencing. Synchronized populations of the outcrossed novel mutants along with wild-type and E424K worms were grown at 15° and 25° (see Materials and Methods) and young adult animals examined using polarized light microscopy and antibody staining for paramyosin or myosin A. At 15° and 25°, most muscle cells in E424K worms contain birefringent accumulations that stain positive for paramyosin but not myosin A (Figure 2.2 C-F), similar to the results obtained at 20° (Figure 2.1, M-P). The G456R mutant had markedly disrupted patterns of myosin A and paramyosin staining at 15° and 25°, and contained some birefringent accumulations at muscle cell ends at both temperatures, but not in the majority of cells (Figure 2.2 G-J; data not shown). Where present, the accumulations contained paramyosin but not myosin A. The S442P S969F mutant is temperature sensitive, having a near wild-type phenotype at 15° (Figure 2.2 K-N), but resembling the E424K mutant at 25°, with paramyosin accumulations, which do not stain for myosin A, present in all cells (Figure 2.2 O-R). Even at 25°, the muscle cells of the S442P S969F mutant have some striations discernible by polarized light and myosin A stain in much of the cell body, and therefore this mutant appears less severe than the other activation segment mutant, G456R. The presence of distinctive paramyosin accumulations in these activation segment missense mutants indicates they are not specific to the E424K lesion. Because the E424K mutant has a high penetrance of paramyosin accumulations at all temperatures, it was chosen for fluorescent tagging experiments to elucidate the interaction of UNC-82 with paramyosin.

Mutant UNC-82 E424K Colocalizes with Abnormal Paramyosin Accumulations

To investigate the relationship between the E424K protein and the formation of the paramyosin -containing accumulations, transgenes expressing fluorescently tagged UNC-82 E424K were generated (see Materials and Methods) and examined in wild-type and *unc-82* mutant backgrounds. When expressed in the *unc-82* null mutant, the tagged E424K UNC-82 proteins reproduced the polarized light phenotype of the chromosomal E424K *unc-82(e1220)* allele, exhibiting brightly birefringent accumulations at the ends of muscle cells (Figure 2.3). Fluorescence microscopy of live animals revealed that the RFP-tagged E424K signal was concentrated in these birefringent accumulations (Figure 3 A-B). The E424K::GFP signal was also found in distinctive accumulations in the *unc-82* null background (Figure 2.3 C), indicating that the behavior was independent of the fluorescent tag. In a wild-type background, the E424K::GFP signal appeared at the M-line (Figure 2.3 D), the pattern typical of the wild-type UNC-82::GFP fusion (Hoppe *et al.*, 2010a), indicating that the presence of wild-type UNC-82 protein allowed normal localization of the GFP-tagged mutant protein. Similarly, wild-type UNC-82::GFP expressed from the extrachromosomal transgene *phEx22* rescued the muscle phenotype of the genomic *unc-82(e1220)* allele, which contains the E424K substitution (data not shown). The significance of the nuclear UNC-82::GFP signal (Figure 2.3 D) is not known but is seen with both wild-type UNC-82::GFP and E424K::GFP. Interestingly, nuclear localization has also been reported for the zinc-finger-containing M-line protein UNC-98/ZnF (Mercer *et al.*, 2003). The mammalian UNC-82 orthologs exhibit nuclear localization under conditions of stress (Kuga *et al.*, 2008; Hou *et al.*, 2011).

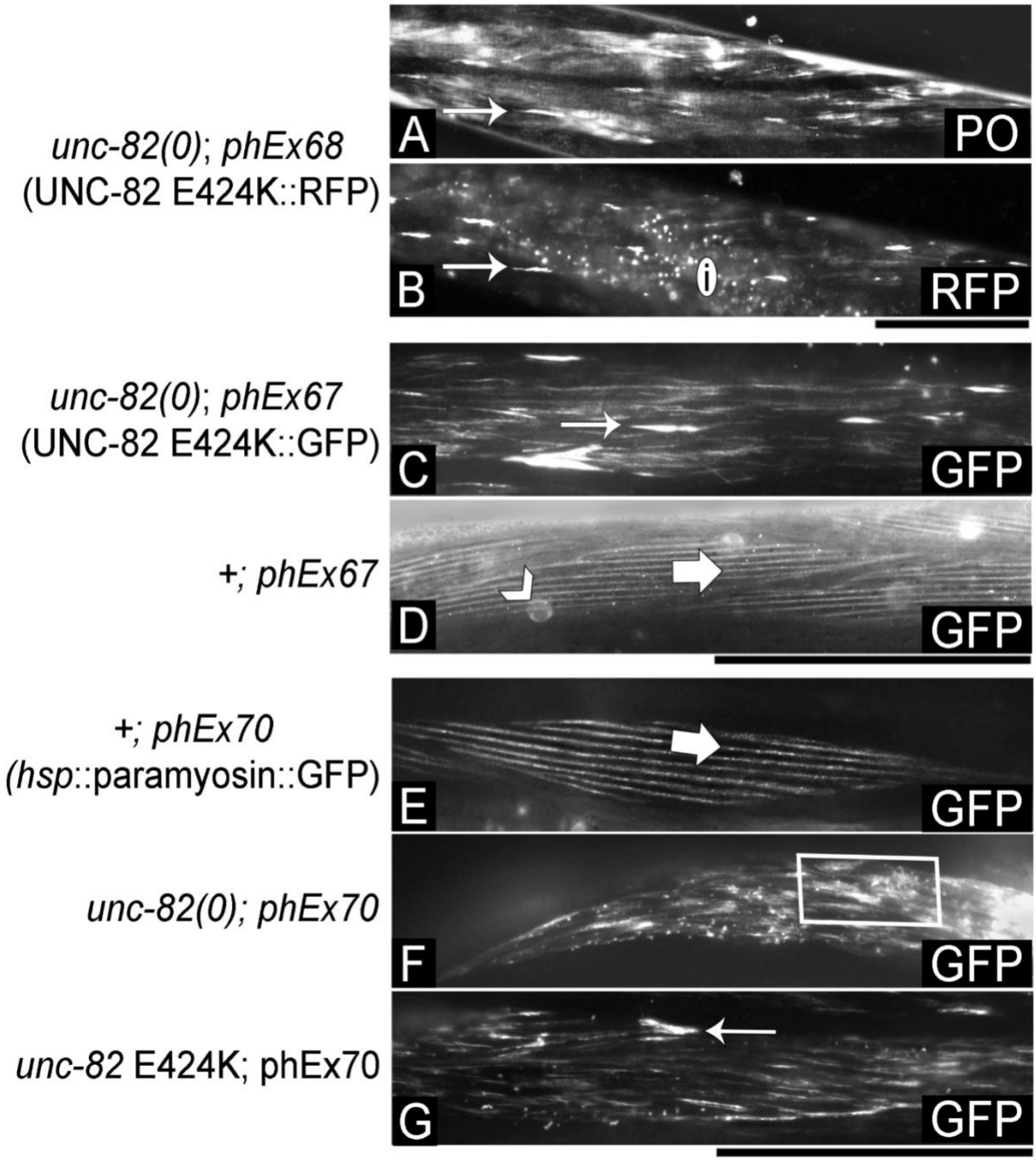

Figure 2.3: UNC-82 protein containing the E424K substitution localizes to the distinctive paramyosin accumulations, which also label with recently synthesized paramyosin. **A-B**. Live worms expressing the mutant UNC-82 E424K::RFP protein in the *unc-82(0)* background [PZ176 *unc-82(e1323);phEx68*] contain birefringent aggregates at the ends of muscle cells (arrow in A), similar to those present in the strain homozygous for the genomic missense E424K mutation *unc-82(e1220)*. UNC-82 E424K::RFP co-localizes with the distinctive birefringent aggregates (arrow in B). The intestine (i) contains round autofluorescent granules. **C.** The UNC-82 E424K protein tagged with GFP

accumulates in distinctive aggregates (arrow in C) in an *unc-82* null mutant background [PZ171 *unc-82(e1323); phEx67*]. **D**. The signal from the same UNC-82 E424K::GFP transgene in a wild-type background [PZ169 *+;phEx67*] is present at the M-line (broad arrow in D) and in the nucleus (chevron in D). **E-G.** Paramyosin::GFP expressed following heat shock goes to the M-line (broad arrow in E) in wild-type worms [PZ182 *+; phEx70*], is disorganized (rectangle in F) in *unc-82* null mutants [PZ187 *unc-82(e1323); phEx70*], and joins distinctive accumulations at the ends of muscle cells (arrow in G) in the E424K mutant [PZ190 *unc-82(e1220); phEx70*]. Scale bars are 20 microns

The colocalization of paramyosin and the mutant UNC-82 E424K protein in the distinctive accumulations suggests that the two proteins physically interact during assembly of the thick filament, and that loss of UNC-82 catalytic activity leads to aggregation of both proteins. If so, wild-type UNC-82 may have chaperone-like activity that promotes proper entry of soluble paramyosin into the thick filament. To test whether UNC-82 influences the localization of recently synthesized paramyosin, an unstable transgenic array in which expression of paramyosin::GFP is driven by a heat shock promoter was generated and crossed into wild type and *unc-82* mutants. Transgenic young adult animals were heat shocked at 30° for 5 hours, and fluorescent images taken within 15 minutes of treatment. In wild type, the paramyosin::GFP fusion protein appeared in stripes at or near the M-line (Figure 2.3 E; Miller *et al.*, 2008). In the *unc-82(0)* background, paramyosin::GFP was seen in a patchy distribution throughout the muscle cell (Figure 2.3 F). In the *unc-82* E424K mutant, some GFP signal was detected in longitudinal stripes that may be abnormal M-lines, while bright signal was seen in distinctive accumulations at the ends of muscle cells (Figure 2.3 G). These observations are consistent with the hypothesis that newly synthesized paramyosin physically associates with UNC-82, and that this complex localizes to the M-

line in wild type, but in distinctive accumulations at the ends of muscle cells in the UNC-82 E424K mutant.

Over Expression of UNC-82 in Paramyosin Mutants

To test the hypothesis that wild-type UNC-82 associates with paramyosin to promote proper assembly, we examined the subcellular localization of wild-type UNC-82::GFP in the paramyosin missense mutant *unc-15(e73).* This mutant contains large needle-like birefringent paramyosin-containing aggregates that are thought to form due to increased affinity of paramyosin for itself (Gengyo-Ando and Kagawa, 1991). The paramyosin *e73* mutation is semi dominant: heterozygotes exhibit slow movement and smaller birefringent aggregates, whereas *e73* homozygotes move very poorly and have prominent aggregates (Waterston *et al.*, 1977). If UNC-82 binds to paramyosin to promote entry into the thick filament, we might expect expression of UNC-82::GFP in the *e73* mutant to reduce the size of the aggregates and improve motility. Increased expression of myosin A has been shown to dramatically suppress the *e73* phenotype by increasing incorporation of mutant paramyosin into normal thick filaments (Riddle and Brenner, 1978; Otsuka, 1986; Hoppe and Waterston, 2000). An extrachromosomal array expressing wild-type UNC-82::GFP (*phEx22*) and carrying the coinjection marker *rol-6* was crossed to *e73* homozygotes. Repeated attempts to obtain a strain that carried the transgene in a homozygous *e73* background were not successful. The transgene, which restores muscle structure in *unc-82(e1323)* mutant worms (Hoppe *et al.*, 2010a), appeared to increase the severity of the movement defect in *e73* heterozygotes.

To better analyze the interaction of increased UNC-82 expression with the paramyosin *e73* mutation, the UNC-82::GFP (*phEx22*) transgene was crossed into a heterozygous line in which *e73* is balanced by a closely linked *gld-1* mutation on the opposite chromosome [PZ290 *unc-15(e73) +/+ gld-1(q485)* I; *phEx22*]. Examination of transgenic progeny revealed that over expression of UNC-82 increased severity of the polarized light muscle phenotype in *e73* heterozygotes and resulted in lethality or developmental arrest in *e73* homozygotes (Figure 2.4). Muscle cells in transgenic heterozygotes contained larger birefringent aggregates than heterozygotes without the transgene, and UNC-82::GFP localized to these aggregates (Figure 2.4 F-H). Wild-type animals carrying the transgene did not contain abnormal birefringent aggregates, although small accumulations of GFP signal were seen outside the contractile apparatus (Figure 2.4 A-B). Enhancement of aggregate formation by over expression of UNC-82 was also observed in animals heterozygous for another missense paramyosin mutation, *su228* [PZ289 *unc-15(su228) +/+ gld-1(q485)* I; *phEx22*]. The s*u228* allele contains an arginine to cysteine substitution near the paramyosin C-terminus (Gengyo-Ando and Kagawa, 1991). Whereas *unc-15(su228)/+* heterozygotes rarely contain birefringent aggregates at the ends of cells, transgenic heterozygotes contained prominent aggregates, most of which colocalized with GFP signal (Figure 2.4 I-K). Therefore, rather than promoting incorporation of mutant paramyosin into normal filaments, increased levels of UNC-82 led to larger aberrant accumulations that contain UNC-82. Interestingly, transgenic animals heterozygous for the paramyosin null mutation [PZ259 *unc-15(e1214) +/+ gld-1(q485)* I*; phEx22*] also had a small number of birefringent accumulations at the end of the cells whereas nontransgenic heterozygotes do not (Figure 2.4 C-E). However, in these animals, no GFP signal was detected on the accumulations.

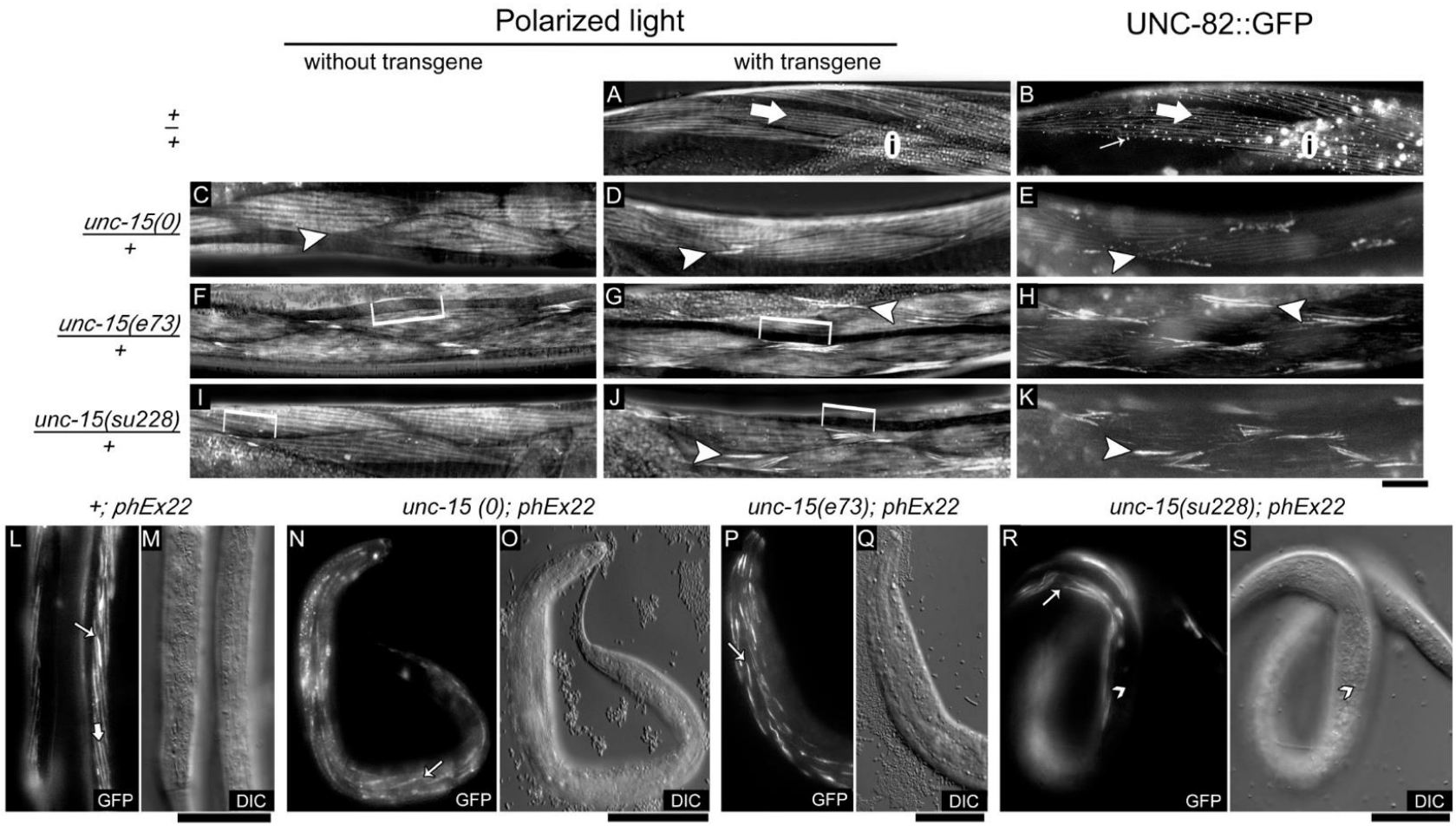
Polarized light
UNC-82::GFP
without transgene
with transgene
+/+
unc-15(0)/+
unc-15(e73)/+
unc-15(su228)/+
A
B
C
D
E
F
G
H
I
J
K
+; phEx22
unc-15 (0); phEx22
unc-15(e73); phEx22
unc-15(su228); phEx22
L
M
N
O
P
Q
R
S
GFP
DIC

Figure 2.4: Over expression of UNC-82 increases the severity of phenotypes in paramyosin mutant heterozygotes and homozygotes. **A-B**. Polarized light microscopy of a live wild-type animal expressing UNC-82::GFP [PZ278+*; phEx22*] reveals wild-type muscle (compare with Figure 1 F) with defined A bands and no ectopic aggregates. Fluorescence microscopy of this animal shows UNC-82::GFP localized to the M-line (broad arrow in B) and in small round ectopic accumulations (thin arrow in B). The intestine, with larger autofluorescent granules, is labeled (i). **C-E.** Muscle cells in *unc-15(0)/+* heterozygotes have near-normal muscle with decreased birefringence at muscle cell ends (arrowhead in C). Expression of UNC-82::GFP in *unc-15(0)/+* results in brightly birefringent accumulations at the ends of some cells; these accumulations do not strongly label with UNC-82::GFP (arrowheads in D and E). **F-H.** Animals heterozygous for the semidominant missense paramyosin mutant *e73* have bright birefringent accumulations at the ends of muscle cells (F). The accumulations are larger in *e73* heterozygotes that carry the UNC-82::GFP transgene (brackets in F and G), and UNC-82::GFP colocalizes with the birefringent structures (arrowheads in G and H). **I-K**. Animals heterozygous for the paramyosin missense mutant *unc-15(su228)* occasionally have small birefringent accumulations at muscle cell ends (I). The accumulations are enhanced in size and prevalence in an *su228* heterozygote expressing UNC-82::GFP (brackets in H and K). UNC-82::GFP colocalizes with the birefringent structures. **L-M.** In early larval stages UNC-82::GFP expressed in wild-type worms is visible in the muscle in stripes and in some accumulations (arrows in L). The corresponding DIC image shows the normal un-kinked hatched larval phenotype (M). **N-O.** This arrested transgenic *unc-15(0)* homozygote shows unorganized UNC-82::GFP signal and a kinked body phenotype. **P-Q.** The head portion of a later-stage arrested *e73* larva shows bright defined accumulations of UNC-82::GFP. **R-S.** This arrested *su228* transgenic homozygote has disorganized UNC-82::GFP signal with areas of apparent muscle detachment, which may account for the kinked body phenotype (chevron in R and S). Scale bars are 5 microns

Therefore, in addition to increasing severity of defects in animals heterozygous for paramyosin missense mutants, increased UNC-82 expression also leads to birefringent accumulations in cells where levels of wild-type paramyosin have simply been reduced. The protein composition of the accumulations in the latter case is not known, but the accumulations do not colocalize with UNC-82 signal.

For all three *unc*-15 alleles, expression of UNC-82::GFP in mutant homozygotes produced lethality or developmental arrest, as determined by brood analysis of transgenic balanced heterozygotes (see Materials and Methods) (Table 2.1). All control nontransgenic heterozygous parent hermaphrodites produced viable Unc progeny (*unc-15* homozygotes) in numbers that were close to the expected 25% proportion based on a Mendelian genotypic ratio of 1:2:1. A small percentage of progeny from nontransgenic *unc-15(e1214)*/+ and *unc-15(su228)*/+ hermaphrodites were scored as dead/arrested (3.6% and 1.8%): all of these were

Table 2.1 Over Expression of UNC-82 Increases the Severity of Paramyosin Mutant Phenotypes

GENOTYPE OF PARENT	**PHENOTYPE OR GENOTYPE OF PROGENY**			
	Unc	+/+	*unc-15*/+	Dead/arrested
e1214/+	25 (18.1%)	30 (21.7%)	78 (56.5%)	4 (3.6%)[a]
e1214/+; phEx22	10 mosaic (5.3%)	42 (22.2%)	89 (47.1%)	48 (25.4%)[a b]
e73/+	32 (19.2%)	59 (35.5%)	75(45.2%)	0 (0%)
e73/+; phEx22	4 mosaic (2.9%)	30 (21.6%)	66 (47.5%)	39 (28.1%)[a b]
su228/+	48 (29.4%)	37 (22.7%)	78 (47.9%)	3 (1.8%)[a]
su228/+; phEx22	1 (1%) 1 mosaic (1%)	28 (29.8%)	53 (56.4%)	14 (14.7%)[b c]

Table 2.1 Each of the three *unc-15* alleles tested was maintained in a balanced strain *unc-15* +/+ *gld-1* with or without the *phEx22* UNC-82::GFP extrachromosomal array. The genotype of the parent hermaphrodite of a given brood is given in the first column. The phenotypes and *unc-15* genotypes scored in each brood are listed in the first row. Each subsequent row contains counts of a brood from a single hermaphrodite, with the percentage of the total progeny from that brood given in parentheses. In control (nontransgenic) broods, all progeny were counted and scored. In broods from transgenic hermaphrodites, only transgenic progeny were included in the analysis (see Materials and Methods). The recessive *gld-1(q485)* mutation is closely linked to *unc-15* (0.2 map units). Progeny homozygous for *gld-1*, which are sterile with a tumorous germ line, were scored as the *unc-15* genotype of +/+. The dead/arrested class includes any animals that did not survive to adulthood. Mosaic animals were those that did not have the unstable transgene expressing UNC-82::GFP in all muscle cells. a: arrested worms elongated in the egg shell but failed to hatch. b: worms hatched but arrested in larval stages, many were kinked or folded. c: eggs that did not develop to the two-fold stage of body elongation were not counted

elongated embryos that failed to hatch. In contrast, transgenic hermaphrodites carrying the UNC-82::GFP array had a decrease in the number of viable Unc offspring with a concomitant increase in the dead/arrested class. Most died as unhatched elongated larvae. Of those that arrested at later developmental stages, the majority had abnormal body elongation and/or kinked morphology, consistent with muscle contraction and attachment defects (see Introduction). A few transgenic *unc-15* homozygotes survived to adulthood. Most were mosaic animals in which UNC-82::GFP was expressed in a subset of the animal's muscle cells.

The UNC-82::GFP signal in arrested larvae homozygous for either missense allele appeared in bright, defined accumulations (Figure 2.4 P-R) like those found in the transgenic heterozygous adults (Figure 2.4 H and K). In contrast the UNC-82::GFP signal in arrested *unc-15(0)* larvae was more diffuse (Figure 2.4 N). Surviving *unc-15(0)* adults that expressed UNC-82::GFP in a subset of muscle cells allowed examination of cell phenotype by polarized light microscopy. In these mosaics (Figure 2.5 A-B), the cells that expressed UNC-82::GFP had irregularly shaped accumulations of GFP signal at the ends of cells, with little GFP signal in the cell body. The GFP-positive cells contained large round birefringent structures that are not typically found in the paramyosin null mutant; these structures were not strongly GFP-positive (Figure 2.5 A-B). Because paramyosin is absent, these structures may arise from aggregation of one or more other muscle proteins during filament assembly, or the later collapse of the contractile apparatus. The observation that transgenic *unc-15(0)*/+ hermaphrodites (Figure 2.4 D) contain birefringent accumulations that are not GFP positive in an otherwise well-ordered cell is consistent with the aggregation model. These results suggest that the stoichiometric relationship between paramyosin and UNC-82 is critical for

proper muscle cell structure, and that the imbalance affects additional proteins other than paramyosin and UNC-82.

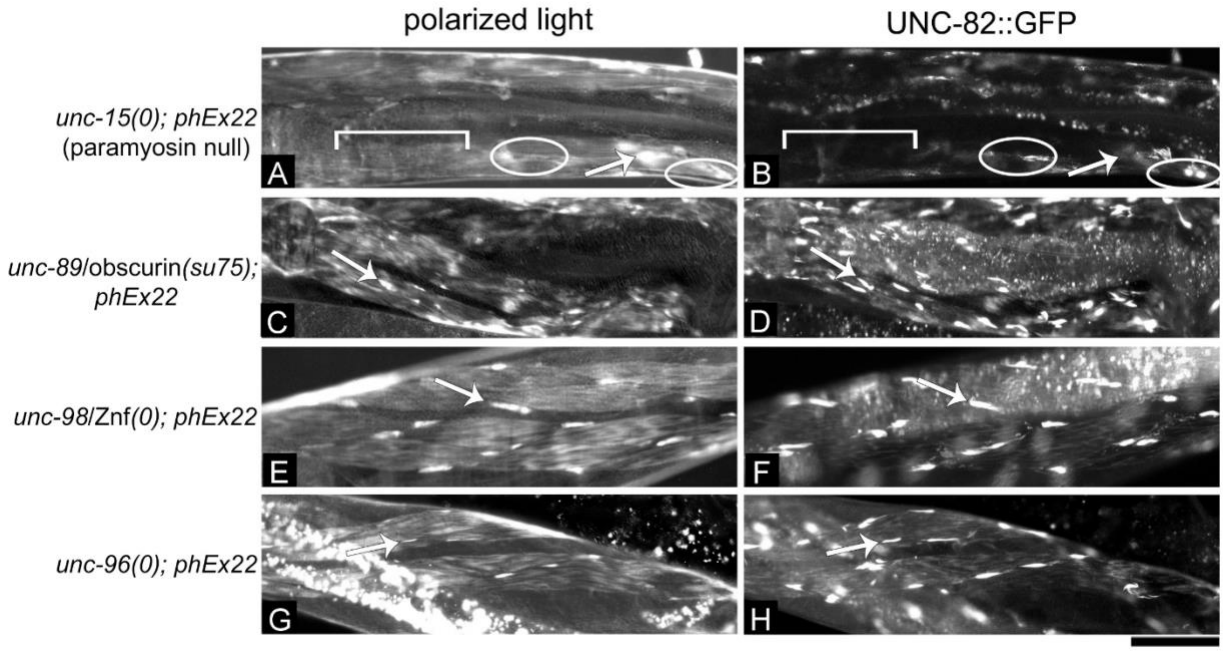

Figure 2.5: UNC-82::GFP localization is affected in mutants that have abnormal paramyosin distribution**. A-B.** An adult escaper homozygous for the paramyosin null mutation and carrying the unstable UNC-82::GFP transgene is a mosaic. Cells lacking paramyosin and expressing UNC-82::GFP contain large birefringent aggregates (arrow in A) that do not coincide with bright GFP signal (arrow in B). Bright GFP signal is found in abnormal accumulations at the ends of cells (ovals in B) where some birefringence is also detected (ovals in A). Cells that do not express UNC-82::GFP (bracket in B) show the uniform, diffuse birefringent signal typical of *e1214* null mutant animals (bracket in A). **C-H**. UNC-82::GFP signal colocalizes with the birefringent paramyosin-containing aggregates at the ends of muscle cells in live adults from strains homozygous for a mutation affecting an M-line protein: UNC-89/obscurin [PZ237 *unc-89(su75)* I*; phEx22*] (C-D); UNC-98/ZnF [PZ236 *unc-98(sf19)* X*; phEx22*] (E-F); UNC-96 [PZ279 *unc-96(sf18)* X*; phEx22*] (G-H). Scale bar is 20 microns

Interaction Between Accumulated Paramyosin and UNC-82 does not Require UNC-96, UNC-98/ZnF, UNC-89/obscurin, Myosin A or Myosin B

The recruitment of UNC-82::GFP to the abnormal aggregates in the paramyosin missense mutant *e73* (Figure 2.4 G-H) is consistent with a physical interaction between UNC-82 and paramyosin. However, because the *e73* aggregates also stain positive for myosin B, and perhaps for myosin A and UNC-89/obscurin (Epstein *et al.,* 1987; Gengyo-Ando and Kagawa, 1991; Qadota *et al.,* 2016) the interaction between UNC-82 and paramyosin might be indirect. We therefore obtained other mutant strains that have ectopic paramyosin accumulations of differing composition. Paramyosin aggregates that do not stain for either myosin A or B are found in *unc-96* mutants (where aggregates also lack UNC-96), in *unc-98* mutants (where aggregates also lack UNC-98/ZnF), and in *unc-89(su75)* (where aggregates also lack UNC-89/obscurin). Interestingly, like the accumulations in *unc-82* missense mutants, the paramyosin accumulations in *unc-96*, *unc-98*/ZnF, and *unc-89(su75)*/obscurin mutants reside at the ends of the muscle cells (Mercer *et al*., 2006; Miller *et al*., 2008; Qadota *et al.,* 2016). The extrachromosomal transgene *phEx22* expressing UNC-82::GFP was crossed into these mutant lines. All three strains were viable and fertile, and in all three UNC-82::GFP colocalized with the ectopic birefringent structures (Figure 2.5 C-H).

Taken together, these data indicate that recruitment of UNC-82 to paramyosin aggregates does not require UNC-96, UNC-98/ZnF, or myosins A or B individually. The three transgenic mutant strains were examined to determine if over expression of UNC-82 altered the muscle phenotype, as it did in the three paramyosin mutants (Figure 2.4). Expression of UNC-82::GFP in the *unc-98(sf19)*/ZnF mutant animals caused no obvious difference in movement or in the morphology of paramyosin aggregates compared to those of the *unc-*

98/ZnF mutant alone (data not shown). The expression of UNC-82::GFP in the *unc-89*/obscurin and *unc-96(sf18)* mutants, which move more slowly than *unc-98*/ZnF mutants, appeared to increase the severity of the movement defects. Because of the unstable nature of the transgene and the abnormal rolling locomotion caused by the *rol-6* marker, quantitative assessment of the decrease in locomotion was not attempted.

Analysis of Double Mutants of *unc-82* with Other Paramyosin-Affecting Mutations

The detrimental effect of increasing UNC-82 expression in the paramyosin missense mutant *e73* is consistent with previous reports that the double mutant containing *e73* and *unc-82(0)* moved better than the *e73* single mutant, and that the appearance of the paramyosin aggregates was altered in doubles with either the *unc-82* null or the missense allele E424K (Waterston *et al.,* 1980; Brown and Riddle 1985). We therefore reisolated the double mutant strains and examined the muscle phenotype by polarized light microscopy. The double mutant *e73; unc-82* E424K [PZ267 *unc-15(e73)* I; *unc-82-e1220)* IV] contained birefringent accumulations at the ends of cells that more closely resembled those found in the *unc-82* mutant rather than the longer defined needles characteristic of *e73* (Figure 2.6 A-F). Similarly, the *e73; unc-82(0)* double [PZ263 *unc-15(e73)* I; *unc-82(e1323)* IV] more closely resembled *unc-82(0)* alone, containing patchy disorganized birefringence and none of the large needle-like accumulations characteristic of *e73* (Figure 2.6 B). The observation that the *e73; unc-82(0)* double mutant has improved movement, rather than an additive more severe phenotype, suggests that the two genes act in a single pathway to organize paramyosin, and that UNC-82 protein promotes paramyosin aggregate formation in the *e73* mutant.

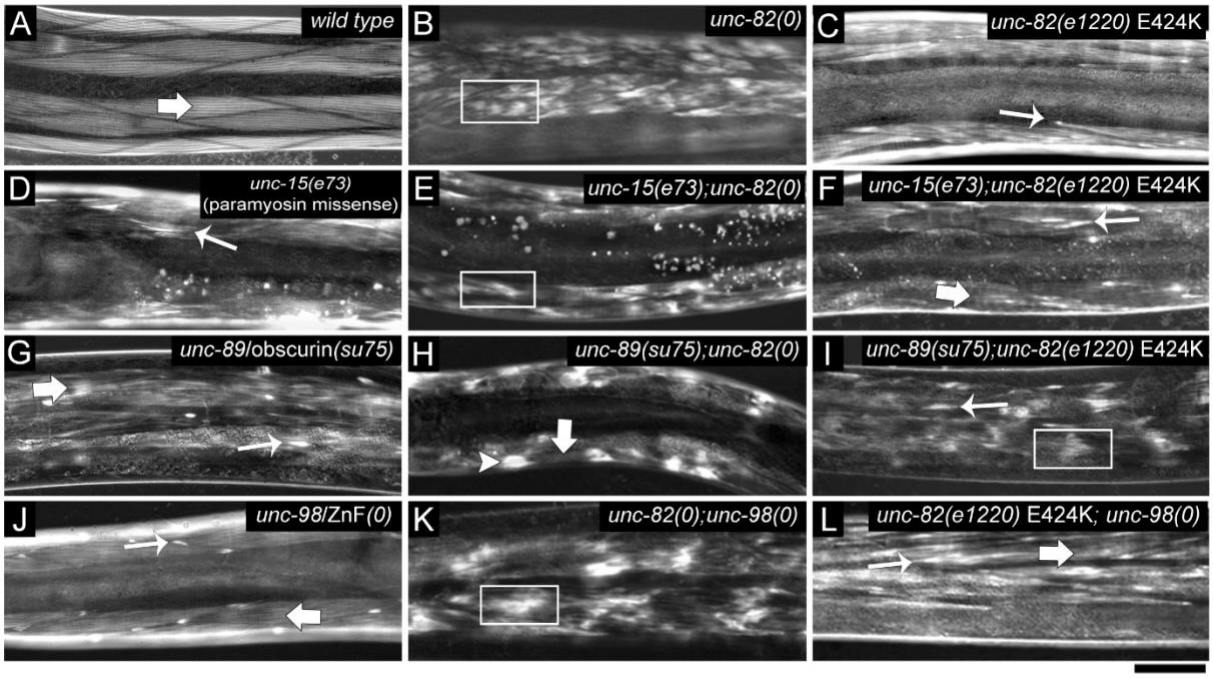

Figure 2.6: Distinct polarized light muscle phenotypes are observed in double mutants of *unc-82* with other mutations that produce paramyosin aggregates. **A.** Wild-type body-wall muscle contains highly regular longitudinal birefringent A-bands (broad arrow). **B.** Worms homozygous for the *unc-82(0)* mutation contain irregular amorphous patches of birefringent material (rectangle). **C.** The missense *unc-82* mutant E424K has brightly birefringent accumulations at the ends of cells (arrow) and, compared to the null mutant, a more uniform distribution of disorganized birefringence in the rest of the cell. **D.** The paramyosin missense mutant *e73* contains large birefringent needles (arrow) and has reduced, unpatterned birefringence in the rest of the cell. **E**. Double mutants homozygous for the missense paramyosin and *unc-82* null mutations [PZ263 *unc-15(e73)* I*; unc-82(e1323)* IV] exhibit patchy birefringence and no needles (rectangle), resembling *unc-82(0)* (compare to B), but are thinner in body width. **F.** Double mutants homozygous for the missense paramyosin and *unc-82* E424K mutations [PZ267 *unc-15(e73)* I*; unc-82(e1220)* IV] have reduced overall birefringence with little organization (broad arrow), and bright accumulations, which lack the definition of the *e73* needles, at the ends of cells (arrow in F). **G**. The *unc-89/*obscurin mutant exhibits bright accumulations at the ends of cells (thin arrow) and reduced, poorly patterned signal in the rest of the cell (broad arrow). **H**. Cells in an *unc-89; unc-82(0)* double mutant that segregated from a strain in which *unc-82* is rescued with an unstable transgene [PZ249 *unc-89(su75)* I; *unc-82(e1323)* IV*; phEx22*] exhibit an enhanced phenotype with large round brightly birefringent accumulations (arrowhead) and little signal in the rest of the cell (broad arrow). **I**. The double mutant of *unc-89/*obscurin with *unc-82* E424K [PZ245 *unc-89(su75)* I*; unc-82(e1220)* IV] is more severe than either mutant alone, with bright accumulations at ends of cells (arrow) and patchy birefringence (rectangle) in the rest of the cell. **J**. The *unc-98(sf19)/* ZnF mutant [GB246] has bright accumulations at the ends of cells (thin arrow) with faint but

relatively well organized A bands (broad arrow) in the rest of the cell. **K**. The double mutant of *unc-98/* ZnF and *unc-82(0)* [PZ240 *unc-82(e1323)* IV*; unc-98(sf19)* X] has amorphous patches of birefringence (rectangle) and no bright accumulations, resembling *unc-82(0)* mutants (compare to B). **L**. Double mutants carrying *unc-98/* ZnF and *unc-82* E424K [PZ250 *unc-82(e1220)* IV*; unc-98(sf19)* X] have bright accumulations at end of cells (small arrow) and disorganized signal in the rest of the cell (broad arrow), resembling the *unc-82* E424K single (compare to C). Scale bar is 20 microns

To test the interaction of *unc-82* with mutations in other genes that result in formation of prominent paramyosin aggregates, double mutant strains of *unc-82* with *unc-89/*obscurin and *unc-98/* ZnF were obtained by genetic crossing (see Materials and Methods). The double of *unc-82(0)* with *unc-89(su75)/*obscurin is sterile, and has a muscle cell phenotype unlike that of either single mutant. The muscle phenotype of the double mutant was studied by constructing a double mutant strain in which *unc-82* is rescued by an unstable transgene expressing UNC-82::GFP [PZ249 *unc-89(su75)* I*; unc-82(e1323)* IV*; phEx22*] and examining progeny that had lost the transgenic array. Muscle cells in these worms lacking UNC-82::GFP had little birefringent signal outside of large round accumulations in the middle of the cell (Figure 2.6 H). To examine the sterile phenotype, single non-rolling adults were picked from this strain. Some of these animals were likely mosaics that had lost the UNC-82::GFP transgene in the epidermis (where the *rol*-6 marker is expressed) but retained the transgene in other cells. Most animals (7 out 12) produced no eggs. The gonad was often grossly abnormal or absent, and in a few, a round clear internal "bubble" of unknown origin was present in the posterior of the animal. The maximum number of progeny produced by a single adult was 29, and the median number was four. The few progeny that were produced

had variable defects, including severe Unc, and dumpy and folded morphologies. None of the progeny were fertile. The double of *unc-89*/obscurin and *unc-82* E424K [PZ245 *unc-89(su75)* I*; unc-82(e1220)* IV] is viable, but has reduced body size, decreased motility, and lower fecundity. The muscle showed an additive polarized light phenotype with patchy birefringence in the cell body and bright birefringent accumulations at the ends of cells (Figure 2.6 I).

In contrast, the doubles of either the *unc-82* null or E424K missense mutation with the presumptive null allele *unc-98(sf19)*/ZnF were viable and fertile, and had polarized light muscle phenotypes similar to those of the *unc-82* mutations alone (Figure 2.6 J-L). The distinctive paramyosin accumulations characteristic of *unc-98*/ZnF were absent in the double with the *unc-82(0)* as determined by polarized light microscopy (Figure 2.6 K) and antibody staining (Figure 2.7 A-C). Brightly birefringent accumulations are found in both single mutants *unc-82* E424K and *unc-98(0)*/ZnF. The double mutant exhibited bright accumulations as well as the more disorganized contractile apparatus characteristic of the *unc-82* missense mutant (Figure 2.6 L). Antibody staining of this double revealed accumulations that contain paramyosin and myosin B (Figure 2.7 D-F), a property of accumulations in the E424K single mutant, but unlike those in the *unc-98*/ZnF single, which do not stain for myosin B. The presence of "*unc-82*-like" accumulations in the double, along with the more severe disorganization of the contractile apparatus in *unc-82(0)* compared to *unc-98(0)*/ZnF, suggests that *unc-82* may act upstream of *unc-98*/ZnF in a single pathway that organizes paramyosin, or that *unc-82* acts in a pathway that affects a larger portion of the paramyosin pool than the *unc-98*/ZnF pathway.

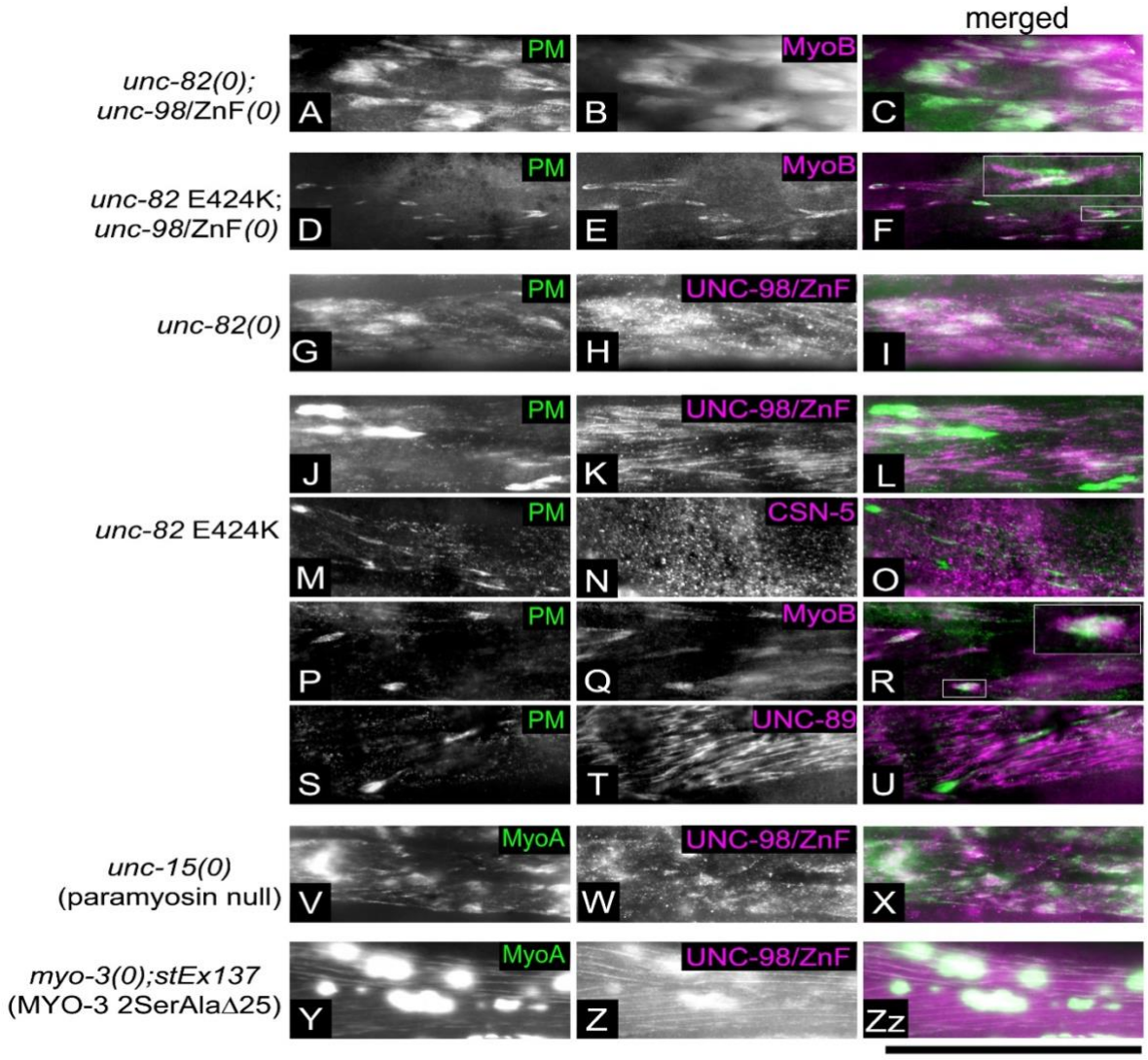

Figure 2.7: Protein composition of muscle cell aggregates investigated by immunostaining. **A-C**. Animals homozygous for presumptive null mutations in both *unc-82* and *unc-98*/ZnF resemble the *unc-82* single, exhibiting patchy paramyosin and myosin B stain with no distinct accumulations at muscle cell ends. **D-F**. The double mutant of *unc-98*/ZnF null with the missense *unc-82* mutation, resembles the *unc-82* E424K single having little paramyosin stain in the contractile apparatus and bright accumulations, which also stain for myosin B, at the ends of cells (P-R). The paramyosin and myosin B stains overlap in the accumulations but are not completely coincident (inset). **G-I**. UNC-98/ZnF colocalizes with paramyosin stain in some areas of the muscle cells in *unc-82(0).* **J-U**. Ectopic accumulations of paramyosin in *unc-82* E424K do not stain with UNC-98/ZnF, CSN-5 or UNC-89/obscurin but are positive for myosin B. **V-X.** In the absence of paramyosin, myosin A and UNC-98/ZnF stains overlap in areas of the disorganized contractile apparatus. **Y-Zz**. Ectopic filamentous balls of myosin A recruit UNC-98/ZnF in strain RW3880, which expresses myosin A with an altered C-terminus (2SerAlaΔ25; Hoppe *et al.* 2010b). Scale bar is 20 microns

Localization of Other M-line Proteins in *unc-82* Mutants

UNC-98/ZnF has been shown to bind to paramyosin and has been proposed to promote the proper assembly of paramyosin into thick filaments (Miller *et al.* 2008). It was therefore of interest to examine the localization of UNC-98/ZnF in *unc-82* mutants. The absence of UNC-82 did not prevent association of UNC-98/ZnF with the disorganized contractile apparatus (Figure 2.7 G-I), where its distribution partially overlapped that of paramyosin. In the *unc-82* E424K mutant, UNC-98/ZnF was again detected in the contractile apparatus where the signal partially overlapped that of anti-paramyosin. However, UNC-98/ZnF signal was not detected in the ectopic paramyosin accumulations (Figure 2.7 J-L), which contain the mutant UNC-82 kinase and myosin B, but not myosin A (Figure 2.1 O-R, Figure 2.3 A-C, and Figure 2.7 P-R). The absence of UNC-98/ZnF from the paramyosin-containing accumulations in UNC-82 E424K mutants suggests that the association of UNC-98/ZnF with paramyosin requires UNC-82 activity in vivo.

The disparity between the paramyosin and UNC-98/ZnF staining patterns prompted us to examine the in vivo interaction of UNC-98/ZnF and myosin A, which have been shown to physically interact (Miller *et al.* 2006). We found that UNC-98/ZnF and myosin A colocalize in *unc-15(0)* animals, which do not contain paramyosin (Figure 2.7 V-X), and in animals that express a mutant myosin A that forms ectopic accumulations (Figure 2.7 Y-Zz). Both myosin A and myosin B contain a C-terminal nonhelical tailpiece that is homologous to the N-terminal nonhelical headpiece of paramyosin, which is phosphorylated by an endogenous kinase (Kagawa *et al.* 1989, Schriefer and Waterston 1989). The myosin A nonhelical tailpiece is 29 amino acids long, and contains three copies of the proposed phosphorylation motif S_S_A that was identified in the paramyosin

headpiece (Hoppe *et al*. 2010b, Schriefer and Waterston 1989). The mutant myosin construct is missing the C-terminal 25 amino acids, and the serine residues within the four remaining residues of the tailpiece (which contain one motif) are changed to alanine. The mutant myosin assembles outside the contractile apparatus, suggesting that this construct has a loss of negative control of myosin assembly that normally occurs through phosphorylation. The ectopic myosin A accumulations appear to be balls of jumbled filaments and do not stain with anti-paramyosin (Hoppe *et al*. 2010b). Therefore, our results suggest that UNC-98/ZnF associates with myosin A in the absence of paramyosin, and that the C-terminal 29 amino acids of myosin A are not required to bind UNC-98/ZnF in vivo. In yeast two-hybrid experiments, the C-terminal 200 amino acids of myosin A were found to be sufficient for binding UNC-98/ZnF, and removal of the last 32 amino acids abolished this binding (Miller *et al*.. 2006). Interestingly, the additional three amino acids removed in the yeast two-hybrid experiment, but present in our mutant myosin construct, are within the four amino acids at the C-terminus of the coiled-coil rod that are essential for viability when tested in double mutants lacking endogenous myosin A and B (Hoppe *et al*., 2003).

The failure of UNC-98/ZnF to associate with the paramyosin aggregates in *unc-82* E424K led us to examine the localization pattern of other M-line proteins in this mutant. The paramyosin aggregates in *unc-96* and *unc-98*/ZnF mutants (Miller et al. 2009) and *unc-89(su75)*/obscurin mutant (Qadota *et al*. 2016) stain positive for CSN-5, a component of the conserved COP9 signalosome complex. CSN-5 interacts with both UNC-96 and with UNC-98/ZnF, and likely promotes the degradation of UNC-98/ZnF. Antibody staining experiments did not detect CSN-5 on the paramyosin/myosin B accumulations in UNC-82 E424K (Figure 2.7 M-O). Experiments using antibodies against UNC-89/obscurin, UNC-

97, UNC-95, CPNA-1, PAT-6 and UNC-112 (see Materials and Methods) indicated that none of these antibodies stain cells in a pattern that resembles the distinctive accumulations at the ends of cells in *unc-82* E424K (Figure 2.8). UNC-89/obscurin, which has been shown to interact with paramyosin (Qadota *et al.*, 2016), does appear in bright irregular patches in E424K (Figure 2.8 G), as it does in the *unc-82(0)* (Hoppe *et al.,* 2010a). A double stain with paramyosin found that, although paramyosin and UNC-89/obscurin stain showed some overlap, the distinctive paramyosin accumulations at ends of cells did not stain for UNC-89/obscurin (Figure 2.7 S – U). Interestingly, in the plane of the cell containing the paramyosin accumulations, the UNC-89/obscurin stain was moderately disorganized (Figure 2.7 T). But in focal planes that were more distal from the integrin complex, which is located in the plasma membrane adjacent to the epidermis, the UNC-89/obscurin stain included large irregular patches (Figure 2.8 G). Therefore, the only proteins detected in the distinctive accumulations formed in the *unc-82* E424K kinase domain missense mutant are the mutant UNC-82 protein itself, paramyosin and myosin B.

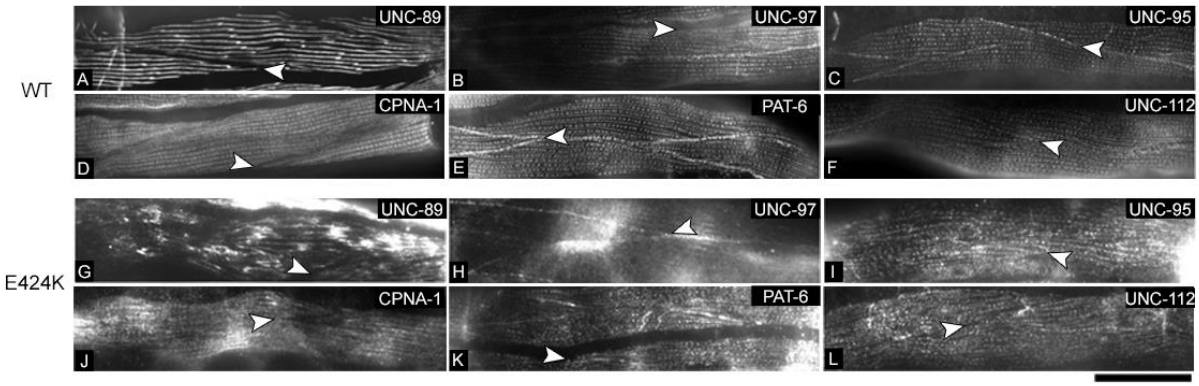

Figure 2.8: Other M-line proteins are not found on abnormal accumulations in the missense mutant *unc-82* E424K. Immunofluorescence images of stained wild type (A-F) and *unc-82* missense mutant E424K (G-L) adults show varying degrees of disorganization of the different M-line components in the *unc-82* mutant. However, none of the proteins is detected in distinctive accumulations at muscle cell ends (arrowheads). Scale bar is 20 microns.

Discussion

Loss of function of the AMPK-related kinase UNC-82 results in defects in thick filament morphology and organization in striated muscle of *C. elegans* (see Introduction). In this study, we present evidence that the major thick filament components paramyosin, myosin A and myosin B are not equally affected by alterations in the catalytic activity of UNC-82. Our analysis of three different *unc-82* missense mutants revealed distinctive ectopic accumulations at the ends of cells, which contain paramyosin but not myosin A. Notably, such accumulations are not found in the null (Figures 1.1 and 1.2). Accumulations in at least one of these mutants (E424K) also contain myosin B (Figure 2.1) and the mutant UNC-82 protein itself (Figure 2.3). We propose that UNC-82 is required in an early step in paramyosin, and probably myosin B, assembly that occurs prior to the association of paramyosin with UNC-98/ZnF, myosin A, or several other M-line proteins (Figure 2.9).

The UNC-82 missense mutations used in this study fall within the kinase domain, either in the catalytic loop, which performs the transfer of phosphate from ATP to peptide substrate, or the activation segment, which regulates catalytic activity of the domain in response to phosphorylation (Figure 2.2). Our results suggest that at least two of these alleles (E424K and S442P S969F), both of which exhibit a high incidence of ectopic paramyosin accumulations, can generate stable but presumably catalytically-impaired protein products. The GFP-tagged E424K protein accumulates and localizes normally to the M-line in wild-type cells, and is strongly detected in the birefringent accumulations at the ends of muscle cells in the *unc-82(0)* background (Figure 2.3). Because the mutant UNC-82 E424K::GFP protein is present in these accumulations, and the accumulations are not present in the *unc-82* null, we propose that these accumulations represent a complex of the

catalytically-impaired UNC-82 protein with its substrate in a stalled intermediate. The protein produced by the second mutant, S442P S969F, is clearly stable at the permissive

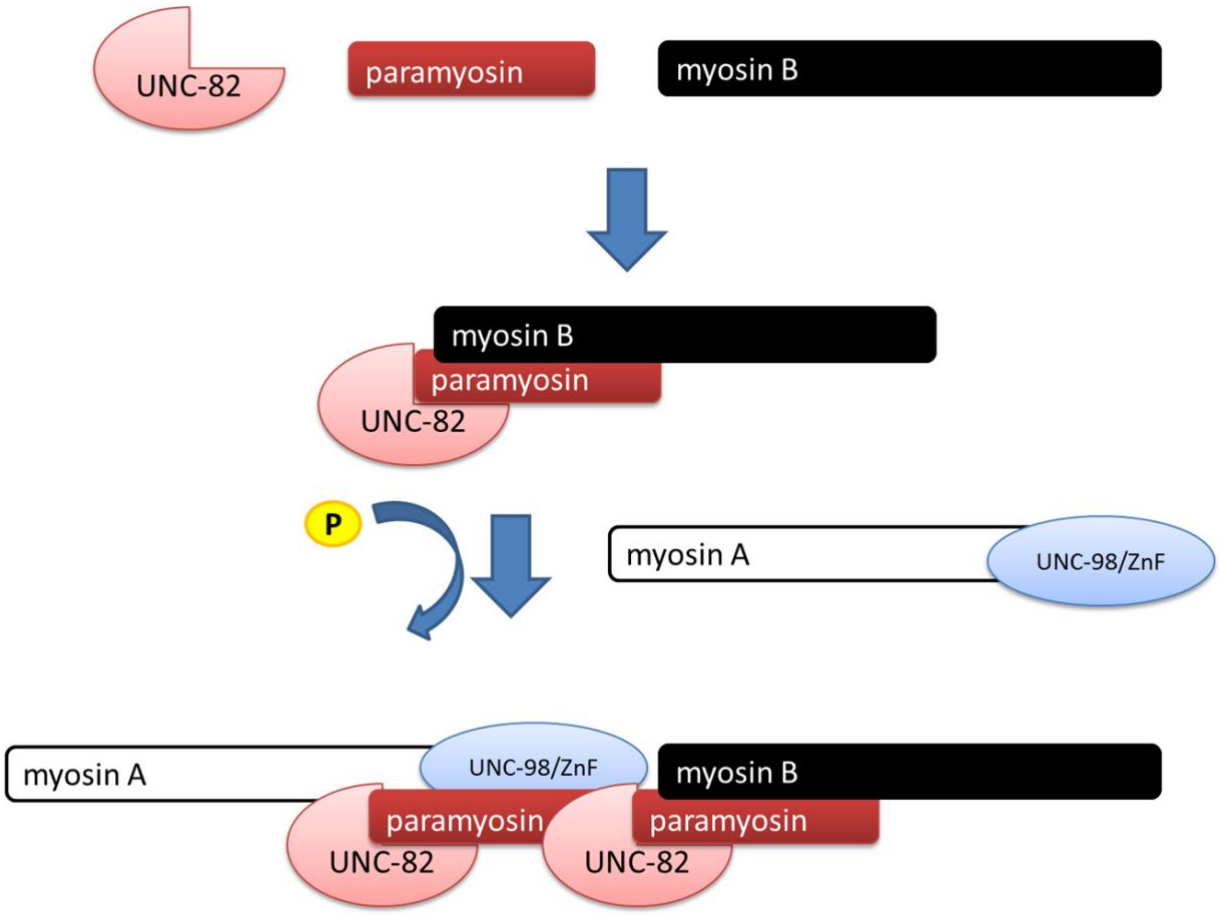

Figure 2.9: Model for the order of UNC-82 protein interactions during early steps of thick filament assembly. UNC-82 first associates with newly made paramyosin and myosin B. UNC-82 kinase activity promotes the subsequent association of this complex with a complex of UNC-98-myosin A during filament and body elongation.

temperature, given the normal muscle structure in the homozygote (Figure 2.2). At the restrictive temperature, we suggest that the S442P change may destabilize the fold adopted

by the activation segment upon phosphorylation, impeding substrate access to the catalytic cleft.

The third mutant, G456R (which also affects the activation segment), contains some accumulations, but not in all muscle cells. Given our model that catalytically-impaired UNC-82 protein produces the distinctive accumulations, one possible explanation for fewer accumulations in the G456R mutant is lower levels of mutant UNC-82 protein. Alternatively, the G456R mutant protein might have a decreased tendency to associate with paramyosin or another component of the aggregates. The G456R substitution affects a highly conserved glycine, and places the large, positively charged arginine side chain within three residues of the threonine that is phosphorylated in the active form of the enzyme (Figure 2.2). The change might impair phosphorylation of the threonine, which would decrease the pool of activated UNC-82, and potentially alter the stability of the mutant UNC-82 or its interactions with other muscle proteins. Similar effects have been demonstrated for unphosphorylated PKA (Iyer *et al*. 2005).

The proposal that UNC-82 interacts with paramyosin early in the assembly pathway is supported by results from three types of experiments. First, recently synthesized paramyosin::GFP colocalizes with both wild-type and a mutant form of UNC-82. In wild type, paramyosin::GFP driven by a brief heat shock is detected at the M-line (Figure 2.3; Miller *et al*. 2008), the site of UNC-82::GFP localization. This initial localization of paramyosin at the M-line may represent a staging area for thick filament components prior to incorporation into growing thick filaments. In the E424K *unc-82(e1220)* genomic mutant, newly made paramyosin associates with distinctive birefringent structures at the ends of cells (Figure 2.3 F), which we have shown stain positive for both paramyosin and myosin B

(Figure 2.1 M-N, Q-R; Figure 2.7 P-R). Similar birefringent structures containing UNC-82 E424K::GFP are formed when the mutant protein is expressed in the *unc-82(0)* (Figure 2.3). This is consistent with our model that the accumulations represent a stalled paramyosin/UNC-82 complex that normally forms as an intermediate prior to incorporation of paramyosin into the thick filament.

The composition of the E424K aggregates provides a second line of evidence that this putative intermediate is formed prior to paramyosin association with other proteins. The accumulations in *unc-82* E424K mutants contain paramyosin, UNC-82 E424K mutant protein, and myosin B, but not proteins of the myosin A-associated complex (myosin A, UNC-98/ZnF) (Figures 1.1 and 1.7), proteins of the integrin-associated complex (UNC-112, UNC-98/ZnF, CPNA-1, PAT-6, or CSN-5) (Figures 1.7 and 1.8), or the giant M-line protein UNC-89/obscurin (Figure 2.7). Conversely, we found that wild-type UNC-82::GFP colocalized with ectopic birefringent aggregates resulting from mutation of four other genes that disrupt thick filament assembly or organization (Figures 1.4 and 1.5). In addition to paramyosin, these aggregates all contain additional proteins (see Results) that are not found in UNC-82 E424K aggregates. These observations suggest that arrest of the assembly process in these other mutants occur at a later step than in UNC-82 E424K mutants.

Finally, the genetic interactions between *unc-82* and other paramyosin-affecting mutations also support its early action in a paramyosin assembly pathway. The phenotype of double mutants of *unc-82* alleles with *unc-98(sf19)*/ZnF is similar to the phenotype of the *unc-82* mutation alone (Figure 2.6 J-L and Figure 2.7 A-B). The lack of an additive increase in severity argues that the two proteins may act in a common linear pathway. The aggregates present in the *unc-98*/ZnF mutant contain UNC-82 (Figure 2.5 E-F); these

aggregates do not form in the absence of UNC-82 in the *unc-82(0)*; *unc-98/*ZnF double mutant (Figure 2.6 K, Figure 2.7 A-C). Further, the accumulations typical of *unc-82* E424K mutants (accumulations that contain myosin B) are present in the double with *unc-98/*ZnF (Figure 2.7 D-F). These observations are consistent with UNC-82 acting upstream of UNC-98/ZnF, and UNC-82 protein playing a role in aggregate formation in *unc-98/*ZnF mutants.

In contrast, the double mutants of *unc-82* alleles with a mutation in *unc-89/*obscurin show a more severe phenotype than either mutation alone (Figure 2.6 G-I). The *unc-89(su75)* allele eliminates all large isoforms of UNC-89/obscurin, which contain the SH3 domain. The SH3 domain is proposed to crosslink thick filaments at the M-line through an interaction with paramyosin (Qadota *et al*. 2016). The double mutant combination of *unc-89(su75*)/obscurin and *unc-82(0)* is sterile, and muscle cells have grossly abnormal structure with birefringent signal appearing in large round accumulations (Figure 2.6 H). This additive interaction suggests that the two proteins function independently, with UNC-82 promoting paramyosin assembly into the thick filament and UNC-89/obscurin mediating filament attachment at the M-line.

Birefringent, and therefore ordered, assemblages of paramyosin form in a variety of mutant backgrounds, and also when wild-type paramyosin is over expressed from transgenes (Hoppe *et al*. 2010b). The more hydrophobic surface of paramyosin compared to myosin (Cohen *et al*. 1987) may be responsible for the apparent propensity to form aggregates. Aggregates may form in a given mutant because the affected protein has a direct role in paramyosin organization. However, because increased dosage of normal paramyosin can lead to aggregate formation, aggregates may form due to a block in a separate step in thick filament assembly that secondarily leads to high levels of cytosolic paramyosin. The

colocalization of UNC-82 with all paramyosin-containing aggregates examined (Figure 2.3, Figure 2.5 C-H) suggests a close interaction of UNC-82 with paramyosin in vivo. Consistent with this hypothesis, the localization pattern of UNC-82::GFP is highly abnormal in the paramyosin null mutant (Figure 2.5 A-B).

Considering the roles of phosphorylation in regulating the assembly of smooth and non-muscle myosin heavy chains (Castellani and Cohen, 1987; Murakami *et al.* 1988; Kelley and Adelstein 1990; Rovner *et al.* 2002), it is tempting to speculate that UNC-82 exerts its effects by phosphorylating paramyosin to regulate its assembly. Several observations are consistent with this model. The level of paramyosin and myosin phosphorylation in purified *C. elegans* thick filaments has been correlated with its state of assembly, and solubilized myosin and paramyosin phosphorylation by a co-purifying kinase was demonstrated (Dey et al. 1992). In worm extracts, paramyosin is phosphorylated by an endogenous kinase on serine residues within the N-terminal nonhelical headpiece (Schriefer and Waterston 1989). Point mutation of the headpiece, or the homologous C-terminal tailpiece residues in myosin A, leads to formation of abnormal aggregates in muscle cells (Hoppe et al. 2010b). Unpublished data cited in Shriefer and Waterston (1989) indicate that the more acidic forms of paramyosin are absent in *unc-82* mutants, consistent with decreased phosphorylation of the protein. This reported effect on paramyosin phosphorylation might occur because paramyosin is an UNC-82 substrate, or through an indirect mechanism. The mammalian UNC-82 ortholog ARK5/NUAK1 increases myosin light chain phosphorylation in human embryonic kidney cells by phosphorylating and inactivating a myosin phosphatase (Zagorska *et al*. 2010).

However, the dosage effects observed in our experiments are not consistent with a simple model in which UNC-82 phosphorylates newly synthesized paramyosin, either to prevent aggregation or to directly promote its assembly into a growing thick filament. The effect of increased expression of wild-type UNC-82 in paramyosin missense mutants was to increase, rather than decrease, aggregate formation in heterozygotes (Figure 2.4 F-K), and to cause synthetic lethality in homozygotes (Figure 2.4 P-S). Increased UNC-82 levels also caused lethality and aggregate formation in the absence of paramyosin (Figure 2.5 A-B). These data indicate that a stoichiometric relationship of UNC-82 and paramyosin is critical for normal muscle structure, and suggest that UNC-82 has both catalytic and structural roles during thick filament assembly.

The synthetic lethality and formation of novel birefringent structures in the muscles cells of paramyosin null animals with increased UNC-82::GFP expression implicates UNC-82 in organizing additional components of the contractile apparatus (Figure 2.5 A-B). The composition of the birefringent aggregates formed in these cells was not determined. Given that the paramyosin accumulations in UNC-82 E424K mutants and paramyosin *e73* missense mutants contain myosin B (Figure 2.1 Q-R, Epstein et al. 1987, Gengyo-Ando and Kagawa 1991), and that the paramyosin accumulations in other mutants do not (Mercer *et al*. 2006; Miller *et al*. 2008; Qadota *et al.* 2016), these aggregates may be assemblages of myosin B. Removal of myosin B in a paramyosin mutant background is lethal (Waterston 1988). Induction of myosin B aggregation in the paramyosin null may mimic that double mutant phenotype. The possibility that UNC-82 is involved in the organization of myosin B and paramyosin (Figure 2.9), which compose the thick filament arms (see Introduction), is consistent with defects in *unc-82(0)* mutant muscle cells becoming apparent during body

elongation stages of embryogenesis, when muscle cells and thick filaments are increasing in length.

Myosin A is not found associated with the UNC-82-containing aggregates (Figure 2.1 O-P). The opposite effects of increasing myosin A dosage in a paramyosin *e73* background, which suppresses (Riddle and Brenner 1978, Otsuka 1986, Hoppe and Waterston 2000), and increasing UNC-82 dosage, which enhances (Figure 2.4 E-H and P-Q), also suggest that UNC-82 and myosin A do not act as part of the same complex in organizing paramyosin. We have found that UNC-98/ZnF colocalizes with myosin A in structures that do not contain paramyosin (Figure 2.7 V-ZZ). We propose that UNC-82 catalytic activity is required in a processing step that precedes the association of paramyosin with UNC-98 and myosin A (Figure 2.9).

There are two mammalian orthologs of UNC-82, ARK5/NUAK1 and SNARK/NUAK2 (Hoppe *et al.* 2010a); both are required in mouse muscle. Phosphoproteome analysis of a muscle-specific knock-out of ARK5/NUAK1 revealed changes in phosphorylation levels of proteins in the actin-myosin cytoskeleton, including myosin (Inazuka *et al.* 2012). Reduction of SNARK/NUAK2 resulted in an age-dependent loss of muscle mass (Lessard *et al.* 2016). These observations suggest potential conserved roles for UNC-82/ARK5/SNARK in the contractile apparatus across diverse animal lineages.

CHAPTER 3

A REGION OF THE MYOSIN A ROD IS DEPENDENT UPON THE AMPK RELATED KINASE UNC-82/ARK-5/SNARK ACTIVITY DURING THICK FILAMENT ELONGATION IN THE BODY WALL MUSCLE OF *C. ELEGANS*

The use of *C. elegans* nematode to study the molecular arrangement of proteins important for proper muscle cell structure and sarcomere function, is a wonderful tool for understanding the complexities within mammalian muscle (reviewed in Waterston, 1988; Moerman and Fire, 1997; Moerman and Williams, 2006; Gieseler *et al.*, 2016). The molecular machinery of *C. elegans* body wall muscle and associating attachment structures have striking similarities to mammalian muscle cell structures. The contractile units of both invertebrate and vertebrate muscle cells contain highly organized myosin thick filaments, anchored to M-lines, and intercalated between actin-containing thin filaments anchored to dense bodies (Z-disks). The basic mechanism of muscle contraction involves the myosin motor domain interacting cyclically in a cross-bridge with actin, requiring the repeated hydrolysis of ATP, which is bound to myosin, to produce a power stroke. This mechanism requires a careful balance between ATP consumption and production for the continuation of contraction, as well as consistent organized interaction between myosin and actin filaments.

Thick Filament and Sarcomere Structure

The myosin thick filaments of *C. elegans* exist in a series of homocentric layers of interacting molecular polymers, with an inner axial core of filagenins and paramyosin that associate

with an intermediate layer of paramyosin (*unc-15*), and an outer coaxial layer of class II myosins, A (*myo-3*) and B (*unc-54*) (Epstein *et al.*, 1985; Deitiker and Epstein, 1993; Liu *et al.*, 1998). The stabilizing inner core of the thick filament is comprised of hydrophobic "headless myosin" molecule, paramyosin, which is homologous to the filament forming light meromyoisn domain of the coiled-coil myosins A and B (Lowey *et al.,* 1969; Cohen *et al.,* 1987; Kagawa *et al,.* 1989). Both the minor M-line associating, filament initiating myosin isoform A and the major filament elongation myosin isoform B assemble into two distinct zones on the more hydrophobic surface of the inner paramyosin core (McLachlan and Karn, 1982; Kagawa *et al.*, 1989). These thick filament structures of striated muscles appear in bipolar arrangements with myosin A molecules in the initiating 2μm center, associated with M-line proteins such as UNC-89/obscurin and UNC-98/Zn packed in an antiparallel arrangement (bare zone) transitioning to a reversed parallel arrangement of a mix of myosin A and myosin B molecules terminating with myosin B associating with UNC-45 in the outer 8um arms of the 10um long thick filament structure (Liu *et al.,* 1997, Miller *et al.*, 1983; Ardissi and Epstein, 1987; Benian *et al.,* 1996; Ao and Pilgrim, 2000; Kachur and Pilgrim, 2008; Qadota *et al.,* 2010). Upon the surface of this stable paramyosin core, the motor domains can cross-bridge with actin filaments that anchored to integrin containing dense bodies, requiring the repeated hydrolysis of ATP, which is bound to myosin, to produce a power stroke interact with actin filaments to slide the two filament systems past each other and accomplish contraction of the muscle cell (Francis and Waterston, 1985).

Muscle Contraction and Embryonic Viability

The body-wall muscles cells of C. elegans are attached to the cuticular exoskeleton of the worm through integrin-mediated attachments between the extra cellular matrix (ECM) and the actin cytoskeleton, and their contractile activity is required for embryonic viability and adult locomotion (Waterston, 1980). Contraction of the body-wall muscles causes sinusoidal body undulations that drive locomotion. In addition, locomotion, the contraction of body-wall muscles is required for embryonic body elongation. The body elongation of embryos is accomplished through constriction of actin filaments along the peripheral circumference of the worm epidermis (Priess and Hirsh, 1986) When this vital muscle contraction is obliterated, body elongation is halted, and worms arrest as deformed L1 larvae with the Pat phenotype (paralyzed, arrested elongation at the two-fold stage) and ultimately die (Waterston, 1989; Williams and Waterston, 1994). The organization and assembly of muscle and epidermal cells together occurs through integrin-mediated signaling at the focal adhesion-like structures of the cytoskeleton. These structures are present at the base of dense bodies and M-lines that anchor actin filaments and myosin filaments, respectively, to the ECM (reviewed in Moerman and Williams, 2006). Forward genetic screens of mutagenized worms were used to identify genes/proteins involved in body wall muscle function and development. Many alleles that produced decreased muscle function and with slow Unc (uncoordinated) movement as adult such as *unc-82(e1323), unc-15(e1214), and unc-54 (e190)* as well as one that produced the more sever Pat phenotypes, such as *myo-3 (st386)* were identified as results of these forward genetic screens. Mutational elimination of paramyosin (*unc-15 (e1214)*) or myosin B (*unc-54 (e190)*) result in paralyzed adult worms with disorganized body-wall muscle sarcomeres, whereas mutational elimination of the minor

isoform myosin A (*myo-3 (st386)*) results in larvae with the lethal Pat phenotype (Epstein *et al.*, 1974; Waterston *et al.*, 1977). These observations implicated myosin A, but not myosin B or paramyosin, as having an essential role in antiparallel arrangement of these myosin A molecules required for proper thick filament initiation (Waterston, 1989). Using chimeric myosin constructs, the myosin A-specific function for antiparallel assembly and filament initiation has been mapped to charge interactions between sets of coiled-coiled molecules involving residues in the central rod (Region 1) and resides located on the c-terminal end of the rod (region 2) (Hoppe and Waterston, 1996). The ability for myosin A to assemble in a parallel manner with paramyosin was mapped to 322 amino acid residues in Region 2 of the myosin A coiled-coil rod (Hoppe and Waterston, 2000)

AMPK-Related Kinase, UNC-82

Electron and polarized light microscopy revealed spatial arrangement abnormalities of thick filament with aberrant aggregates of paramyosin in worms with mutations in the *unc-82* gene which codes for the AMPK-related kinase, UNC-82 (Waterston *et al.*, 1980; Hoppe *et al.*, 2010a). The kinase activity of the conserved AMPK related kinase UNC-82, orthologous to ARK5/NUAK1 and SNARK/NUAK2, which is highly expressed in mammalian striated muscle, is required for proper sarcomere organization in *C. elegans* body-wall muscle (Waterston, 1980, Lefebvre and Rosen, 2005, Hoppe *et al.,* 2010a, Schiller *et al.,* 2017). Previous studies in mice, implicate these orthologues as having a role in mammalian sarcomere function, with alterations in sarcomere proteins after muscle specific knock down of ARK5/NUAK1, as well as age-dependent decrease in muscle mass with disruption of SNARK/NUAK2 expression profiles (Inazuka *et al.,* 2012; Lessard *et al.,* 2016). Double

knockouts of both orthologues, however, resulted in embryonic arrest due to neural tube closure defects (Ohmura *et al.,* 2012). Evidence of ARK5/NUAK/SNARK activity in regulation of light chain phosphorylation levels on non-muscle myosin has also been reported in cultured human kidney cells (Zagórska *et al.,* 2010).

While the mechanism of UNC-82 kinase activation, and its role in sarcomere organization, is not well understood, a few studies have provided evidence for UNC-82 involvement in organizing myosin filaments (Hoppe *et al.,* 2010a; Schiller *et al.,* 2017). Antibody staining of the *unc-82(0)* mutant revealed severely disrupted localization of myosin A, paramyosin and myosin B (Hoppe *et al* 2010a; Schiller *et al.,* 2017). It is possible that UNC-82 is directly required for organization of all three of these homologous proteins individually. Alternatively, disorganization of one component in *unc-82* mutants may have indirect effects on the localization of the others. Analysis of protein distribution in the kinase-impaired missense mutant *unc-82* E424K provided evidence that UNC-82 kinase domain physically interacts with myosin B and paramyosin, but not myosin A (Schiller *et al.* 2017, Figure 1), suggesting that either myosin B or paramyosin may be a direct substrate of UNC-82 kinase activity. Additionally, given the mis-localization of myosin A in *unc-82(0)* mutants, but not kinase impaired mutants, it is also possible that residues outside of the kinase domain of UNC-82 may be required for proper myosin A localization. This investigation proposes to identify a role for UNC-82 in organizing class II myosin rods in the contractile apparatus of *C. elegans* body wall muscle. Our results identify a 531-amino acid central region of the myosin A rod that is dependent on UNC-82 activity for the parallel association with paramyosin in thick filaments of *C. elegans* body-wall muscle.

Materials and Methods

Genetic Crosses

Generation of Non Transgenic Double Mutants

Generation of non-transgenic double mutants involving paralyzed unc-15(e1214), unc-15(e73), or unc-54(e190) mutants: These crosses were started by heat shocking the nonparalyzed mobile single mutant to generate males. These mobile males were allowed to mate with the paralyzed hermaphrodites for 24 hrs. After 24 hours the males removed from the plate and sacrificed via flame (flamed) and the mated hermaphrodites were separated and allowed to produce F1 progeny. Four days post mating, F2 cross progeny, identified by their ability to move on the agar, were picked to 12 well culture plates and allowed to self for 3 days. On day three, moving L3-L4 F3 worms were individually picked from the 12 well plate to a 24 well plate and allowed to self for 48 hours. After 48 hours, the F3 parents of each well in the 24 well plate were mounted on slides and their muscle phenotype screened by polarizing light microscopy to identify those worms exhibiting the muscle phenotype of the original moving single mutant genotype from which the male originated. These wells were marked as homozygous for that single mutation and the F4 larva were allowed to develop for 2 more days. At which point, any wells segregating paralyzed F4 worms were singly picked to a 12 well plate and further analyzed as double mutants. If no paralyzed worms were identified, the wells were assayed for arrested F4 larva and documented as non-viable double mutants. All viable double mutant strains were verified by outcross to N2 and re-isolation of each single mutant.

Generation of unc-15(e1214); unc-54(e190) double: Males generated from a wild type N2 strain were mated to *unc-54(e190)* paralyzed hermaphrodites to generate heterozygous males. Heterozygous *unc-54(e190)/+* males were then crossed into the paralyzed *unc-15(e1214)* mutant background and allowed to mate for 24hrs. After 24hrs the heterozygous *unc-54(e190)/+* males were flamed and the mated *unc-15(e1214)* hermaphrodites were separated to new plates and allowed to produce embryos. On day 4 the mated *unc-15(e1214)* hermaphrodites were screened for moving L3 F1 hermaphrodites which were individually picked into single wells in a 12 well culture plate then allowed to self for 5 days. After 5 days, 48 F3 paralyzed L4-adult worms were single picked to two 24 well culture plates and allowed to self. The wells that segregated arrested F4 larva were analyzed further.

Generation of Transgenic Lines

Transgenes in this study were followed in genetic crosses by the presence of a dominant rolling (Rol) phenotype, GFP expression in the cuticle, or GFP expression in the pharynx conferred by co-injection marker plasmids pRF4 *rol-6(su1006),* pPHgfp-1 *(prol-6::*GFP*)*, and *myo-2::gfp* respectively (Park and Kramer 1994, Hoppe and Waterston 2000). To easily distinguished cross progeny from the hermaphrodites' self-progeny, passing the GPF or rolling transgene from the male is best. Because Rol and Unc males mate poorly, well moving, non-paralyzed hermaphrodites were temporarily immobilized by treatment with TT: M9 with 0.1% tricaine and 0.01% tetramisole (Sigma Inc.) (McCarter *et al*. 2005). Adult transgenic males were mated with anesthetized adult hermaphrodites, about four per male, in a manner previously described in Schiller *et al.* 2017.

Crossing transgenes marked with rol-6(su1006) into mutant backgrounds: To introduce a transgene into a single mutant background, transgenic males were crossed to anaesthetized homozygous mutant hermaphrodites (see above), and the rolling or fluorescent F1 heterozygous progeny picked singly and allowed to self. The rolling or fluorescent F2 progeny were picked singly, and mutant homozygotes identified by movement and polarized light phenotypes of the F2 parent and its F3 progeny. All viable double mutant strains were verified by outcross to N2 and re-isolation of each single mutant.
Two extrachromosomal arrays expressing UNC-82::GFP (*phEx22* and *phEx21*) that were made previously (Hoppe *et al.* 2010) were used in this study. The *phEx21* array was integrated into a random chromosomal location using a UV irradiation protocol (Mariol *et al*. 2013) to create *phIs2*.

Myosin Transgenes

The details for the creation of wild-type myosin and chimeric myosin transgenes used in this study have been described in Hoppe and Waterston, 1996.
Myosin A (stEx80): Wild-type myosin A (*myo-3*) construct transformed into worms with GFP co-injection marker driven by *rol-6* collagen gene promoter (*rol-6::gfp)* (Park and Kramer 1994, Hoppe and Waterston, 1996).
Myosin B (stEx59): Wild-type myosin B (*unc-54*) construct with hemagglutinin (HA) epitope-tag transformed into worms with GFP under the *myo-2* promoter driving expression in the pharynx. collagen gene promoter (Hoppe and Waterston, 1996).

Chimera 2 (stEx85): Chimeric myosin construct which contains the entire myosin A head and rod residues (M1-I1079) adjacent to C-terminal myosin B rod and tail residues co-injected with *rol-6::gfp*.

Chimera 8 (stEx89): Chimeric myosin construct containing 531 amino acid residues (D1080-Q1611) of myosin A, including region 1 residues, flanked by myosin B motor, rod and tail residues co-injected with *rol-6::gfp*.

Chimera 11 (stEx23): Chimeric myosin containing c-terminal myosin A rod residues (A1612-1933), including region 2 residues, flanked by myosin B motor, rod and tail residues co-injected with *rol-6(su1006)*.

The myosin B extrachromosomal arrays in *unc-54; unc-82* mutants were generated as described (Mello et al. 1991), using a 25:25:1 ratio of pPHgfp-1/Bluescript/myosin B (pucBB) at 200 ng/ml in 10 mm Tris, 1 mm EDTA, pH 8.

Nematode Strains Used in this Study

All worm strains in this study were maintained at 20 C on nematode growth medium (NGM) plates seeded with the uracil mutant OP50 strain of *Escherichia coli* (Brenner, 1974). *Strains obtained from Guy Benian or The Caenorhabditis Genetics Center (CGC) are as follows*: Bristol N2 [wild type]; CB1220 [*unc-82(e1220)* IV]; CB1323 [*unc-82(e1323)* IV]; CB73[*unc-15(e73)* I]; GB246 [*unc-98(sf19)* X]; CB190 [*unc-54(e190)* I] and CB1214 [*unc-15(e1214)* I].

Transgenic strains carrying fluorescently tagged wild-type UNC-82::GFP (phEx22 or phEx21): PZ236 [*unc-98(sf19)* X*; phEx22*]; PZ84 [+*; phEx22*] PZ286 [+; *phIs2* I (integrant of *phEx21* (UNC-82::GFP))]; PZ235 [*myo-3(st386)* V*; phEx22; stEx137*];

Transgenic strains carrying wild-type myosin A (stEx80): PZ256 [+*; stEx80(myo-3)*]; PZ260 [*unc-82(e1323)* IV*; stEx80*]; PZ266 [*unc-82(e1220)* IV*; stEx80*]; PZ312 [*unc-54(e190) I; stEx80*]; PZ270 [*unc-54(e190) I; unc-82(e1323) IV; stEx80*]; PZ271 [*unc-54(e190) I; unc-82(e1220) IV; stEx80*]

Transgenic strains carrying wild-type myosin B (stEx59): PZ285 [+*; stEx59(unc-54)*]; PZ288 [*unc-82(e1323)* IV*; stEx59*]; PZ284 [*unc-82(e1220)* IV*; stEx59*]; RW3773 [*unc-54(e190) I; stEx59*]

Transgenic strains carrying chimera 2 (stEx85): PZ253 [+*; stEx85*]; PZ261 [*unc-82(e1323)* IV*; stEx85*]; PZ269 [*unc-82(e1220)* IV*; stEx85*]; PZ274 [*unc-54(e190) I; stEx85*]; PZ272 [*unc-54(e190) I; unc-82(e1323) IV; stEx85*]; PZ273 [*unc-54(e190) I; unc-82(e1220) IV; stEx85*]

Transgenic strains carrying chimera 8 (stEx89): [*unc-54(e190); stEx89*]

Transgenic strains carrying chimera 11 (stEx23): PZ309 [*unc-54(e190); stEx23*];

PZ311 [*unc-82(e1323)* IV*; stEx23*]; PZ310 [*unc-54(e190) I; unc-82(e1323) IV; stEx23*]; PZ308 [*unc-54(e190) I; unc-82(e1220) IV; stEx23*]

Microscopy

Adult worms were fixed using either the Nonet method (Nonet *et al.*, 1993) or the French press method (Francis and Waterston, 1985) and incubated in primary antibodies overnight at room temperature. Mouse monoclonal antibodies 5-6 (1:500 dilution), 5-8 (1-500), and 5-23 (1:200 dilution) were used for immunofluorescence localization of myosin A, myosin B, and paramyosin respectively (Miller *et al.*1983). Alexa Fluor 488- and 594-conjugated secondary antibodies from Jackson ImmunoResearch Laboratories were used at 1:400 dilutions. Worms were incubated in secondary antibodies for two hours. In the myosin A and myosin B co-stained worm fragments Rhodamine conjugated 5-6 (1:200) and FITC conjugated 5-8 (1:200) antibodies were used. For staining of Beta-integrin the MH25

(1:200, from The Developmental Studies Hybridoma Bank) antibody was used (Francis and Waterston, 1985). GFP staining was done using a GFP rat monoclonal antibody (1:200) from Invitrogen. Polarized light microscopy procedures of Mackenzie *et al*. (1978) were followed.

Embryos were stained using paraformaldehyde and methanol fixation methods of Hresko, Williams, & Waterston (1994) and incubated on primary antibodies at room temperature for 1 hour followed by incubation with secondary antibodies at room temperature for 1 hour. All images were acquired in ImagePro 6.0 (Rockville, MD) using a Retiga Exi Fast cooling mono12-bit Qimaging camera mounted to a Leica DM5500 microscope equipped with a polarizing lens. All images processed using Adobe Photoshop CS6 software (San Jose, CA).

All strains and reagents generated in this study are available upon request.

Thrashing Assay

All worm strains assayed for thrashing were maintained at 20 C on nematode growth medium (NGM) plates seeded with the uracil mutant OP50 strain of *Escherichia coli* (Brenner, 1974). All worms picked were healthy and at least F4 from last starved state. 30 young adult hermaphrodites were picked to 500µl of sterile M9 in a single well of a 24 well plate. Worms were allowed to normalize to the M9 for 5 minutes prior to videography. Live bright field thrashing was visualized on a computer and monitor equipped with th ImagePro 6.0 program (Rockville, MD) using a Retiga Exi Fast cooling mono12-bit Qimaging camera mounted to a dissecting Leica Microscope. Due to computational limits, 70 second 1080p HD video recording (30 fps) of the live preview from the monitor was acquired by the use of

an iPhone 5S equipped with an iSight Camera. Videos were emailed from the iPhone and analyzed at half speed using Windows Movie Maker (2012 Microsoft Corporation). The thrashing counts of 10 worms were recorded for each strain assayed (except where otherwise noted). One thrash was counted every time the head or tail moved past the midline, to the other side, of the dorsal-ventral axis. Statistics for the average, StDevA, and two-tailed T-tests with unequal variance were calculated using Microsoft Office 365 ProPlus, Excel 2016. Graphs were generated in Excel 2016. Movement relationship maps were created using CmapTools program developed by The Institute for Human & Machine Cognition (Pensacola, Fl). All thrashing assays were repeated blind.

Embryo Development Videos

Prior to addition of the embryos, 2% molten agarose was dropped on to a glass microscope slide and pressed to a think agarose pad using the weight of a second microscope slide. Once cooled, the second slide was removed, and the thin agarose pad was cut with a clean surgical blade to a 3x3 grid small enough to fit under a 12 mm x 12 mm (L x W) glass coverslip. Unhatched comma stage embryos, from transgenic parents, were single picked, using a dissection microscope to 0.5ul of M9 buffer atop each pad in the grid. A 12 mm x 12 mm glass coverslip was outlined with petroleum jelly and placed on top of the embryo grid to prevent drying of the embryos. All grid spots on the slide were marked on the bottom of the slide with a row and a letter. A series of time laps images were taken over the period of 8 hours using Nomarski optics on a scanning confocal microscope. The embryos were allowed to continue development for another 10 hours on the grid, at which point all embryos we assessed for the presence of the GFP marked transgene by mounting

the grid to a compound microscope equipped with UV light and cross referenced to the associating time lapse video file.

Results

UNC-82 Associates with Sarcomere Structures Independently of Paramyosin, Myosin B and the Myosin Co-chaperone UNC-98/ZnF

Previously published results of disorganized sarcomere components in *unc-82* mutants suggested physical interactions between UNC-82, paramyosin and myosin B. In wild-type worms expressing a *rol-6* marked *unc-82::gfp* transgene (*phEx22*), UNC-82::GFP localizes to the m-line and thick filament regions of the muscle sarcomere (Hoppe *et al* 2010a). This UNC-82 transgene produces synthetic lethality in mutants homozygous for missense or nonsense paramyosin alleles where organization or amount of paramyosin in the sarcomere is altered (Schiller *et al* 2017). To better define the mechanism by which UNC-82 is involved in organizing thick filaments, we examined the distribution of UNC-82::GFP in live worms lacking various thick filament components. While, introducing a transgene of *unc-82::gfp* in paramyosin mutants results in synthetic lethality, we examined the distribution of UNC-82::GFP more closely in the rare surviving mosaic adult worms that were segregated from a previously established *unc-15 +/ + gld-1* balanced line PZ259 [*unc-15(e1214) +/+ gld-1(q485) I; phEx22*] to clarify localization of UNC-82 in muscle cells when paramyosin is absent. Under lower magnification, in these cells, the pattern of UNC-82 localization appears in elongated accumulations, at the ends of cells, these accumulations are also birefringent when viewed by polarized light and readily seen at 40x magnification indicating they contain ordered assemblages of molecules (Schiller *et al.,* 2017). But when examined at 100x magnification, we see that UNC-82::GFP is also in discernable striations in the region of the muscle cell containing the contractile apparatus (Figure 3.1 A). This prompted us to ask if the localization of UNC-82 in stripes or accumulations in *unc-15(0)*

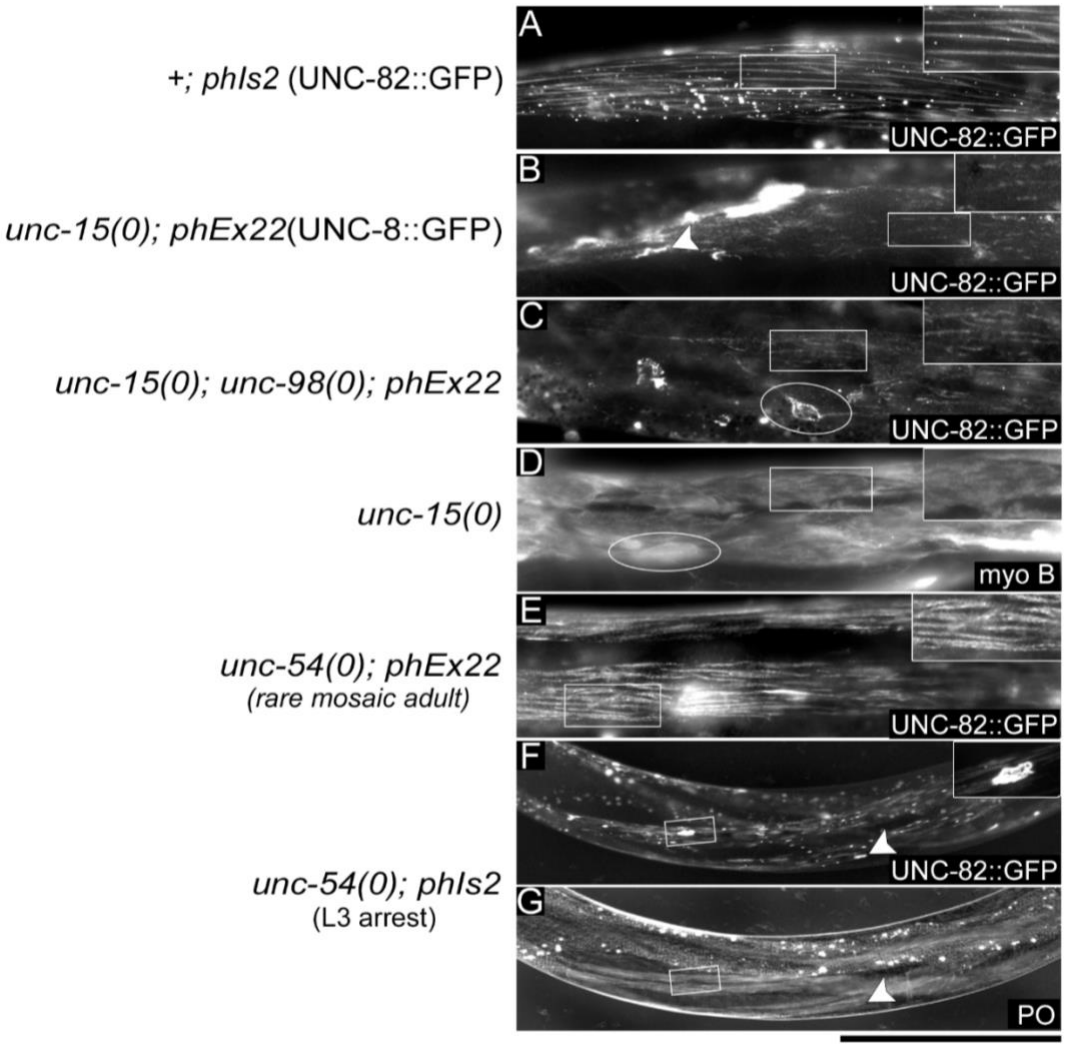

Figure 3.1: UNC-82 associates with sarcomere components in the absence of myosin B, paramyosin, and UNC-98. **A**. Fluorescence microscopy of live transgenic *unc-82::gfp* (*phEx22*) expression in a mosaic single mutant *unc-15(0*) adult exhibits UNC-82::GFP localization to discontinuous lines within the contractile apparatus (arrow in A) as well as to accumulations at the ends of muscle cells (arrowhead in A). **B**. Transgenic expression of *unc-82::gfp* expression in a rare surviving mosaic double mutant worm that lacks paramyosin and UNC-98 reveals UNC-82::GFP localizing to the contractile apparatus (arrow in B) and to ectopic punctate accumulations (rectangle in B) with no obvious distinct accumulations at the ends of muscle cells (arrowhead in B). **C**. Antibody staining reveals myosin B in paramyosin mutant, unc-15(0), is diffuse throughout the muscle cell with abnormal accumulations at the ends of cells (rectangle in C). **D**. UNC-82::GFP is visible in stripes in the contractile apparatus (arrow in D) of worms lacking myosin B (*unc-54(0)*). **E-F**. Fluorescence and polarized light phenotype of a typical live L3 worm lacking myosin B and expressing *unc-82::gfp* (*phIs2*). UNC-82::GFP is visible in lines in the contractile apparatus, as well as in non-birefringent filamentous accumulations at the ends of cells (rectangles in E and F). Scale bar is 20 microns

animals is dependent on UNC-98. Due to the sterility associated with *unc-15(0); unc-98(0)* animals, the cross was performed using viable rolling *unc-98(0)* males carrying the UNC-82::GFP transgene (Schiller *et al.* 2017). Transgenic animals homozygous for *unc-98(0)* and heterozygous for *unc-15(0)* produced mosaic sterile adults and arrested L1 larvae. In the mosaic mutants, UNC-82:GFP localizes in a striated pattern in regions of the cell associated with structures in the sarcomere but does not localize to the ends of cells (Figure 3.1B). Instead, UNC-82::GFP appears in punctate ball like accumulations in areas of the muscle cell outside of regions of the contractile apparatus.

To investigate if myosin B is in similar patterns in paramyosin nonsense mutant muscle, worms lacking paramyosin were subjected to immunofluorescence French press procedures described in Francis and Waterston, 1985 and stained with antibodies for myosin B. In these mutants, myosin B appears in cloud like accumulations throughout the muscle cell with some small areas of striated staining that suggest some organization into the sarcomere. At the ends of cells more dense accumulations of myosin B form birefringent accumulations (Figure 3.1 C; data not shown). The pattern of myosin B stain in *unc-15(0)* is similar to that of UNC-82::GFP in this mutant but distinctly different from the patterns of myosin A and UNC-98 in this mutant, where the two proteins colocalize in patches in apparently random distribution (Miller *et al* 2006, Schiller *et al* 2017).

The similarity in distribution of myosin B and UNC-82 in the absence of paramyosin prompted a reciprocal experiment to test the localization of UNC-82::GFP in the absence of myosin B [*unc-54(e190)*] (Figure 3.1 D-F). Initial attempts to cross the unstable UNC-82::GFP transgene phEx22 into the myosin B null produced only mosaic adults of *unc-54(e190); phEx22* genotype from heterozygous parents. Transgenic cells contained in the

mosaic animals showed UNC-82::GFP present in organized striations resembling the M-line localization of UNC-82 in wild type. The failure to generate a homozygous transgenic line with could be due to the inability to detect the rolling marker of the *unc-82::gfp* transgene in the paralyzed *unc-54(0)* mutant; thus, we attempted to generate a homozygous transgenic line using a UV-integrated transgene of *unc-82::gfp* (*phIs2*). The homozygous animals segregating from transgenic heterozygous heterozygotes arrested as L3 paralyzed larvae. Upon inspection of these larvae, UNC-82::GFP was present in stripes in the muscle sarcomeres as well as in non-birefringent dense accumulations at the ends of cells and linear accumulations in the middle of the cells. These observations argue that the localization of UNC-82 to the contractile apparatus is more dependent upon paramyosin than on myosin B. But does not rule out a role for UNC-82 in organizing myosin B. Additionally, these data support that the roles of UNC-98/ZnF, paramyosin, and myosin B do not include localization of UNC-82.

Myosin-Isoform-Specific Interactions with UNC-82

UNC-82 indirectly interacts with myosin A in organizing thick filaments

To further test the hypothesis that UNC-82 acts through myosin B, we examined the distribution of myosin A and paramyosin in adult animals that lack myosin B and also differ in levels of UNC-82 activity. If myosin B is the primary target of UNC-82 modulation, then we expect that by removing myosin B in the *unc-82(0)* mutant background the localization defects observed in myosin A and paramyosin pattern would be improved or no more severe compared to either mutant alone. Using immunocytochemistry techniques, we examined the distribution of paramyosin and myosin A in these mutant backgrounds. The single

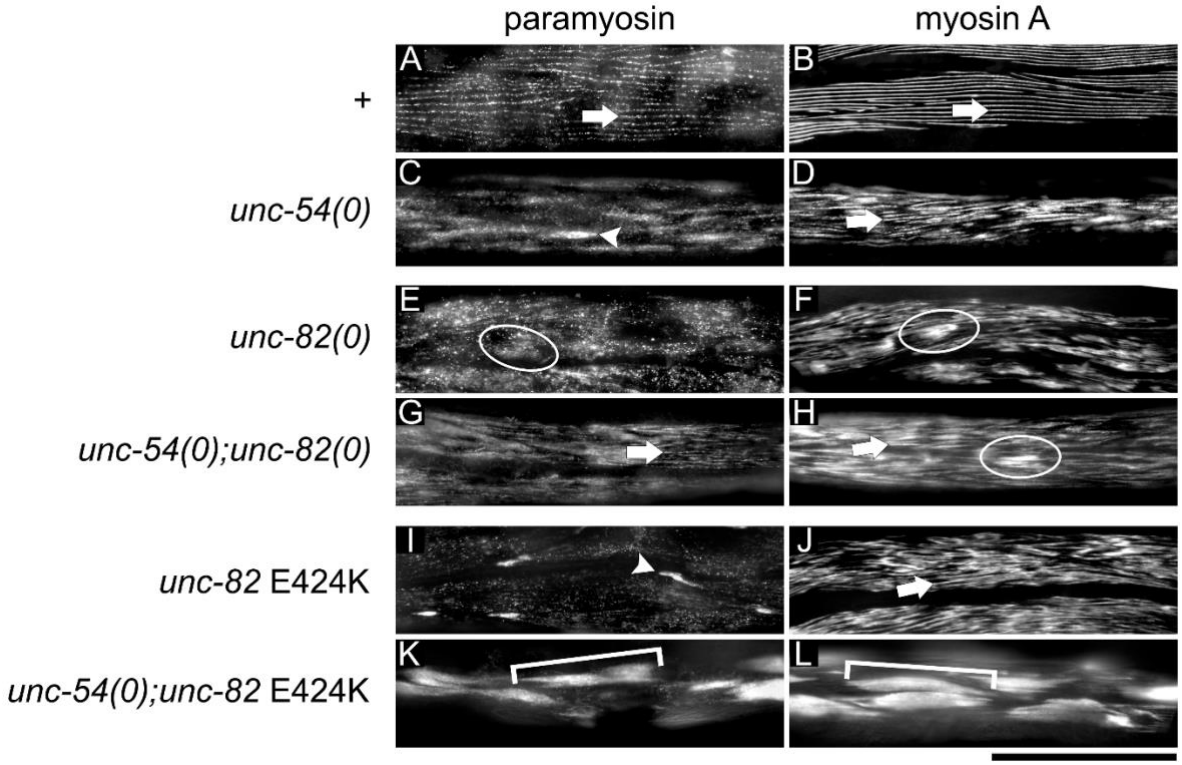

Figure 3.2: In the absence of myosin B, the distribution of myosin A and paramyosin is strongly affected by UNC-82 activity. **A-B.** Paramyosin and myosin A, antibody stains produce signal in regular longitudinal stripes in wild type worms (arrows in A and B). **C-D.** Worms lacking myosin B have a loss of paramyosin organization with accumulations of paramyosin at the end of cells (arrowhead in C) whereas myosin A signal remains in stripes, associated with the disorganized A bands (arrow in D). **E-F.** Paramyosin is present in amorphous accumulations in worms lacking UNC-82 (oval in E). Whereas myosin A appears less affected, with some striations as well as amorphous patches found throughout the muscle cell (oval in F). **G-H.** Paramyosin in double mutants lacking both myosin B and UNC-82 is present at the M line [arrow in (G)]. In these same mutants myosin A is present in irregular A band stripes (arrow in H) as well as in small accumulations (oval in H). **I-J.** In the *unc-82* E424K mutant paramyosin is strongly detected in distinctive accumulations at the ends of cells (arrowhead in I) and weakly seen in the contractile apparatus. Myosin A is present in irregular stripes in these mutants (arrow in J). **K-L.** In double mutants containing kinase impaired UNC-82 E424K but lacking myosin B, both paramyosin and myosin A are present in large, brightly-staining accumulations in the region of the contractile apparatus (brackets in K and J). Scale bar is 20 microns.

mutants of either *unc-54(0)* or *unc-82(0)* have disorganized myosin A, which is less uniformly distributed in worms lacking UNC-82 compared to worms lacking myosin B. In the severely paralyzed double mutant lacking both myosin B and UNC-82, however, myosin A appears primarily in short, irregular stripes and bright accumulations, a phenotype more severe than either single mutant. Suggesting separable roles for both UNC-82 and myosin B in organizing myosin. Strikingly, the paramyosin stain in this double mutant has areas of regular stripes, and is therefore appears (Hoppe *et al.*, 2010a, Waterston, 1980, Figure 3.2 G).

The observation that paramyosin appears better organized in the presence of myosin A when both myosin B and UNC-82 are absent, is consistent with the possibility that UNC-82 may act as both an assemblase and a chaperone for paramyosin, aiding in its assembly into the thick filament while concurrently preventing inappropriate early interactions with each of the two muscle myosin isoforms. These results further suggest that the organization of myosin A in the sarcomere may be dependent on its appropriate interaction with paramyosin, evidence further supported by the apparently random localization pattern of myosin A in mutants lacking paramyosin. Additionally, organization of myosin A may be independent of UNC-82 activity and raises the possibility that mutations in *unc-82* affect myosin A indirectly by altering myosin B interactions with paramyosin.

To address this possibility, we assessed the distribution of myosin A and paramyosin in double mutants lacking myosin B and containing a kinase-impaired mutation within the catalytic loop of *unc-82, unc-82(e1220) (unc-82* E424K*)* (Schiller *et al.,* 2017). The kinase-impaired missense mutant UNC-82 E424K contains distinctive accumulations of myosin B, paramyosin, and the mutant UNC-82 protein, but not myosin A (Schiller *et al.,* 2017). To

test if formation of these distinct paramyosin containing accumulations is a consequence of an aberrant interaction of the kinase-impaired UNC-82 with myosin B, we generated the double mutant *unc-54(0); unc-82* E424K and compared the muscle phenotype to that of the double null *unc-54(0); unc-82(0).* The polarized light and immunofluorescence assessments of these doubles revealed dramatically different muscle phenotypes. The double with missense E424K had an increased disruption of muscle structure with a novel staining pattern in which both paramyosin and myosin A appear in large uniformly stained patches (Figure 3.2 K-L). This severely abnormal phenotype of myosin A staining prompted us to investigate if the cells themselves have collapsed. Further assessment of these mutant muscle cells by beta-integrin immunostaining reveals that the cells membranes and the filament attachment structures are intact, but the thick filament material is severely disorganized (Figure 3.3 A-C). This prompted us to investigate if these the thick filament components become disorganized after embryonic elongation, which requires the embryo to move, or if this disorganization occurs prior to the start of embryonic movement. Previous research has shown that myosin A and paramyosin defects appear most obvious after embryonic elongation begins, with obvious muscle defects seen by the 2-fold stage of embryonic development in *unc-82(0)* mutants (Hoppe *et al.,* 2010b). Immunohistochemical assessment of the *unc*-82 E424K missense mutant embryo reveals disruptions in paramyosin, but not myosin A as early as the 1.5-fold stage, prior to elongation, with obvious distinct paramyosin accumulations present by the fully elongated 3-fold stage, prior to hatching (Figure 3.3 H-K). Whereas defects in both paramyosin and myosin A patterning are apparent by the 1.5-fold stage in the double *unc-54(0); unc*-82 E424K mutant embryo (Figure 3.3 L-O).

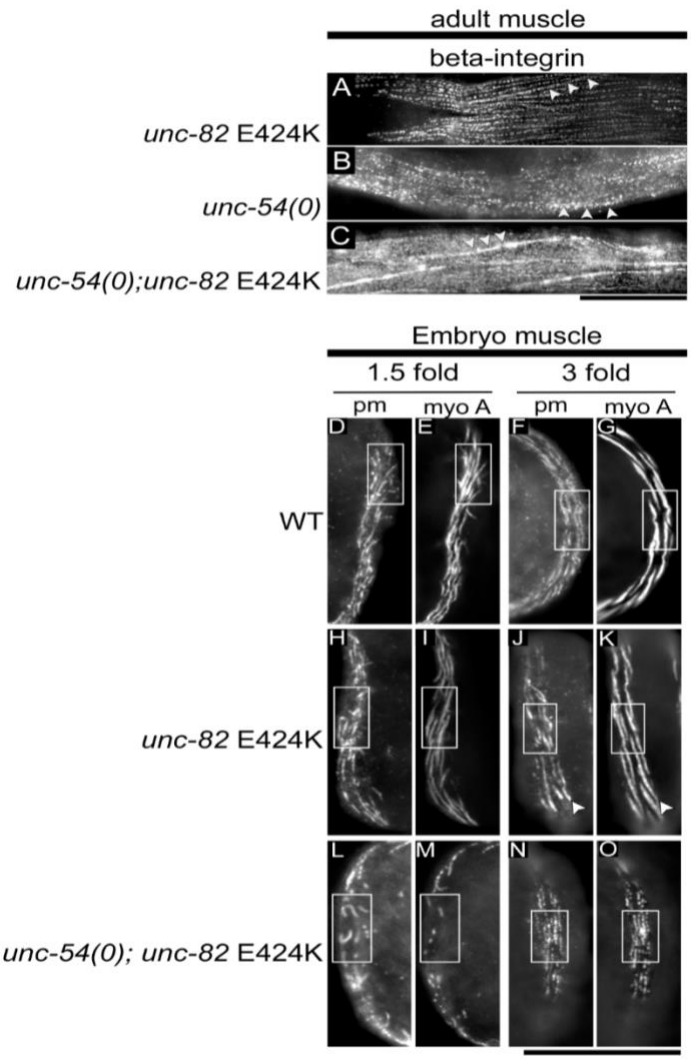

Figure 3.3. Cell shape and cell-cell contacts are maintained in mutants with large accumulations of thick filament components. **A-C** Fixed adult worms, which exhibit abnormal thick filament accumulations were stained with anti-beta-integrin to stain the membrane insertion sites of the actin and myosin filament attachment structures and cell-cell contacts. The mutants exhibit normal cell boundaries (arrowheads in A, B, and C) **D-O**. The defects in thick filament protein localization occur prior to embryonic elongation in embryos of single *unc-82* E424K (H-K) and double *unc-54(0); unc-82* E424K. (L-O) Single muscle quadrants of embryos, stained with Paramyosin and myosin A, at the 1.5-fold pre-elongation (left columns) and 3-fold post elongation (right columns) stages of development are depicted in corresponding columns. **D-G**. Paramyosin and myosin Aare detectable in stripes in early developing 1.5-fold and 3-fold embryos, with paramyosin in similar stipes to myosin A (rectangles). **H-K**. unc-82 E424K embryos display abnormal paramyosin patterning as early as 1.5-fold stage prior to elongation (rectangles in H-K) with distinct accumulations of paramyosin visible by 3-fold stage (arrowheads in J and K). **L-O**. Double mutant *unc-54(0); unc-82* E424K embryos display a lack of paramyosin and myosin A patterning at 1.5-fold stage with punctate accumulations of both proteins visible at the 3-fold stage (Rectangles in L-O). Scale bars are 20 microns

These data suggest that there may be myosin isoform-specific interactions with UNC-82. It appears that the kinase-impaired UNC-82 E424K severely impacts the localization of paramyosin and myosin A require UNC-82 kinase activity to organize properly. Further, myosin B may have a role in organizing paramyosin and myosin A that is not dependent on UNC-82 kinase activity. The observation that the presence or absence of myosin B greatly influences the distribution of myosin A and paramyosin in the *unc*-82 E424K background, suggests that myosin A can inappropriately assemble with the aberrant structures of paramyosin generated in the presence of the impaired UNC-82 E424K kinase and the presence of myosin B likely acts to mitigate this inappropriate interaction by assembling with paramyosin outside of the contractile apparatus in a manner that is independent of myosin A. Alternatively, the dramatic increase in size of accumulations in the *unc-54(0); unc-82* E424K double may simply result from a large reduction in overall myosin content in the cell, in which myosin A, the minor isoform, is simple not present in sufficient quantity to counter the deleterious effect of kinase-impaired UNC-82 on sarcomere assembly.

To investigate possible myosin-isoform-specific interactions with UNC-82, we tested the effect of increasing myosin A in the *unc-82* E424K and *unc-82(0)* backgrounds. A myosin A transgene, that is expressed at sufficient levels to restore movement in the *unc-54(e190)* myosin B null mutant, was crossed into single and double mutant backgrounds and muscle cell structure was assessed using polarized light microscopy and immunohistochemistry (Hoppe and Waterston, 1996). The transgenic expression of myosin A (*stEx80*) in worms lacking myosin B increases organization within muscle cells (Figure 3.4 A-B) and rescues movement defects in these mutants (Hoppe and Waterston, 1996).

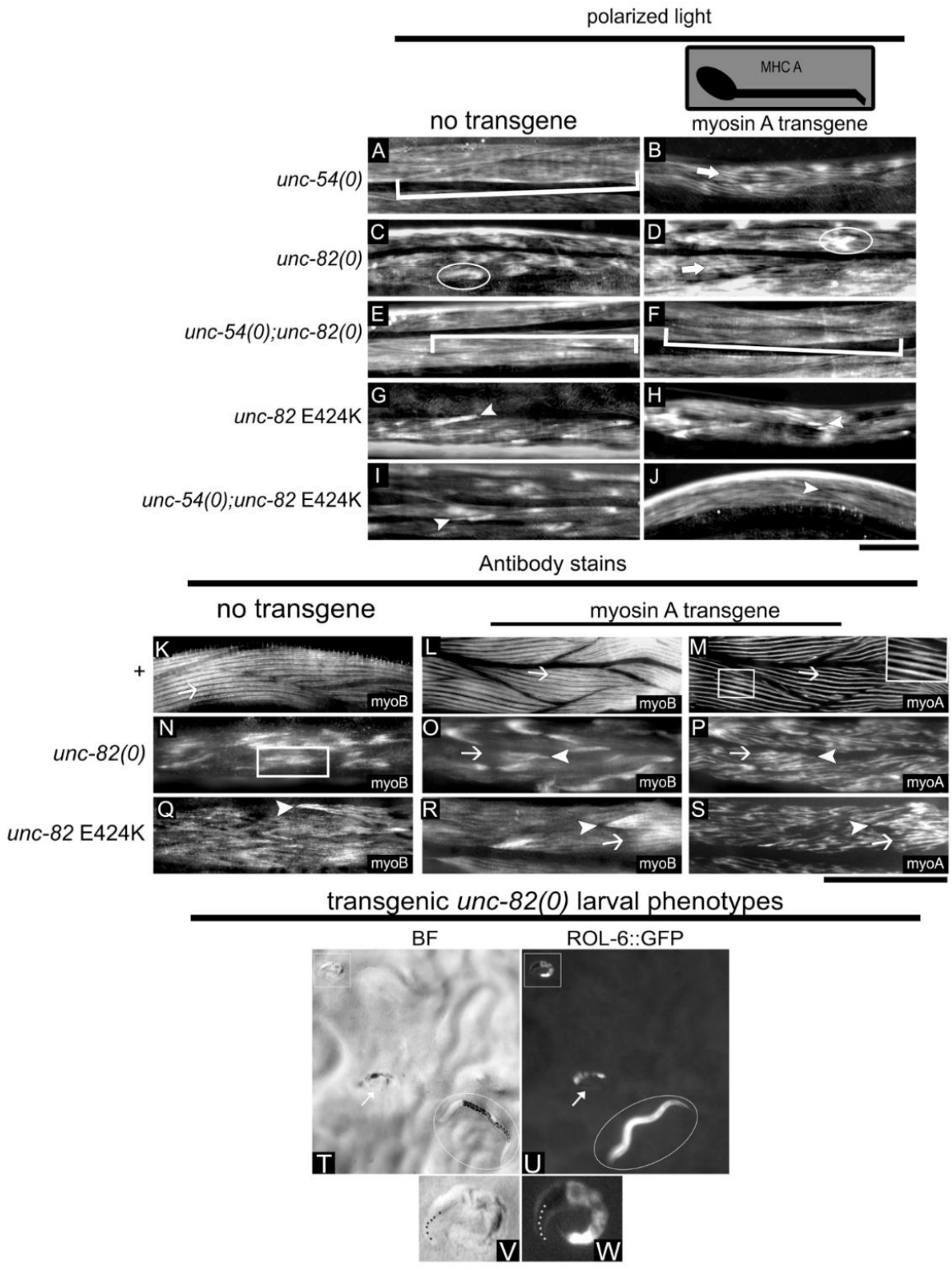
polarized light
MHC A
no transgene
myosin A transgene
unc-54(0)
unc-82(0)
unc-54(0);unc-82(0)
unc-82 E424K
unc-54(0);unc-82 E424K
A
B
C
D
E
F
G
H
I
J
Antibody stains
no transgene
myosin A transgene
+
unc-82(0)
unc-82 E424K
K
L
M
N
O
P
Q
R
S
myoB
myoA
transgenic unc-82(0) larval phenotypes
BF
ROL-6::GFP
T
U
V
W

Figure 3.4: Overexpression of myosin A cannot compensate for loss of myosin B in *unc-82* mutants. To determine if increased myosin A assembly into thick filaments is independent of UNC-82, muscle phenotypes of mutant strains were examined with and without the unstable extrachromosomal transgene *stEx80* expressing myosin A. **A-J** Polarized light images show the adult muscle phenotypes of nontransgenic (left column) and transgenic animals (right column) segregating from mutant strains. cells. **A-B** Myosin B [*unc-54(0)*] mutants exhibit a uniform smear of birefringence throughout the muscle (bracket in in A). Transgenic siblings expressing extra myosin heavy chain A (MHC A) exhibit increased birefringence and discernable striations in muscle (arrow in B). **C-D**. Muscle cells in *unc-82(0)* mutants contain birefringent patches (oval in C). In siblings expressing extra myosin A, there are fewer patches and more organization in stripes (oval and arrow in D). **E-F**. The muscle birefringence in the double mutant *unc-54(0); unc-82(0)* appears as a uniform smear in both nontransgenic and transgenic siblings (bracket in E and F). **G-H**. Kinase-impaired UNC-82 E424K mutant muscle presents with distinct birefringent accumulations at the ends of muscle cells (arrowhead in G). Increased expression of myosin A (arrowhead in H) alters the appearance of the accumulations. **I-J**. The double mutant *unc-54(0); unc-82* E424K contains birefringent accumulations at the ends of cells (arrowhead in I) which are decreased in the presence of increased myosin A expression (arrowhead in J). **K-S** Double antibody stains of *unc-82* mutants show change in distribution of myosins in response to over expression of myosin A. **K-M**. In wild type, the canonical myosin B antibody staining appears in the A bands but is absent from the M-line (arrow in K). Antibody stains of myosin B in worms over expressing myosin A from the transgene *stEx80* exhibit a similar wild-type pattern (arrow in L). Myosin A staining in these transgenic worms shows normal localization at the center of the A band, (arrow in M) with some expansion of the width of the band of myosin A stain (zoomed box in M) consistent with previous reports (Epstein *et al.* 1986). **N-P.** Myosin B staining in *unc-82(0)* mutants appears as large amorphous accumulations (rectangle in N). Myosin B staining in *unc-82(0)* mutants expressing extra myosin A appears in large accumulations at the ends of cells (arrowhead) and is absent or reduced in the cell body (arrow in O). In contrast, the myosin A in these transgenic mutants appears primarily in irregular stripes in the cell body (arrow in P). **Q-S.** Myosin B staining in *unc-82* E424K mutants appears disorganized with accumulations at the ends of cells (arrowhead in Q). In transgenic animals, myosin B is present in accumulations at the ends of cells (arrowhead in R) but also shows improved organization into stripes in the cell body (arrow in R). Myosin A staining in these worms appears unaffected (compare to Figure 1 J) and colocalizes with myosin B in the disorganized A bands (arrow in S). Scale bar is 20 microns. **T-W** Over expression of myosin A causes early lethality and abnormal development in some *unc-82(0)* animals. Transgenic progeny in broods collected from wild-type and *unc-82(0)* transgenic animals were identified by GFP expression in the skin. **T-U**. Brightfield (BF) and fluorescent images of typical transgenic *unc-82(0)* offspring on a culture plate show a paralyzed larva with failed body elongation (box in T and U), a larva arrested at a slightly later stage (arrow in T and U), and a moving, apparently normal larval sibling (oval in T and U). **V-W**. An enlarged view of the severely affected larva from A and B shows deformed body (stars indicate the position of the developed pharynx).

Polarized light images of *unc-82(0)* mutants expressing increased myosin A show continued presence of large amorphous patches characteristic of this mutant, but some increase in signal appearing in stripes (Figure 3.4 C-D). The myosin A transgene in double mutants lacking both myosin B and UNC-82, fails to improve organization of birefringent signal, and the animals are Unc (Figure 3.4 E-F). This observation suggests that UNC-82 is involved in organization of myosin A in the filament arms when myosin B is absent. Expression of the same transgene in *unc*-82 E424K does not eliminate the birefringent accumulations at the ends of cells (Figure 3.4 G-H). Interestingly, in the double of *unc*-82 E424K with the myosin B null these accumulations, which are composed of paramyosin, myosin B and mutant UNC-82 E424K, are eliminated with an increase in myosin A dosage (Figure 3.4 I-J). However, the cells have no discernable striations and these animals are Unc.

To better understand the effects of increased myosin A expression in these mutants, double antibody stains for myosin A and myosin B were performed in *unc-82* single mutants expressing extra myosin A. In wild-type worms, the expression of myosin A produces only a minor expansion of the stripe of myosin A stain at the M-line, as previously reported (Epstein *et* al 1986, Figure 3.4 K-M). *unc-82(0)* animals expressing transgenic myosin A display improved myosin A localization to the contractile apparatus, but abnormal myosin B localization at the ends of muscle cells (Figure 3.4 O-P compared to Figure 3.4 Q-R and Figure 3.2 F). No difference in paramyosin organization compared to non-transgenic siblings was found (data not shown, Figure 3.2 E). Although over expression of myosin A appears to improve the muscle structure of *unc-82(0)* adults, the transgene caused a significant increase in larval lethality and abnormal development in this mutant (19.2%)

compared to a wild type background (2.5%) (Table 3.1). Most defective transgenic *unc-82(0)* worms presented as mild Pats or arrested Lpy-Dpy larvae (Figure 3.4 T-W, S1 video). These data indicate a dosage interaction between UNC-82 and myosin A that is similar to the synthetic lethal dosage interactions reported for UNC-82 and paramyosin (Schiller *et al.,* 2017).

Over expression of myosin A did not produce lethality, or any detectable developmental defects in development, in the *unc-82* E242K single mutant (Table 3.1). UNC-82 E424K adults expressing transgenic myosin A have larger birefringent accumulations at the ends of some cells, thicker A-bands, and areas of muscle where birefringence appears to vary in intensity (Figure 3.4 G-H).

Table 3.1: Comparative Brood Analysis of Wild Type and *unc-82(0)* Mutants with Increased Myosin A Expression

Increased expression from myosin A transgene (*stEx80*)			
Genotype	**wt**	***unc-82(0)***	***unc-82 E424K***
Total population	550	326	230
Total non-transgenic	195	92	174
Total transgenic	355	234	56
Apparently normal transgenic	345	189	56
Abnormal/arrested non-transgenic	0	0	0
Abnormal/arrested transgenic	10(2.8%)	45 (19.2%)*	0

Table 3.1: Comparative brood analysis of wild type and *unc-82(0)* mutants expressing a GFP marked myosin A (*stEx80*) transgene are displayed in the table. These mutants exhibit a higher percentage of abnormality and mortality (19.2%) compared to wild-type worms expressing the same construct (2.8%). Chi-sq : 36.29285 *p value: <.0001.

Antibody staining of these transgenic mutants revealed altered myosin B localization with increased myosin B at the ends of the muscle cells (Figure 3.4 Q-R). Myosin A distribution does not appear to be altered compared to non-transgenic *unc-82* E424K mutants (Figure 3.4 S compared to Figure 3.2 J). Paramyosin staining in these mutants resembles the paramyosin staining of non-transgenic siblings (data not shown).

UNC-82 indirectly interacts with myosin B in organizing thick filaments

We then examined the effect of introducing a myosin B transgene into *unc-82* mutant backgrounds. The transgene was able to restore near wild-type muscle structure in the myosin B null mutant and caused mild disruption of striations in wild-type worms (Figure 3.5 A and B, Hoppe and Waterston 1996). Increased expression of myosin B in both *unc-82* mutants improved the polarized light muscle phenotype by increasing the presence of birefringent stripes (Figure 3.5 C and D). Despite this apparent improvement viewed in adult *unc-82(0)* worms, the transgene did not affect the large birefringent amorphous patches, that are typical of *unc-82(0)* (Figure 3.5 C, E and F), and produced embryonic lethality. In the case of the *unc-82* E424K mutant, increased expression of myosin B did reduce the prevalence of the distinctive birefringent accumulations as the ends of cells (Figure 3.5 D) and no embryonic lethality was detected. This myosin transgene rescues the movement defect of the myosin B null mutant, but, caused a decrease in thrashing in wild type animals, consistent with previously reported effects of myosin B dosage (Fire and Waterston, 1989). Similarly, over expression of myosin B negatively affected movement of the *unc-82(0)* mutant. In contrast, the movement of transgenic *unc-82* E424K mutants was significantly

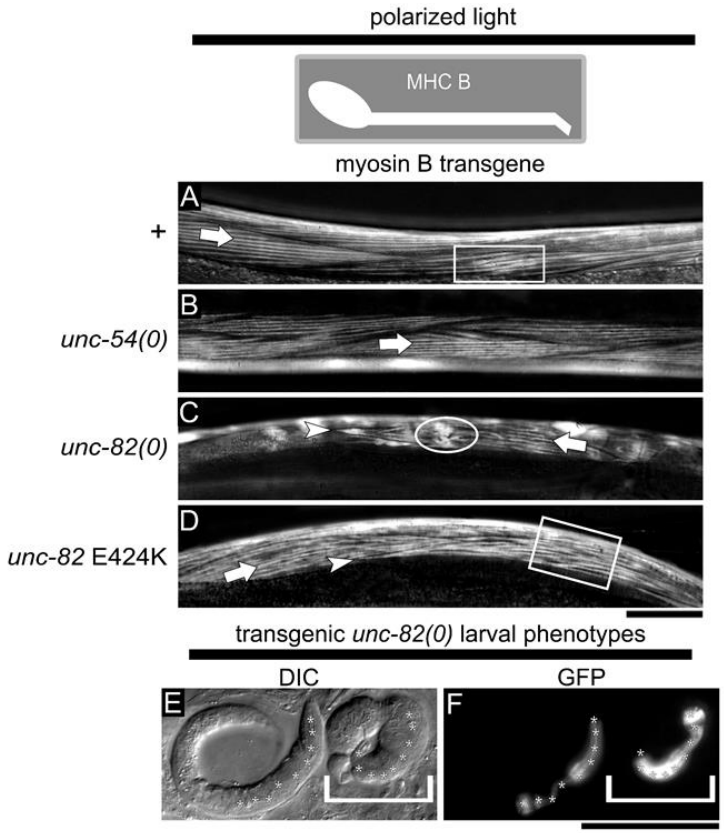
polarized light
MHC B
myosin B transgene
A
+
B
unc-54(0)
C
unc-82(0)
D
unc-82 E424K
transgenic unc-82(0) larval phenotypes
DIC
GFP
E
F

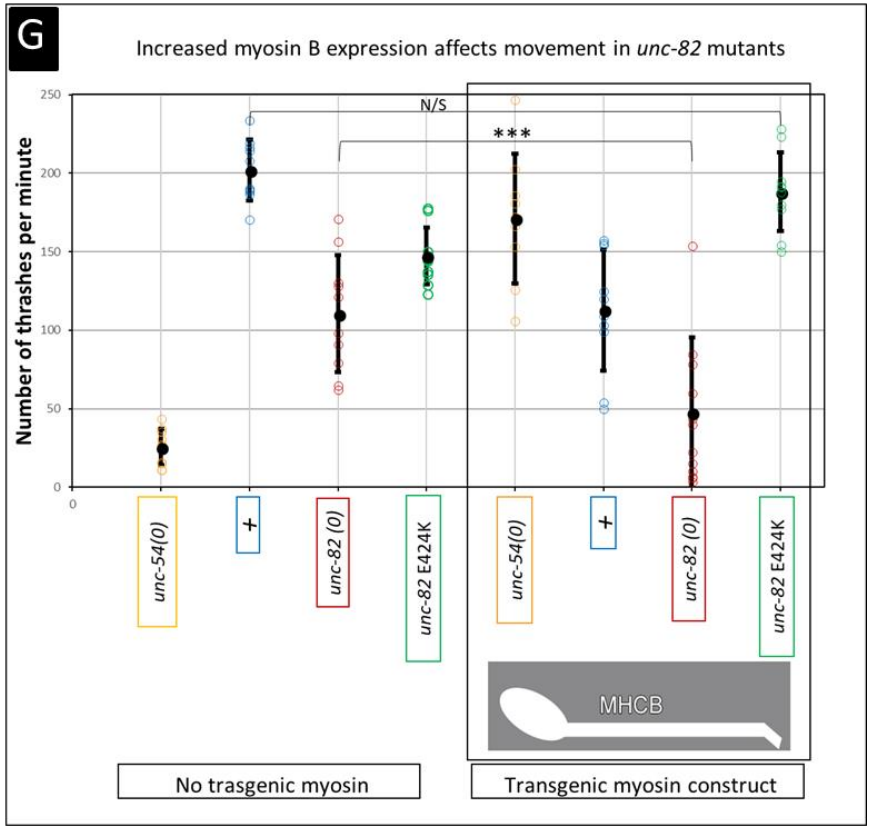
G
Increased myosin B expression affects movement in unc-82 mutants
Number of thrashes per minute
250
200
150
100
50
0
N/S
***
unc-54(0)
+
unc-82 (0)
unc-82 E424K
unc-54(0)
+
unc-82 (0)
unc-82 E424K
MHCB
No trasgenic myosin
Transgenic myosin construct

Figure 3.5: Over expression of myosin B suppresses muscle organization defects in *unc-82* mutant adults. **A**. In wild-type worms, increased expression of myosin B from the *stEx59* transgene causes mild disruption of some birefringent A-bands (rectangle in A) with a majority of A-bands appearing in the normal regular striped pattern (arrow in A). **B**. Expression of myosin B from the *stEx59* transgene in worms lacking endogenous myosin B restores muscles structure to near wild type (arrow in B). **C**. Transgenic expression of myosin B in *unc-82(0)* worms alters muscle organization with an increase in the appearance of areas of birefringent stripes (broad arrow in C) but also with abnormal birefringent accumulations in the middle (oval in C) and at the ends of muscle cells (arrow head in C). **D**. Over expression of myosin B in *unc-82* E424K mutants reduces the prevalence of distinct paramyosin accumulations at muscle cell ends (arrowhead in D) while increasing organization into stripes (arrow in D). **E-F** Differential interference contrast (DIC) and fluorescent images of typical transgenic *unc-82(0)* offspring show paralyzed larvae with failed body elongation (bracket in E and F) and an apparently normal larval sibling (rectangle in E and F). Stars indicate the position of the developed pharynx in each. **G.** Increased myosin expression affects movement in *unc-82* mutants**.** A graph depicting the rate of thrashing of *unc-82* mutants without transgenic myosin (left side) and with transgenic myosin B (right rectangle in G). Number of thrashes per minute is along the Y axis. Genotypes are color coded with each colored circle indicating a data point from a single worm. Transgenic myosin B is depicted along the x-axis as a picture. Open circles represent individual worms. Filled black circles represent mean thrashes per minute. Black bars indicate the standard deviation from the mean. *** indicates statistically significant difference in thrashes per minute between groups. N/S indicates no significant difference in thrashes per minute between groups. Rectangular box is used to separate sets of data for ease of comparison. Significance was calculated using an unpaired two tailed t-tests with unequal variance.

improved, and indistinguishable from that of wild type. Increases in myosin B or myosin A were not sufficient enough to suppress the muscle phenotype of the null *unc*-82 mutant suggesting that there may be a functional role for potions of the UNC-82 protein outside of the kinase domain. The ability of myosin B, but not myosin A, to suppress muscle cell defects in the missense *unc-82* mutant E424K suggests an isoform specific a role for UNC-82 in organizing myosin containing thick filaments that is dependent on the kinase activity.

Myosin A Requires UNC-82 Activity for Adult Movement

While double mutants lacking both myosin B and UNC-82 appear to have better paramyosin and perhaps myosin A organization within the contractile apparatus compared to single *unc-82(0)* mutants (Figure 3.2 E-H), they remain paralyzed as adults when cultured on agar, a phenotype typical of *unc-54(0)* single mutants. Thrashing assays revealed the movement of the double mutant is significantly ($p < 0.0002$) reduced compared to *unc-54(0)* (Figure 6), with the double mutant *unc-54(0); unc-82(0)* moving an average of 4.5±2.3 thrashes per minute compared to *unc-54(0)* alone, which moves an average of 25.6±11.5 thrashes per minute. *unc-54(0); unc-82* E424K adult worms had similar movement phenotypes with an average rate of 5.1±2.4 thrashes per minute ($p<0.0002$).

Expression of the myosin A transgene in myosin B and *unc-82* double mutants did not improve movement, in agreement with the poor muscle structure (Figure 3.4 F and J). The average rate of thrashing for both the *unc-54(0); unc-82(0)* and *unc-54(0); unc-82 E424K* worms expressing the myosin A transgene (*stEx80*) was not statistically different from their nontransgenic siblings with rates of 5.9±6.3 and 6.5±6.2 thrashes per minute respectively. These worms were, however, statistically slower that the *unc-54(0); stEx80* worms which had an average rate of 189.7±34 thrashes per minute $p<0.00001$ (Figure 3.6).

Attempts to establish a strain of either *unc-54(0); unc-82(0)* or *unc-54(0); unc-82* E424K expressing the myosin B transgene (*stEx59*) via mating crosses were unsuccessful and resulted in severe larval arrest in heterozygous worms. This lethality is likely a result of an imbalance in dosage amount thick filament components. We therefore injected plasmids containing a myosin B gene and a *rol-6::gfp* injection marker directly into the double mutants of *unc-54(0); unc-82(0)* and *unc*-54(0); unc-82 E424K. Green viable F1 progeny were obtained,

indicating that introducing myosin B transgene in these double mutant backgrounds can suppress the paralyzed movement phenotype of the double mutants on culture plates. These results suggest that myosin A, but not myosin B, required UNC-82 activity to form the functional thick filament arms.

Myosin A Requirement for UNC-82 Maps to the Central Region of the Rod

The differential requirement for UNC-82 observed between the two myosins prompted us to map this interaction using chimeric myosin transgenes that contain different regions of sequence from myosins A and B (Figure 3.7). Each construct had been previously shown to rescue the movement and sarcomere defects of *unc-54(0)* mutants (Fire and Waterston 1989, Hoppe and Waterston, 1996). To map the myosin A dependence on UNC-82 for filament elongation, genetic crosses were used to introduce three different chimeric myosins into double mutants lacking myosin B and UNC-82. If the chimera could rescue the movement defects in the absence of UNC-82 those portions of myosin A present were considered to not require UNC-82 activity for filament elongation. Whereas any portion of myosin A in a chimera that produced lethality or did not rescue movement was considered to have a dependence on UNC-82 activity for assembly into filament arms.

Chimera 2 contains the myosin A head and hinge region as well as N-terminal portions of the myosin A rod (M1-I1079). This chimera was sufficient to rescue movement defects in the double mutant (Figure 3.7). Assessment of thrashing of the transgenic double mutants revealed significant ($p<0.0001$) improvement compared to nontransgenic counterparts, with transgenic *unc-54(0); unc-82(0)* worms thrashing an average of 101.89±23.79 thrashes per

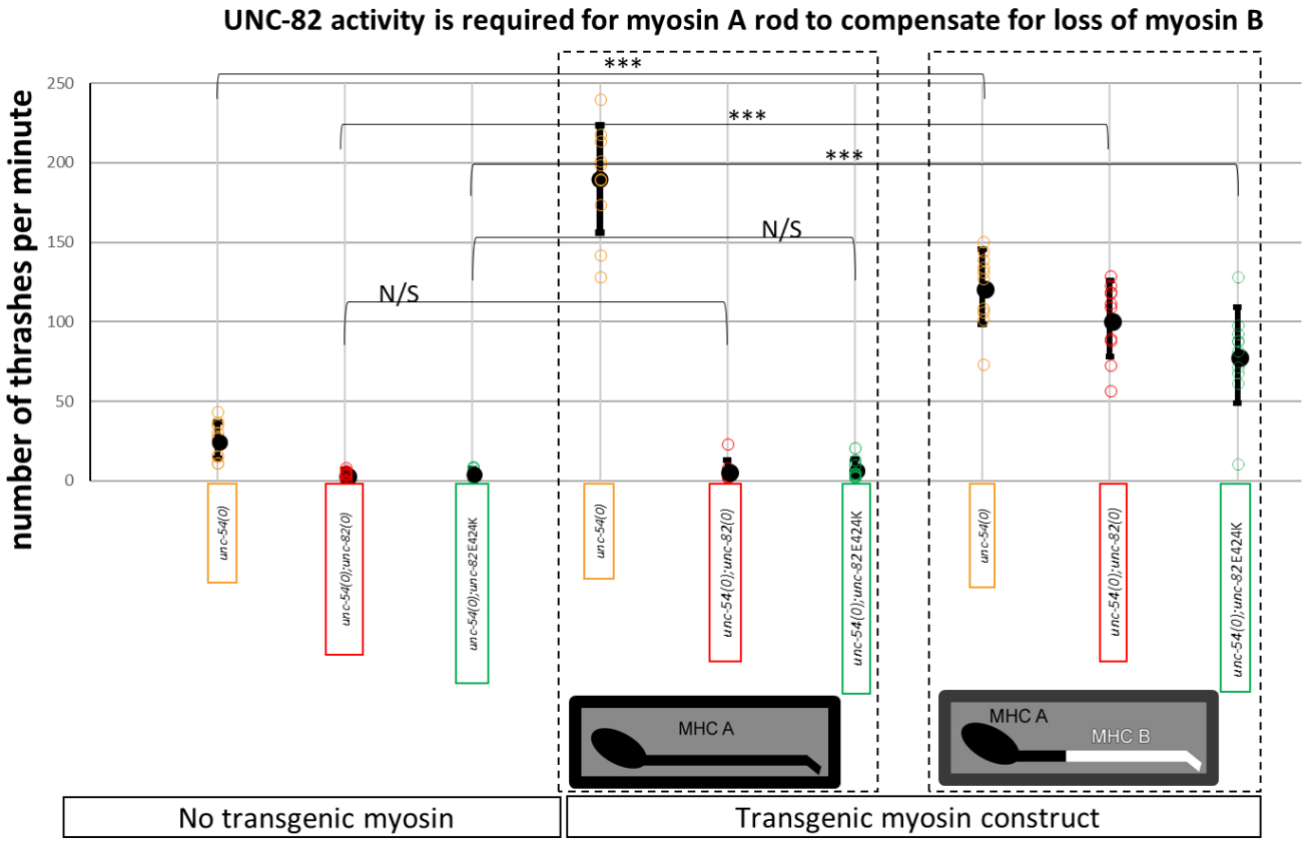

Figure 3.6. The ability of myosin B to function in the absence of UNC-82 maps to the myosin B rod. Myosin A transgene cannot restore movement in mutants lacking both myosin B and UNC-82. A graph depicting the rate of thrashing of Unc worms with transgenic myosin. Number of thrashes per minute is along the Y axis. Genotypes are color coded with each colored circle indicating a data point from a single worm. The sequence content of the myosin transgene is indicated by a schematic myosin with myosin A (MHCA, black) or myosin B (MHCB, white) portions labeled accordingly. Open circles represent individual worms. Filled black circles represent mean thrashes per minute. Black bars indicate the standard deviation from the mean. * indicates statistically significant difference in thrashes per minute between groups. N/S indicates no significant difference in thrashes per minute between groups. Dashed lines are used to separate sets of data for ease of comparison. Significance was calculated using unpaired two tailed t-tests with unequal variance.

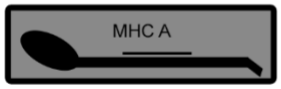

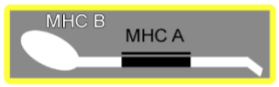

		MHC A residues	rescues lethality	Restores movement		
			myo-3(0)	*unc-54(0)*	*unc-54(0); unc-82(0)*	*unc-15(e73)*
	Myosin A (*stEx80)*	M1-L1969	+	+	-	+
	Myosin B (*stEx59*)		-	+	+	-
	Chimera 2 (*stEx85*)	M1-I1079	-	+	+	-
	Chimera 8 (*stEx87*)	D1080-Q1611	+	+	lethal	lethal
	Chimera 11 (*stEx23*)	A1612-M1933	+	+	+	+

Figure 3.7: UNC-82 interaction with myosin A maps to MHC rod. Schematic myosin molecules represent the portions of MHC A (black) and MHC B (white) included in each construct. The construct name and the extrachromosomal transgene used are shown in the second column, and the specific numbered positions of MHC A amino acids are shown in the third. The remaining four columns summarize the results of in vivo rescue experiments in different genotypes (defined as ability to rescue movement in the presence of *unc-54* mutations) in double mutant *unc-54; unc-82* worms. The data from genotypes *myo-3(0)* and *unc-54(0)* was published in Hoppe and Waterston, 1996, and the *unc-15(e73)* data was from Hoppe and Waterston 2000. While transgenic copies of either MHC isoform can compensate for the loss of myosin B in the *unc-54 single mutant,* myosin A cannot restore movement in the absence of functional *unc-82*. The portion of myosin A that requires UNC-82 and maps to the MHC rod residues 1080-1611.

minute. This increase in movement was not significantly different compared to the double mutants expressing UNC-82 E424K and this chimera (79.11±30.32 thrashes per minute). Chimera 8 contains 531 amino acids from the central region of the myosin A rod (D1080-Q1611. This chimera produced severe larval lethality with rare surviving paralyzed adults in the double mutant background (Figure 3.7). Due to lethality and fecundity issues in these worms, thrashing assays could not be performed.

Chimera 11, which is marked by a dominant rolling (Rol) phenotype, contains the C-terminal portions of the myosin A rod (A1612-M193) including the second minimal filament initiating region, region 2, flanked by myosin B head and c-terminal rod amino acid residues. This chimera rescued movement phenotypes in both double mutants tested (Figure 3.7). Due to the rolling phenotype produced by this extrachromosomal array, thrashing assays were not done. These data implicate a region within the central 531 amino acid portion of the myosin A rod located in chimera 8 as having a dependence on UNC-82 activity for filament elongation.

U**NC-82 Kinase Mediates an Interaction Between Myosin A and Paramyosin**

The proposal that myosin A requires UNC-82 to participate in elongation of the filament arms suggests that UNC-82 may mediates the interaction on myosin A with paramyosin in parallel assembly. Myosin A has an isoform-specific interaction with the paramyosin missense mutant *unc-15(e73)* that has been proposed to occur in parallel assembly. To test the hypothesis that UNC-82 is required for myosin A interactions with paramyosin, we tested if UNC-82 is required for myosin A-specific suppression of this mutant. We introduced the wild-type transgene of myosin in to double mutants of paramyosin *unc-15(e73)* and *unc-82(0)* then assessed the polarize light and movement

phenotypes of the transgenic adults (Figure 3.8). If myosin A is not dependent on UNC-82 to interact with paramyosin, then increasing myosin A expression in the *unc-15(e73)* E342K paramyosin mutant, in the absence of UNC-82, should still rescue the near paralyzed movement defects of the single mutant. Conversely, if myosin A is dependent on UNC-82 to interact with paramyosin, then the increase in myosin A expression will not suppress the. The transgene failed to improve movement or muscle structure in the double mutant (Figure 3.8 G-H). When the myosin A transgene was introduced in to *unc-15(e73); unc-82(0)* mutants no detectable changes in movement occurred, however, an enhancement in sarcomere disruption with large round amorphous accumulations in the middle of the cell and a distinct loss of birefringence in other areas of the muscle cell was observed (Figure 3.8 G-H).

To test whether other paramyosin mutants show suppression by myosin A, we introduced this same transgene into a second missense paramyosin mutant unc-15(su228). Increased expression of myosin A in this mutant background produced no detectable changes in movement or birefringent muscle structure (Figure 3.8 C-D). Introduction of this myosin A transgene did not improve the paramyosin null mutant but did alter the birefringent muscle pattern (Figure 3.8 E-F). Due to the sterility of double mutants lacking paramyosin and UNC-82, no attempts were made to introduce this transgene into that mutant background. We did attempt to introduce the myosin A transgene in to double mutants lacking paramyosin with impaired UNC-82 E424K kinase, but this attempt resulted in larval arrest (Figure 3.8 I-J).

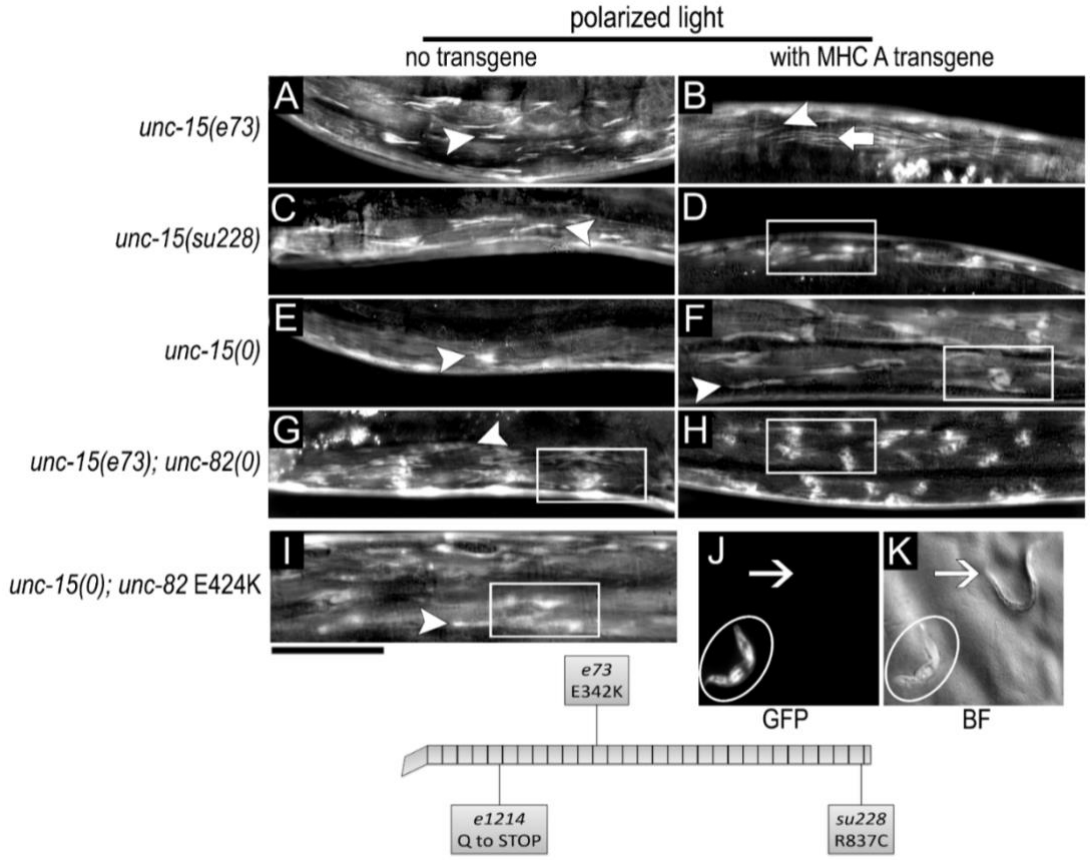

Figure 3.8: UNC-82 activity is required for myosin A suppression of paramyosin mutants. **A-F** Polarized light microscopy phenotypes of single paramyosin mutants (A, C, and E) compared to transgenic siblings (B, D, and F). The paramyosin point mutant *unc-15(e73)* contains large birefringent paramyosin accumulations at the ends of muscle cells (arrowhead in A). These same mutants expressing the myosin A transgene (*stEx80*) exhibit reduced birefringent accumulations at the ends of muscle cells (arrowhead in B) and increased birefringence in stripes throughout the cells (arrow in B). The missense paramyosin mutant *unc-15(su228)* exhibits similar large birefringent accumulations at the end of cells (arrowhead in C), which are altered but not reduced in transgenic siblings (rectangle in D). A similar alteration in birefringent accumulations at the ends of cells occurs in *unc-15(0)* in the presence of the myosin A transgene (Arrowhead in E and F). Transgenic animals also have round birefringent accumulations in the middle of the cell (rectangle in F). **G**. Paramyosin *unc-51(e73)* mutants lacking *unc-82* have muscle phenotypes that are altered compared to either mutant alone (compare G to A and Figure 2 C) with large birefringent accumulations in the middle (rectangle in G) and at the ends (arrowhead in G) of muscle cells. **H**. The transgenic *unc-15(e73); unc-82(0)* mutants are Unc, with more pronounced accumulations in the middle of the cell (rectangle in H) and no striations visible. **I**. A typical adult worm lacking paramyosin with impaired *unc-82* E424K exhibits large birefringent accumulations (arrowhead in I) at the ends of muscle cells with some birefringent anomalies (rectangle in I) in the middle of the cell. **J-K**. Early larval arrest (oval in J and K) occurs in *unc-15(0); unc-82* E424K worms expressing transgenic myosin A (*stEx80*) compared to nontransgenic siblings (arrow in J and K).

UNC-82 Co-localizes with Ectopic Myosin A Structures

With the observations that UNC-82 can associate with the contractile apparatus independently of either paramyosin and myosin B (Figure 3.1 G), and the suppression of myosin B and paramyosin mutants with increased myosin A cannot occur when UNC-82 is absent (Figures 2.4, 2.7 and 2.8), we sought to identify if UNC-82 can associate, in vivo, with myosin A. Since myosin A is required for embryonic viability, we introduced a transgene of *unc-82::gfp* into *myo-3(0)* worms carrying a rescuing myosin A transgene (*myo-3* 2SerAlaΔ25) that initiates filaments and supports movement, but also produces abnormal ectopic ball-like accumulations in muscle cells outside of the contractile apparatus that stain for both myosin A and UNC-98, but not paramyosin or myosin B (Schiller *et al.,* 2017, Hoppe *et al.,* 2010a, data not shown). We assessed embryos from this mutant strain using antibodies to myosin A and GPF to assess if UNC-82::GFP associates with these abnormal accumulations of myosin A. The staining reveals UNC-82::GFP colocalizes with the abnormal accumulations of myosin A (Figure 3.9 A-B). Supporting the hypothesis that UNC-82 can associate with myosin A in the absence of paramyosin and myosin B.

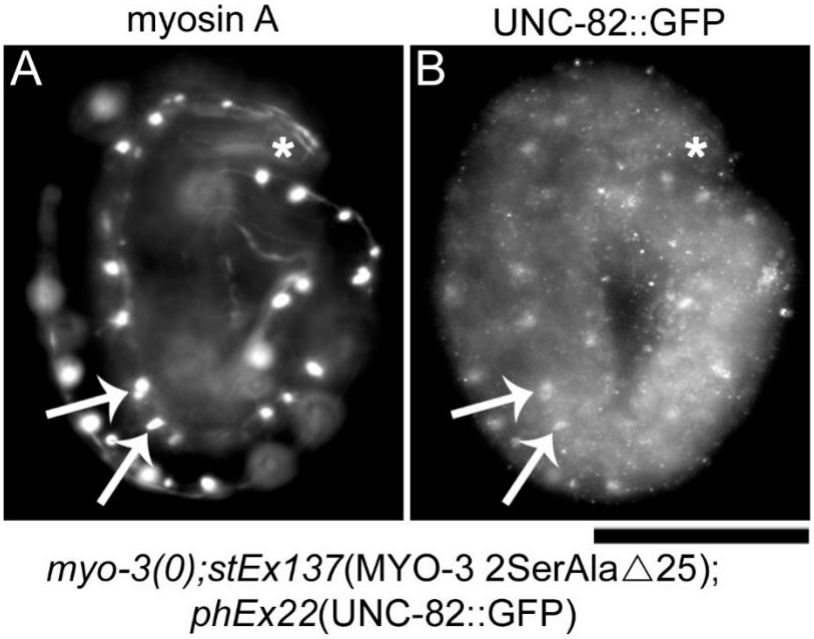

Figure 3.9: UNC-82 associates with ectopic accumulations of myosin A. **A-B.** A typical 3-fold embryo lacking wild-type myosin A, expressing transgenic UNC-82::GFP(*phEx22*), shows UNC-82::GFP associating with the ectopic myosin A balls formed as a result of the rescuing MYO-3 2SerAlaΔ25 (*stEx137*) transgenic construct (arrows). Asterisks mark the embryo head. Scale bar is 20 microns

CHAPTER 4

DISCUSSION

It has been established that UNC-82 is involved in the assembly of thick filaments, but the protein targets of this mechanism of action are not known. Antibody stains showing disorganized thick filament components in *unc-82* mutants implicate myosin A, myosin B, and paramyosin as potential targets (See Introduction). In this present study, we show that UNC-82 has an isoform-specific interaction with the myosin A rod, and this interaction is specifically required for parallel assembly between myosin A and paramyosin.

Our analysis of UNC-82 localization in transgenic single and double thick filament mutants revealed UNC-82::GFP associating in M-line like structures in muscle cells, indicating that localization of UNC-82 does not depend on any one of these proteins, or even combinations of some two proteins. Elimination of myosin B has the least effect on UNC-82 organization, whereas paramyosin organization has the greater impact on UNC-82 localization (Figure 3.1), suggesting a close interaction between UNC-82 and paramyosin. Loss of the myosin-A- and paramyosin-associating protein UNC-98 in the paramyosin null mutant background altered the appearance of UNC-82 accumulations outside of the contractile apparatus but had no obvious effect on UNC-82 organization in the region of the sarcomere (Figure 3.1). This is consistent with the role of UNC-82 being upstream of UNC-98 (Schiller *et al.,* 2017). The UNC-82 filament-like accumulations present in myosin B mutants expressing a chromosomally integrated UNC-82::GFP indicates an ability of UNC-

82 to assemble in filamentous type structures (Figure 3.1), consistent with a proposed structural role in filament assembly.

Myosin A Requires UNC-82 to Produce Functional Sarcomeres

Based on the near wild-type M-line localization pattern of UNC-82 in the absence of myosin B, we investigated the effects of UNC-82 activity on the organizational patterns of the thick filament proteins paramyosin and myosin A, when myosin B is absent. The obvious paralyzed phenotype of worms lacking this major myosin isoform helped simplify this endeavor. Initial assessment of the organizational patterns of myosin A and paramyosin in the single *unc-54(0)* mutant and the single *unc-82(0)* mutant indicated a role for myosin B and for UNC-82 in organizing paramyosin. However, when we did similar assessments in worms lacking both myosin B and UNC-82, the paramyosin organization appeared to improve. This observation suggests that the remaining myosin, myosin A, in addition to filament initiation, is able to organize paramyosin in the sarcomere of muscle cells (Figure 3.2, Miller *et al.,* 1983). These data are consistent with previous reports where increased expression of myosin A can assemble in the outer thick filament arms, and in *unc-54* mutants the myosin A can functionally substitute for myosin B, sustaining movement in adults (Riddle and Brenner, 1978; Epstein *et* al., 1986, Waterston, 1988; Hoppe and Waterston, 1996). In each of these cases, the increase in myosin A, either through a complex genomic rearrangement in the *myo-3* gene (leading to *sup-3* allele) or by transgenic expression of cloned myosin A, results in suppression of paralysis in *unc-54(0*) worms.

Myosin B Interactions with Paramyosin do not Require UNC-82 Kinase Activity

The observation that paramyosin is more disorganized when either myosin B or UNC-82 is absent than in the double mutant suggests that in the single mutants there is an aberrant interaction of paramyosin with itself or some other protein. In a previous study, we demonstrated that in the missense UNC-82 E424K mutant abnormal aggregates form that contain paramyosin, myosin B, and the kinase-impaired UNC-82 itself. We proposed that the content of these aggregates represented a stalled intermediate complex that forms in the normal assembly pathway but requires the kinase activity of UNC-82 to successfully join normal thick filaments. An alternative model is that UNC-82 and myosin B independently act to organize paramyosin, and that the presence of myosin B on paramyosin accumulations in *unc-82* E424K mutants might be due to an inappropriate interaction with myosin B and paramyosin or the mutant UNC-82 E424K protein (Schiller *et al.,* 2017). The drastically enhanced paramyosin and myosin A phenotype in *unc-82* E424K mutants that also lack myosin B (Figure 3.2) suggests that myosin B and UNC-82 act independently to organize paramyosin and raises the possibility for a function of UNC-82 that involves modulating myosin A interactions with paramyosin in thick filaments. These data are more consistent with the model that the paramyosin mislocalization defects seen in single *unc-82* E424K mutants are result of a stalled step in the assembly of paramyosin, and that the accumulation of myosin B on these structures is likely due to an interaction of myosin B with the mislocalized accumulating paramyosin.

Other instances of abnormal aggregates in muscle are reported in previously published studies of paramyosin mislocalizing M-line mutants *unc-98(sf18)*, *unc-96(sf19)*, and *unc-89(su75)*, in which UNC-82 and paramyosin and other M-line associating proteins are

present in the distinct accumulations, whereas myosin B is not. The presence of wild-type UNC-82 and lack of myosin B on the paramyosin accumulations produced by mutations in M-line associating proteins, suggest that these paramyosin accumulations are not being produced as a result of disruption of an interaction between paramyosin and UNC-82.

UNC-82 Kinase Modulates Paramyosin Interactions with Myosin A

In the absence of UNC-82, myosin A and paramyosin localization are worse than in the absence of myosin B, but not as severe as the double *unc-54(0); unc-82* E424K and not as well organized as in the double *unc-54(0); unc-82(0)* (Figure 3.1, Figure 3.2). Interestingly, increases in myosin A expression in worms lacking UNC-82, had no obvious effects on paramyosin (data not shown), marginal improvements in myosin A, and altered myosin B staining patterns (Figure 3.1, Figure 3.4). Taken together these data suggest the protective action of UNC-82 with paramyosin involves the activity of the kinase domain and a myosin-isoform specific interaction. This protective action of UNC-82 is important early in embryonic development, prior to embryonic 2-fold elongation (Figure 3.3).

We showed that myosin A can no longer replace myosin B activity in the thick filament arms when UNC-82 activity is impaired (Figure 3.4). Conversely, transgenic increases in myosin B expression can suppress the birefringent paramyosin defects of the impaired UNC-82 E424K kinase and improve movement in these mutants (Figure 3.5, Figure 3.6). However, similar to myosin A, this transgene produces synthetic lethality in worms lacking UNC-82 altogether (Figure 3.4, Figure 3.5, Table 3.1). Because extra myosin B suppresses defects in the kinase-impaired, but not the null *unc-82* mutant, this implicates a special function of UNC-82 protein regions outside of the kinase domain in the organization of

thick filament components. This premise is further supported by the ability of increased myosin A expression to improve the paramyosin defects in double mutants lacking myosin B with impaired UNC-82 E424K kinase activity (Figure 3.4). In these transgenic double mutants, the birefringent accumulations are drastically reduced but the worm remains paralyzed (Figure 3.4, Figure 3.6). It is likely that C-terminal residues of UNC-82, outside of the kinase domain, are required for the myosin A isoform specific interaction with paramyosin resulting in this improvement in muscle cell birefringence.

UNC-82 Associates with the Middle Region of the Myosin A Rod

We mapped the myosin A specific interaction with UNC-82, by introducing chimeric myosin transgenes, which contain different portions of myosin A and myosin B sequences, into paralyzed double mutants that lack myosin B and have either the null or missense unc-82 mutation and asked if the constructs could rescue the movement defects. Constructs containing the myosin A rod 531 amino acid residues D1080-Q1611 (both full length myosin A and chimera 8) were not able to rescue movement in these double mutants (Figure 3.6, and 2.7). The full-length myosin A has been previously shown to suppress the paramyosin missense mutant *unc-15(e73)* E342K (Riddle and Brenner, 1978; Waterston *et al.*, 1982; Brown and Riddle, 1985, Hoppe and Waterston, 2000). The mechanism of mis-assembly in the *unc-15(e73)* E342K mutants is thought to include preferential association between the positively charged lysine introduced by the *e73* mutation and a negatively charged glutamic acid that is normally present in the C-terminal paramyosin rod (Gengyo-Ando and Kagawa, 1991). The mechanism of suppression by increased myosin A expression is hypothesized to be due to increasing myosin A expression to a level that

mitigates the preferential assembly of the mutant paramyosin with itself by outcompeting the mutant paramyosin in a manner that involves parallel rod associations (Kagawa *et al.*, 1989, Hoppe and Waterston 1996, 2000, Figure 3.7). This ability to suppress *e73* is lost when UNC-82 is absent (Figure 3.8). This loss suggests a role for UNC-82 in mediating the parallel rod associations between myosin A and the mutant paramyosin protein. Further, in double mutants lacking myosin B and functional UNC-82, the inability for increased myosin A to assemble into the filament arms in a manner that can sustain movement may be due to similar disruptions in the parallel assembly interactions between myosin A and paramyosin. Taken together these data have resulted in the refinement of a thick filament elongation model in which myosin A associates with UNC-82 prior to association with paramyosin and myosin B (Figure 4.1).

Myosin A rod residues N1348-Q1611 (Region 1), within the 531-amino acid region of Chimera 8, have been shown to confer myosin A specific functions, antiparallel myosin A rod associations in initiating filaments (Hoppe and Waterston, 1996). This chimera induces lethality in double mutants lacking myosin B and UNC-82 activity (Figure 3.7). Similarly, this chimera is lethal in paramyosin missense *unc-15(e73)* mutants (Hoppe and Waterston 2000, Figure 3.7). This synthetic lethality is likely due to an imbalance of thick filament components. Here we have shown that larval arrest and sterility phenotypes result from disruptions in the stoichiometric relationships between myosin A and other thick filament associating proteins such as myosin B, UNC-89, UNC-98, and UNC-82 (Table 4.1; Schiller et al 2017). Given the similarity in these results, and the role of UNC-82 in organizing paramyosin, it is possible that the lethality produced in these two different genetic backgrounds is due to similar inappropriate interactions with this construct and

paramyosin. This interaction likely requires UNC-82 Kinase activity and the site of the *e73* mutation, the glutamic acid at position 342 in the paramyosin rod. The failure of extra myosin A to suppress a missense allele with a mutation near the C-terminus of paramyosin is further support for the *e73* site being involved in the interaction with myosin A. The proposed involvement of UNC-82 in the interaction of myosin A with the e73 site of paramyosin is supported by the inability of myosin A to suppress the *unc-15(e73)* mutant muscle phenotype when UNC-82 is absent (Figure 3.8).

UNC-82 can Associate with Myosin A Outside of the Contractile Apparatus

Here we show that UNC-82 can interact with ectopic accumulations that form in muscle cells outside of the region of the sarcomere as a result of worms expressing myosin A molecules that lack myosin tail phosphorylation motifs (Ser2AlaΔ25, *stEx137*) (Hoppe *et al.*, 2010a; Figure 3.9). The only other known component of these accumulations is UNC-98 (Schiller *et al.,* 2017). The association of UNC-82 protein with these ectopic accumulations of myosin A supports a direct association between myosin A and UNC-82. If the myosin A tailpiece, which contains several putative phosphorylation sites is a target of UNC-82, the accumulations may be a result of UNC-82 lacking the ability to phosphorylate myosin A to modulate the parallel rod interactions with paramyosin. Alternatively, these ectopic accumulations may be driven by an inappropriate interaction of mutant Ser2AlaΔ25 myosin A with a stalled UNC-82 protein.

Given the requirement of the two mammalian UNC-82 orthologues ARK5/NUAK1 and SNARK/NUAK2 in mammalian muscle (See Introduction, Hoppe *et al.,* 2010a; Inazuka *et al.*, 2012; Lessard *et al.,* 2016), the results of this study suggest the role of UNC-

82/ARK-5/SNARK in modulating assembly of myosins into thick filament structures is conserved between invertebrates and vertebrate animals.

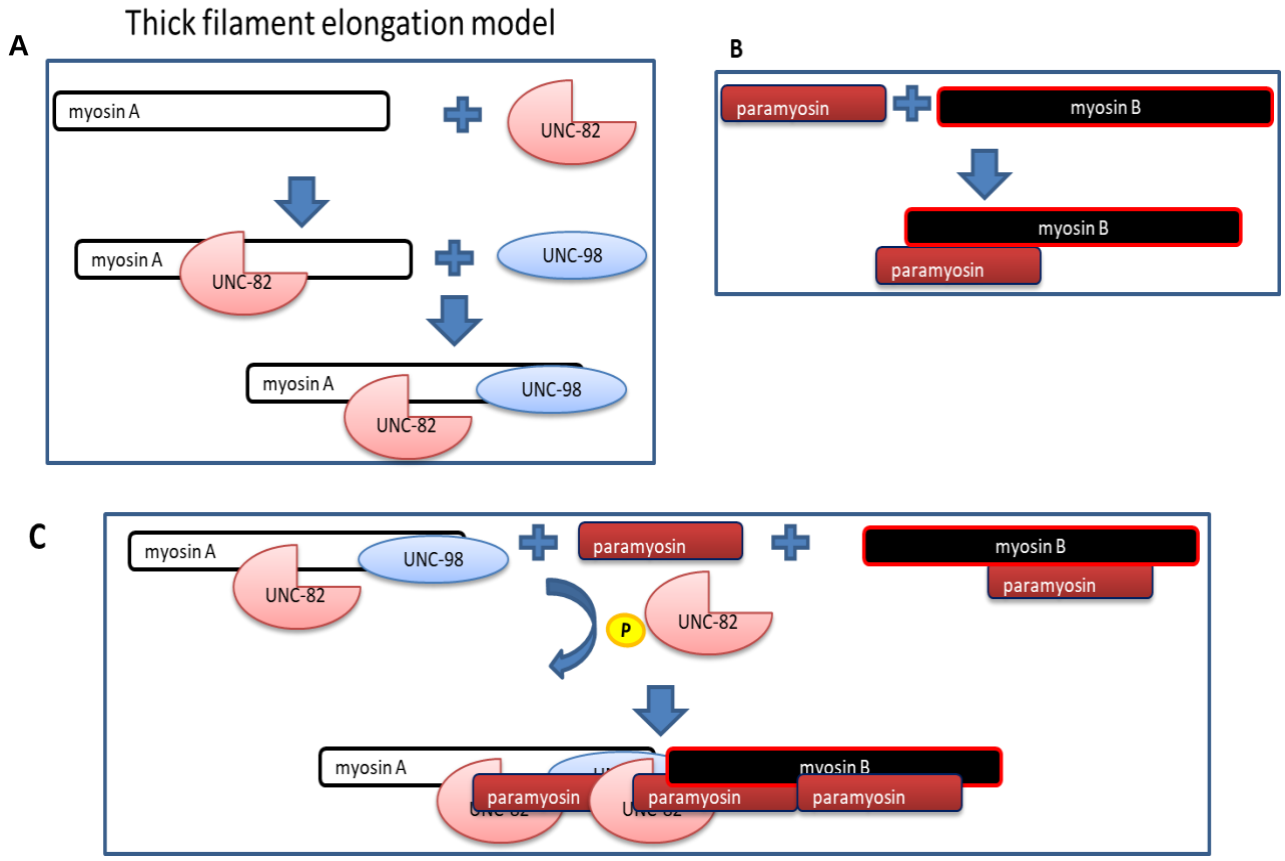

Figure 4.1: Model for the order of thick filament associating protein interactions during early thick filament elongation. **A**. UNC-82 and myosin A associate with newly made paramyosin. **B.** Complexes of myosin B: paramyosin and UNC_82:myosin A:paramyoisin associate. **C.** UNC-82 kinase activity promotes the association of the UNC-82:paramyoisin:myosin B complex with a complex of myosin A:UNC-98 forming the thick filament.

Table 4.1: Synthetic non-viable thick filament genotype combinations

genotype	Sarcomere protein state	Synthetic non-viable phenotype
myo-3(0)	no MHC A	severe larval arrest
unc-54(0); unc-98(0)	no MHC B, no UNC-98	severe larval arrest
unc-15(0); unc-98(0)	no paramyosin, no UNC-98	Sterile adult
unc-54(0); unc-15(0)	no MHC B, no paramyosin	severe larval arrest
unc-89(su75); unc-82(0)	Kinase inactive UNC-89, no UNC-82	severe larval arrest
unc-15(0); unc-82(0)	no paramyosin, no UNC-82	Sterile adult
unc-54(0); unc-82::gfp	no MHC B, increased UNC-82	severe larval arrest
unc-15(0); unc-82::gfp	no paramyosin, increased UNC-82	severe larval arrest
unc-15(e73); unc-82::gfp	mislocalized paramyoinsin, increased UNC-82	severe larval arrest
unc-15(su228); unc-82::gfp	mislocalized paramyoinsin, increased UNC-82	severe larval arrest
unc-82(0); stEx80	no UNC-82 and increased myosin A	mild larval arrest
unc-82(0); stEx59	no UNC-82 and increased myosin B	severe larval arrest
unc-54(0)/+; unc-82(0); stEx59	no UNC-82 and increased myosin B	severe larval arrest
unc-54(0)/+; unc-82 E424K*; stEx59*	Impaired UNC-82 and increased myosin B	severe larval arrest
unc-54(0);unc-82(0); stEx87	no myosin B, no UNC-82, expressing chimeric myosin B with central myosin A rod residues D1080-Q1611	severe larval arrest
unc-54(0); unc-82(e1220); stEx87	no myoisn B, kinase impaired UNC-82, expressing chimeric myosin B with central myosin A rod residues D1080-Q1611	severe larval arrest
unc-15(0); unc-82(e1220); stEx80	no paramyoins, kinase impaired UNC-82, increased myosin A	severe larval arrest

Table 4.1: Synthetic non-viable thick filament genotype combinations. Genotypes are depicted in the column on the left. The null alleles are as follows: *myo-3(st386)*, *unc-54(e190)*, *unc-98(sf19)*, *unc-15(e1214)*, and *unc-82(e1323).* UNC-82::GFP refers to either the *phEx22* or the uv-integrated *phex21*(*phIs2*) transgenes. The state of sarcomere protein products as a result of the alleles is depicted in the center column. The phenotype produced as a result of the abnormal protein interactions is listed in the column on the right. All genotypes that displayed arrest occurred at the L3 stage or younger. Sterile adults were defined as worms with fully developed gonads but did not produce viable fertilized eggs.

CHAPTER 5

CONCLUSION

The mechanism of development and the maintenance of the complex sarcomeres of striated muscle is of great importance to those interested in the public health issues related to skeletal muscle, diabetes, and heart disease. Sarcomeres require a careful balance between ATP production and subsequent consumption for sustaining contractions throughout the life of humans, this intimate connection raises the possibility of the existence of a protein that serves to regulate this interaction and contribute to the structural organization of the sarcomere. Both ARK5 and SNARK were identified based on their highly conserved sequence identity to AMPK kinases which are well-studied enzymatic sensors of intracellular adenosine nucleotide levels and promote metabolic ATP production under stress or glucose starvation conditions. Sequence comparisons of ARK5 and SNARK suggest that the activation of each enzyme occurs by different mechanisms. SNARK lacks the phosphorylation site for the metabolic regulatory serine/threonine kinase, Akt. Whereas ARK5 contains these residues, and has been shown, in human cell lines, to be activated by phosphorylation at this site by Akt in conditions of glucose starvation. In *C. elegans,* UNC-82 can also be found in isoform populations that differ in the presence or absence of this Akt regulatory phosphorylation site. While theses mammalian orthologues are both expressed in muscle, studies of muscle-specific single-gene knock outs or of expression of a dominant-negative SNARK construct have not reported changes in the structure of muscle cells. The role of these proteins in muscle structure has likely been over

looked in muscle-specific targeting assays due to expression of the paralog protein, which may act redundantly to organize myosin thick filaments. Redundant function of ARK5/NUAK1 and SNARK/NUAK2 has been demonstrated for the nonmuscle myosin II- dependent cell shape changes that drive folding of embryonic epithelial sheets during morphogenesis (Ohmura *et al.,* 2012). In double mutant mouse neuroepithelium tissue, early embryonic reduction in localization of phosphorylated myosin light chain II to the apical surface, but not a reduction in overall phosphorylation levels of the myosin light chain, was evident and is consistent with both ARK5/NUAK1 and SNARK/NUAK2 having a redundant role in regulation of nonmuscle myosin II. The mechanism by which ARK5/NUAK1 regulates nonmuscle myosin is proposed to include inhibition of the myosin phosphatase (MYPT), which regulates phosphorylation levels of nonmuscle myosin light chain (Zagorska *et al.,* 2010). SNARK/NUAK2 is also reported to control nonmuscle myosin by acting on myosin light chain in HeLa cells and Human U2OS osteosarcoma cells (Vallenius *et al.* 2011). These studies suggest there may be conserved elements in the roles of UNC-82/ARK5/SNARK/NUAK kinases in regulating both metabolism and myosin II activity in muscle and nonmuscle cells. The results presented in this study have identified a potential molecular link between myosin filament organization, and metabolic syndromes such as diabetes.

Future Work

Metabolic function research in *C. elegans* has previously looked at the role of metabolism through insulin signaling and glycolytic flux and their effects on lifespan, yet none have addressed metabolic function looking at muscle specific protein function. In this study, I

have provided evidence that links the structure and function of muscles with that of metabolic flux through the function of the UNC-82/ARK5/SNARK kinase and its structural interactions with myosin II rods. A rather straightforward experiment would be to test various thick filament affecting mutants for differences in glycolytic flux patterns. Additionally, since NUAK1 is preferentially expressed in cardiac tissue, using an atrial cardiomyocyte cell line (HL-1) derived from mice would be a great tool for investigating the role of these proteins in mammalian muscle organization as well as the thick filament mutations and their impact on the metabolic activity of these cell. Results from these proposed experiments would help bridge our knowledge and possibly identify a direct protein link between sarcomere structure and metabolic function, and thus advance our understanding of the relationship between metabolic syndromes, like diabetes, and cardiomyopathies.

APPENDIX

Genetics Society of America LICENSE TERMS AND CONDITIONS

May 16, 2018

This is a License Agreement between Lee Dion - Production Test Customer ("You") and Genetics Society of America ("Genetics Society of America") provided by Copyright Clearance Center ("CCC"). The license consists of your order details, the terms and conditions provided by Genetics Society of America, and the payment terms and conditions.

All payments must be made in full to CCC. For payment instructions, please see information listed at the bottom of this form.

License Number	4350260881683
License date	May 15, 2018
Licensed content publisher	Genetics Society of America
Licensed content title	Genetics
Licensed content date	Dec 31, 1969
Type of Use	Thesis/Dissertation
Requestor type	Author of requested content
Format	Print, Electronic
Portion	chapter/article
The requesting person/organization is:	NaTasha R. Schiller
Title or numeric reference of the portion(s)	Full Article
Title of the article or chapter the portion is from	The Role of the UNC-82 Protein Kinase in Organizing Myosin Filaments in Striated Muscle of Caenorhabditis elegans pp 1195-1213
Editor of portion(s)	N/A
Author of portion(s)	NaTasha R. Schiller, Christopher D. Duchesneau, Latrisha S. Lane, April R. Reedy, Emily R. Manzon and Pamela E. Hoppe
Volume of serial or monograph.	205
Issue, if republishing an article from a serial	3
Page range of the portion	
Publication date of portion	March 2017
Rights for	Main product
Duration of use	Life of current edition
Creation of copies for the disabled	no
With minor editing privileges	no
For distribution to	Worldwide
In the following language(s)	Original language of publication
With incidental promotional use	no

The lifetime unit quantity of new product	Up to 999
Title	MYOSIN ASSEMBLY INTO ELONGATING THICK FILAMENTS IS DEPENDENT ON THE FUNCTION OF CONSERVED APMK-RELATED KINASE UNC-82 IN C. ELEGANS
Instructor name	Pamela Hoppe
Institution name	Western Michigan University
Expected presentation date	May 2018
Order reference number	CAO2755
Billing Type	Invoice
Billing Address	Lee Dion 222 Rosewood Drive Danvers, MA 01902 United States Attn: Lee Dion
Total (may include CCC user fee)	0.00 USD
Terms and Conditions	

TERMS AND CONDITIONS

The following terms are individual to this publisher:

None

Other Terms and Conditions:

STANDARD TERMS AND CONDITIONS

1. Description of Service; Defined Terms. This Republication License enables the User to obtain licenses for republication of one or more copyrighted works as described in detail on the relevant Order Confirmation (the "Work(s)"). Copyright Clearance Center, Inc. ("CCC") grants licenses through the Service on behalf of the rightsholder identified on the Order Confirmation (the "Rightsholder"). "Republication", as used herein, generally means the inclusion of a Work, in whole or in part, in a new work or works, also as described on the Order Confirmation. "User", as used herein, means the person or entity making such republication.

2. The terms set forth in the relevant Order Confirmation, and any terms set by the Rightsholder with respect to a particular Work, govern the terms of use of Works in connection with the Service. By using the Service, the person transacting for a republication license on behalf of the User represents and warrants that he/she/it (a) has been duly authorized by the User to accept, and hereby does accept, all such terms and conditions on behalf of User, and (b) shall inform User of all such terms and conditions. In the event such person is a "freelancer" or other third party independent of User and CCC, such party shall be deemed jointly a "User" for purposes of these terms and conditions. In any event, User shall be deemed to have accepted and agreed to all such terms and conditions if User republishes the Work in any fashion.

3. Scope of License; Limitations and Obligations.

3.1 All Works and all rights therein, including copyright rights, remain the sole and exclusive property of the Rightsholder. The license created by the exchange of an Order Confirmation (and/or any invoice) and payment by User of the full amount set forth on that document includes only those rights expressly set forth in the Order Confirmation and in these terms and conditions, and conveys no other rights in the Work(s) to User. All rights not expressly granted are hereby reserved.

3.2 General Payment Terms: You may pay by credit card or through an account with us payable at the end of the month. If you and we agree that you may establish a standing

account with CCC, then the following terms apply: Remit Payment to: Copyright Clearance Center, 29118 Network Place, Chicago, IL 60673-1291. Payments Due: Invoices are payable upon their delivery to you (or upon our notice to you that they are available to you for downloading). After 30 days, outstanding amounts will be subject to a service charge of 1-1/2% per month or, if less, the maximum rate allowed by applicable law. Unless otherwise specifically set forth in the Order Confirmation or in a separate written agreement signed by CCC, invoices are due and payable on "net 30" terms. While User may exercise the rights licensed immediately upon issuance of the Order Confirmation, the license is automatically revoked and is null and void, as if it had never been issued, if complete payment for the license is not received on a timely basis either from User directly or through a payment agent, such as a credit card company.

3.3 Unless otherwise provided in the Order Confirmation, any grant of rights to User (i) is "one-time" (including the editions and product family specified in the license), (ii) is non-exclusive and non-transferable and (iii) is subject to any and all limitations and restrictions (such as, but not limited to, limitations on duration of use or circulation) included in the Order Confirmation or invoice and/or in these terms and conditions. Upon completion of the licensed use, User shall either secure a new permission for further use of the Work(s) or immediately cease any new use of the Work(s) and shall render inaccessible (such as by deleting or by removing or severing links or other locators) any further copies of the Work (except for copies printed on paper in accordance with this license and still in User's stock at the end of such period).

3.4 In the event that the material for which a republication license is sought includes third party materials (such as photographs, illustrations, graphs, inserts and similar materials) which are identified in such material as having been used by permission, User is responsible for identifying, and seeking separate licenses (under this Service or otherwise) for, any of such third party materials; without a separate license, such third party materials may not be used.

3.5 Use of proper copyright notice for a Work is required as a condition of any license granted under the Service. Unless otherwise provided in the Order Confirmation, a proper copyright notice will read substantially as follows: "Republished with permission of [Rightsholder's name], from [Work's title, author, volume, edition number and year of copyright]; permission conveyed through Copyright Clearance Center, Inc. " Such notice must be provided in a reasonably legible font size and must be placed either immediately adjacent to the Work as used (for example, as part of a by-line or footnote but not as a separate electronic link) or in the place where substantially all other credits or notices for the new work containing the republished Work are located. Failure to include the required notice results in loss to the Rightsholder and CCC, and the User shall be liable to pay liquidated damages for each such failure equal to twice the use fee specified in the Order Confirmation, in addition to the use fee itself and any other fees and charges specified.

3.6 User may only make alterations to the Work if and as expressly set forth in the Order Confirmation. No Work may be used in any way that is defamatory, violates the rights of third parties (including such third parties' rights of copyright, privacy, publicity, or other tangible or intangible property), or is otherwise illegal, sexually explicit or obscene. In addition, User may not conjoin a Work with any other material that may result in damage to the reputation of the Rightsholder. User agrees to inform CCC if it becomes aware of any infringement of any rights in a Work and to cooperate with any reasonable request of CCC or the Rightsholder in connection therewith.

4. Indemnity. User hereby indemnifies and agrees to defend the Rightsholder and CCC, and their respective employees and directors, against all claims, liability, damages, costs and expenses, including legal fees and expenses, arising out of any use of a Work beyond the scope of the rights granted herein, or any use of a Work which has been altered in any unauthorized way by User, including claims of defamation or infringement of rights of copyright, publicity, privacy or other tangible or intangible property.

5. Limitation of Liability. UNDER NO CIRCUMSTANCES WILL CCC OR THE RIGHTSHOLDER BE LIABLE FOR ANY DIRECT, INDIRECT, CONSEQUENTIAL OR INCIDENTAL DAMAGES (INCLUDING WITHOUT LIMITATION DAMAGES FOR LOSS OF BUSINESS PROFITS OR INFORMATION, OR FOR BUSINESS INTERRUPTION) ARISING OUT OF THE USE OR INABILITY TO USE A WORK, EVEN IF ONE OF THEM HAS BEEN ADVISED OF THE POSSIBILITY OF SUCH DAMAGES. In any event, the total liability of the Rightsholder and CCC (including their respective employees and directors) shall not exceed the total amount actually paid by User for this license. User assumes full liability for the actions and omissions of its principals, employees, agents, affiliates, successors and assigns.

6. Limited Warranties. THE WORK(S) AND RIGHT(S) ARE PROVIDED "AS IS". CCC HAS THE RIGHT TO GRANT TO USER THE RIGHTS GRANTED IN THE ORDER CONFIRMATION DOCUMENT. CCC AND THE RIGHTSHOLDER DISCLAIM ALL OTHER WARRANTIES RELATING TO THE WORK(S) AND RIGHT(S), EITHER EXPRESS OR IMPLIED, INCLUDING WITHOUT LIMITATION IMPLIED WARRANTIES OF MERCHANTABILITY OR FITNESS FOR A PARTICULAR PURPOSE. ADDITIONAL RIGHTS MAY BE REQUIRED TO USE ILLUSTRATIONS, GRAPHS, PHOTOGRAPHS, ABSTRACTS, INSERTS OR OTHER PORTIONS OF THE WORK (AS OPPOSED TO THE ENTIRE WORK) IN A MANNER CONTEMPLATED BY USER; USER UNDERSTANDS AND AGREES THAT NEITHER CCC NOR THE RIGHTSHOLDER MAY HAVE SUCH ADDITIONAL RIGHTS TO GRANT.

7. Effect of Breach. Any failure by User to pay any amount when due, or any use by User of a Work beyond the scope of the license set forth in the Order Confirmation and/or these terms and conditions, shall be a material breach of the license created by the Order Confirmation and these terms and conditions. Any breach not cured within 30 days of written notice thereof shall result in immediate termination of such license without further notice. Any unauthorized (but licensable) use of a Work that is terminated immediately upon notice thereof may be liquidated by payment of the Rightsholder's ordinary license price therefor; any unauthorized (and unlicensable) use that is not terminated immediately for any reason (including, for example, because materials containing the Work cannot reasonably be recalled) will be subject to all remedies available at law or in equity, but in no event to a payment of less than three times the Rightsholder's ordinary license price for the most closely analogous licensable use plus Rightsholder's and/or CCC's costs and expenses incurred in collecting such payment.

8. **Miscellaneous.**

8.1 User acknowledges that CCC may, from time to time, make changes or additions to the Service or to these terms and conditions, and CCC reserves the right to send notice to the User by electronic mail or otherwise for the purposes of notifying User of such changes or additions; provided that any such changes or additions shall not apply to permissions already secured and paid for.

8.2 Use of User-related information collected through the Service is governed by CCC's privacy policy, available online here:
http://www.copyright.com/content/cc3/en/tools/footer/privacypolicy.html.

8.3 The licensing transaction described in the Order Confirmation is personal to User. Therefore, User may not assign or transfer to any other person (whether a natural person or an organization of any kind) the license created by the Order Confirmation and these terms and conditions or any rights granted hereunder; provided, however, that User may assign such license in its entirety on written notice to CCC in the event of a transfer of all or substantially all of User's rights in the new material which includes the Work(s) licensed under this Service.

8.4 No amendment or waiver of any terms is binding unless set forth in writing and signed by the parties. The Rightsholder and CCC hereby object to any terms contained in any writing prepared by the User or its principals, employees, agents or affiliates and purporting to govern or otherwise relate to the licensing transaction described in the Order

Confirmation, which terms are in any way inconsistent with any terms set forth in the Order Confirmation and/or in these terms and conditions or CCC's standard operating procedures, whether such writing is prepared prior to, simultaneously with or subsequent to the Order Confirmation, and whether such writing appears on a copy of the Order Confirmation or in a separate instrument.

8.5 The licensing transaction described in the Order Confirmation document shall be governed by and construed under the law of the State of New York, USA, without regard to the principles thereof of conflicts of law. Any case, controversy, suit, action, or proceeding arising out of, in connection with, or related to such licensing transaction shall be brought, at CCC's sole discretion, in any federal or state court located in the County of New York, State of New York, USA, or in any federal or state court whose geographical jurisdiction covers the location of the Rightsholder set forth in the Order Confirmation. The parties expressly submit to the personal jurisdiction and venue of each such federal or state court.If you have any comments or questions about the Service or Copyright Clearance Center, please contact us at 978-750-8400 or send an e-mail to info@copyright.com.

v 1.1

Questions? customercare@copyright.com or +1-855-239-3415 (toll free in the US) or +1-978-646-2777.

BIBLIOGRAPHY

Amburgey, K, *et al.,* 2011. *Prevalence of congenital myopathies in a representative pediatric United States population.* Ann. Neurol. 70 (4) 662–665.

Benian G.M., Tinley T.L., Tang X., Borodovsky M., 1996 *The Caenorhabditis elegans gene unc-89, required for muscle M-line assembly, encodes a giant modular protein composed of Ig and signal transduction domains*. J Cell Biol. 132: 835-48.

Brenner S., 1974 *The genetics of Caenorhabditis elegans*. Genetics. 77: 71-94.

Brown, S. J., and D. L. Riddle., 1985 *Gene interactions affecting muscle organization in Caenorhabditis elegans.* Genetics. 110: 421-440.

Castellani L, Cohen C, 1987 *Rod phosphorylation favors folding in a catch muscle myosin*. Proc Natl Acad Sci USA 84(12):4058–4062.

Clark KA, McElhinny AS, Beckerle MC, Gregorio CC. 2002 *Striated muscle cytoarchitecture: an intricate web of form and function*. Annu Rev Cell Dev Biol. 18:637–706.

Cohen, C., D. E. Lanar, and D. A. D. Parry, 1987 *Amino acid sequence and structural repeats in schistosome paramyosin match those of myosin*. Biosci. Rep. 7: 11-16.

Deitiker, P. R., and H. F. Epstein, 1993 *Thick filament substructures in Caenorhabditis elegans: evidence for two populations of paramyosin.* J. Cell Biol. 123: 303–311.

Dey, C. S., P. R. Deitiker, & H. F. Epstein, 1992. *Assembly-dependent phosphorylation of myosin and paramyosin of native thick filaments in Caenorhabditis elegans.* Biochem Biophys Res Commun, 186: 1528-32.

Epstein H. F., R. H. Waterston, S. Brenner, 1974 *A mutant affecting the heavy chain of myosin in Caenorhabditis elegans.* J Mol Biol. 90(2): 291-300.

Epstein, H. F., D. M. Miller, I. Ortiz and G. C. Berliner, 1985 *Myosin and paramyosin are organized about a newly identified the core structure.* J. Cell Biol. 100: 904–915.

Epstein, H. F., I. Ortiz, and G. C. Berliner, 1987 *Assemblages of multiple thick filaments in nematode mutants.* J. Muscle Res. Cell, Motil. 8: 527-536.

Fukuzawa A., Lange S., Holt M., Vihola A., Carmignac V., Ferreiro A., Udd B., Gautel M. 2008. *Interactions with titin and myomesin target obscurin and obscurin-like 1 to the M-band: implications for hereditary myopathies*. J. Cell Sci. 121, 1841–1851

Gautel M. (2011). *The sarcomeric cytoskeleton: who picks up the strain?* Curr. Opin. Cell Biol. 23, 39–46

Gieseler, K., Qadota, H., and Benian, G.M. *Development, structure, and maintenance of C. elegans body wall muscle* (August 23, 2016), WormBook, ed. The C. elegans Research Community, WormBook, doi/10.1895/wormbook.1.81.2, http://www.wormbook.org.

Geisler S. B., Robinson D., Hauringa M., Raeker M. O., Borisov A. B., Westfall M. V., Russell M. W. (2007). *Obscurin-like 1, OBSL1, is a novel cytoskeletal protein related to obscurin.* Genomics 89, 521–531

Gengyo-Ando, K., and H. Kagawa, 1991 *Single charge change on the helical surface of the paramyosin rod dramatically disrupts thick filament assembly in Caenorhabditis elegans*. J. Mol, Biol. 219: 429-441.

Gibbs, C. S., and M. J. Zoller, 1991 *Rational scanning mutagenesis of a protein kinase identifies functional regions involved in catalysis and substrate interactions.* J. Biol. Chem. 266: 8923–8931.

Goldstein MA, Schroeter JP, Sass RL. 1990 *Two structural states of the vertebrate Z band*. Electron Microsc Rev. 3:227–248.

Hikita, T., Qadota, H., Tsuboi, D., Taya, S., Moerman, D. G., and Kaibuchi, K. 2005 *Identification of a novel Cdc42 GEF that is localized to the PAT-3-mediated adhesive structure*. Biochem. Biophys. Res. Commun. 335:139–145.

Hoppe, P. E. and R. H. Waterston, 1996. *Hydrophobicity variations along the surface of the coiled-coil rod may mediate striated muscle myosin assembly in Caenorhabditis elegans.* J Cell Biol. 135: 371-382.

Hoppe, P. E., and R. H. Waterston, 2000 *A region of the myosin rod important for interaction with paramyosin in Caenorhabditis elegans striated muscle.* Genetics. 156: 631–643.

Hoppe, P. E., R. C. Andrews and P. D. Parikh, 2003 *Differential requirement for the nonhelical tailpiece and the C-terminus of the myosin rod in C. elegans muscle*. Mol. Biol. Cell 14: 1677–1690

Hoppe P. E., J. Chau, K. A. Flanagan, A. R. Reedy, L. A. Schriefer, 2010a *Caenorhabditis elegans unc-82 encodes a serine/threonine kinase important for myosin filament organization in muscle during growth.* Genetics. 184: 79–90.

Hoppe, P. E., R. J. Heustis, K. A. Flanagan, and A. R. Reedy, 2010b *Phosphorylation Motifs in the Nonhelical Domains of Myosin Heavy Chain and Paramyosin May Negatively Regulate Assembly in Caenorhabditis elegans Striated Muscle.* Cytoskeleton. 67: 309–321

Hou, X., J.E. Liu, W. Liu, C.Y. Liu, Z.Y. Liu and Z.Y. Sun, 2011 *A new role of NUAK1: directly phosphorylating p53 and regulating cell proliferation.* Oncogene. 30: 2933-2942.

Huse M. and J. Kuriyan Cell. 2002 *The conformational plasticity of protein kinases.* Cell. 109: 275-82

Hutter H., M. P. Ng, and N. Chen. 2009 *GExplore: a web server for integrated queries of protein domains, gene expression and mutant phenotypes.* BMC Genomics. 10: 529

Inazuka F., N. Sugiyama, M. Tomita, T. Abe, G. Shioi, and H. Esumi, 2012 *Muscle-specific knock-out of NUAK family SNF1-like kinase 1 (NUAK1) prevents high fat diet-induced glucose intolerance.* J Biol Chem. 287: 16379-16389

Iyer G.H., Garrod, S., Woods Jr V.L., and S. S. Taylor, 2005 *Catalytic independent funcitons of a protein kinase as revealed by a kinase-dead mutant: study of the Lys72His mutant of cAMP-dependent kinase*. J Mol Biol. 351: 1110-1122.

Johnson L. N., and R. J. Lewis, 2001 *Structural basis for control by phosphorylation.* Chem Rev. 101:2209-42.

Kagawa, H., K. Gengyo, A. D. McLachlan, S. Brenner and J. Karn, 1989 *Paramyosin gene (unc-15) of Caenorhabditis elegans: molecular cloning, nucleotide sequence and models for thick filament structure*. J. Mol. Biol. 207: 311–333

Kahn BB, et al., 2005 *AMP-activated protein kinase: ancient energy gauge provides clues to modern understanding of metabolism* Cell Met.1:15–25.

Kelley CA, and Adelstein RS, 1990 *The 204-kDa smooth muscle myosin heavy chain is phosphorylated in intact cells by casein kinase II on a serine near the carboxyl terminus*. J Biol Chem 265: 17876-17882

Kontrogianni–Konstantopoulos A., Ackermann M. A., Bowman A. L., Yap S. V., Bloch R. J. (2009). *Muscle giants: molecular scaffolds in sarcomerogenesis*. Physiol. Rev. 89, 1217–1267

Kuga W, K. Tsuchihara, T. Ogura, S. Kanehara, M. Saito, A. Suzuki, and H. Esumi. 2008 *Nuclear localization of SNARK; its impact on gene expression.* Biochem Biophys Res Commun. 377:1062-6

Lessard S. J., D. A. Rivas, K. So, H. J. Koh, A. L. Queiroz, *et al.*, 2016 *The AMPK-related kinase SNARK regulates muscle mass and myocyte survival.* J Clin Invest. 126: 560-70.

Lefebvre DL, Rosen CF, 2005 *Regulation of SNARK activity in response to cellular stresses*. Biochim Biophys Acta 1724:71–85

Liu, F., C. C. Bauer, I. Oritz, R. G. Cook, M. F. Schmid et al., 1998 *Beta-Filagenin, a newly identified protein coassembling with myosin and paramyosin in C. elegans*. J. Cell Biol. 140: 347-353

Luther PK, Barry JS, Squire JM. 2002 *The three-dimensional structure of a vertebrate wide (slow muscle) Z-band: lessons on Z-band assembly*. J Mol Biol. ;315:9–20

Mackenzie J. M., F. Schachat, H.F. Epstein, 1978 *Immunocytochemical localization of two myosins within the same muscle cells in Caenorhabditis elegans.* Cell. 14: 413–419

Madhusudan, P. Akamine, N. H. Xuong, and S. S. Taylor, 2002 *Crystal structure of a transition state mimic of the catalytic subunit of cAMP-dependent protein kinase* Nat. Struct. Biol. 9: 273–277

McCarter, J., B. Bartlett, T. Dang, and T. Schedl, 1999 *On the Control of Oocyte Meiotic Maturation and Ovulation in Caenorhabditis elegans.* Developmental Biology 205: 111–128

Mello, C. C., J. M. Kramer, D. Stinchcomb and V. Ambros, 1991 *Efficient gene transfer in C. elegans: extrachromosomal maintenance and integration of transforming sequences*. EMBO J. 10:3959–3970

Mercer, K. B., D. B. Flaherty, R. K. Miller, H. Qadota, T. L. Tinley, *et al.*, 2003 *Caenorhabditis elegans UNC-98, a C2H2 Zn Finger Protein, Is a Novel Partner of UNC-97/PINCH in Muscle Adhesion Complexes.* Molecular Biology of the Cell. 14: 2492–2507

Mercer, K. B., R. K. Miller, T. L. Tinley, S. Sheth, H. Qadota, *et al.,* 2006 *Caenorhabditis elegans UNC-96 Is a New Component of M-Lines That Interacts with UNC-98 and Paramyosin and Is Required in Adult Muscle for Assembly and/or Maintenance of Thick Filaments.* Molecular Biology of the Cell. 17: 3832–3847

Miller D. M., I. Ortiz, G. C. Berliner, and H. F. Epstein, 1983 *Differential localization of two myosins within nematode thick filaments.* Cell. 34: 477–490.

Miller, R. K., H. Qadota, M. L. Landsverk, K. B. Mercer, H. F. Epstein, and G. M. Benian, 2006 *UNC-98 links an integrin-associated complex to thick filaments in Caenorhabditis elegans muscle.* JCB vol. 175(6): 853-859

Miller, R. K., H. Qadota, K. B. Mercer, K. M. Gernert, and G. M. Benian, 2008 *UNC-98 and UNC-96 interact with paramyosin to promote its incorporation into thick filaments of Caenorhabditis elegans.* Mol Biol Cell. 19(4):1529-39

Miller, R. K., Qadota H, T.J. Stark, K. B. Mercer, T.S. Wortham, A. Anyanful, and G. M. Benian, 2009 *CSN-5, a component of the COP9 signalosome complex, regulates the levels of UNC-96 and UNC-98, two components of M-lines in Caenorhabditis elegans muscle.* Mol Biol Cell. 20(15): 3608–3616

Moerman DG, Fire A., 1997 *Muscle: Structure, Function, and Development*. Chapter 16 in *C. elegans II. 2nd edition*, edited by Riddle DL, Blumenthal T, Meyer BJ, *et al*. Cold Spring Harbor Laboratory Press, Cold Spring Harbor (NY)

Moerman D. G., B. D. Williams, 2006 *Sarcomere assembly in C. elegans muscle.* WormBook. 16: 1-16.

Murakami N, Kumon A, Matsumura S, Hara S, Ikenaka T, 1988 *Phosphorylation of the heavy chain of skeletal muscle myosin by casein kinase II: Localization of the phosphorylation site to the amino terminus*. J Biochem 103(2):209–211

Nonet, M. L., K. Grundahl, B. J. Meyer, and J. B. Rand, 1993 *Synaptic function is impaired but not eliminated in C. elegans mutants lacking synaptotagmin.* Cell. 73:1291–1305

Ohmura, T., G. Shioi, M. Hirano, S. Aizawa, 2012 *Neural tube defects by NUAK1 and NUAK2 double mutation.* Dev Dyn. 241(8): 1350-64.

Otsuka, A. J., 1986 *sup-3 suppression affects muscle structure and myosin heavy chain accumulation in Caenhorhabditis elegans.* UCLA Syrup. Mol, Cell, Biol. New Ser. 29:619-628.

Priess, J. R., D. I. Hirsh, 1986 *Caenorhabditis elegans morphogenesis: the role of the cytoskeleton in elongation of the embryo.* Dev Biol 117: 156-173.

Qadota H., K. B. Mercer, R. K. Miller, K. Kaibuchi, and G. M. Benian, 2007 *Two LIM domain proteins and UNC-96 link UNC-97/pinch to myosin thick filaments in Caenorhabditis elegans muscle.* Mol Biol Cell. 18(11): 4317-4326.

Qadota H, and G. M. Benian, 2010 *Molecular structure of sarcomere-to-membrane attachment at M-lines in C. elegans muscle*. (Review). J. Biomed. Biotech.

Qadota, H., O. Mayans, Y. Matsunaga, J. L. McMurry, K. J. Wilson, *et al.*, 2016 *The SH3 domain of UNC-89 (obscurin) interacts with paramyosin, a coiled-coil protein, in Caenorhabditis elegans muscle.* Mol Biol Cell. 27(10): 1606-20.

Rovner AS, Fagnant PM, Lowey S, Trybus KM, 2002 *The carboxyl-terminal isoforms of smooth muscle myosin heavy chain determine thick filament assembly properties*. J Cell Biol 156(1):113–123.

Riddle, D. L., and S. Brenner, 1978. *Indirect suppression in Caenhorhabditis elegans.* Genetics. 89:299-314.

Schiller, NT, Duchesneau CD, Lane LS, Reedy AR, Manzon ER and Hoppe PE. 2017 *The role of the UNC-82 protein kinase in organizing myosin filaments in striated muscle of Caenorhabditis elegans.* Genetics. 205, 1195–1213. PMID: 28040740

Schriefer, L., and R. H. Waterston, 1989 *Phosphorylation of the N-terminal region of Caenorhabditis elegans paramyosin.* J. Mol. Biol. 207: 451–454

Squire JM, Al-Khayat HA, Knupp C, Luther PK. 2005 *Molecular architecture in muscle contractile assemblies*. Adv Protein Chem. 71:17–87.

Stiernagle, T., 2006 *Maintenance of C. elegans.* Wormbook. The C. elegans Research Community. http://www.wormbook.org.

Thompson, O., M. Edgley, P. Strasbourger, S. Flibotte, B. Ewing, *et al.*, 2013 *The million mutation project: a new approach to genetics in Caenorhabditis elegans.* Genome Res, 23: 1749–1762

Vallenius, T., K. *et al.*, 2011. *An association between NUAK2 and MRIP reveals a novel mechanism for regulation of actin stress fibers*. J. Cell Sci. 124:384–393

Warner, A., G. Xiong, H. Qadota, T. Rogalski, A. W. Vogl, *et al.*, 2013 *CPNA-1, a copine domain protein, is located at integrin adhesion sites and is required for myofilament stability in Caenorhabditis elegans.* Mol Biol Cell. 24(5):601-616

Waterston, R. H., R. M. Fishpool, S. Brenner, 1977 *Mutants affecting paramyosin in C. elegans.* J Mol Biol 117:679–697.

Waterston, R. H., J. N. Thomson, S. Brenner, 1980 *Mutants with altered muscle structure of Caenorhabditis elegans.* Dev Biol 77(2):271–302.

Waterston R. H., 1989 *The minor myosin heavy chain, mhcA, of Caenorhabditis elegans is necessary for the initiation of thick filament assembly.* EMBO J. 8(11):3429-36.

White GE, Petry CM, Schachat F 2003 *The pathway of myofibrillogenesis determines the interrelationship between myosin and paramyosin synthesis in Caenorhabditis elegans.* J Exp Biol 206: 1899–906.

Williams, B. D. and R. H. Waterston, 1994 *Genes critical for muscle development and function in Caenorhabditis elegans identified through lethal mutation.* J. Cell Biol. 124: 475-490.

Xiao B, et al. Structure of mammalian AMPK and its regulation by ADP. Nature.;472:230–233. 2011

Yuan, A., M. Dourado, A. Butler, N. Walton, A. Wei, et al., 2000 *SLO-2, a K1 channel with an unusual Cl- dependence.* Nat. Neurosci. 3: 771–779.

Zagórska, A., M. Deak, D. G. Campbell, S. Banerjee, M. Hirano, *et al.*, 2010 *New Roles for the LKB1-NUAK Pathway in Controlling Myosin Phosphatase Complexes and Cell Adhesion* Science Signaling. 3(115), ra25.

Zengel, J. M. and Epstein, H. F. 1980 *Mutants altering coordinate synthesis of specific myosins during nematode muscle development.* Proc.Natl. Acad. Sci. USA 77: 852-856.